Estimation of regional-scale wind and gust speeds for Europe by statistical-dynamical downscaling

I n a u g u r a l - D i s s e r t a t i o n

zur

Erlangung des Doktorgrades

der Mathematisch-Naturwissenschaftlichen Fakultät

der Universität zu Köln

vorgelegt von

Rabea Haas

aus Iserlohn

Hamburg, 2015

Berichterstatter: Prof. Dr. Michael Kerschgens

                           Prof. Dr. Andreas Fink

Tag der mündlichen Prüfung: 10. Juni 2014

Contents

Abstract

The winter season 2013 / 14 has shown once again that mid-latitude windstorms have a strong impact on Europe in terms of potential damages and insured losses caused by gusts or indirectly by storm surges. To analyze windstorm occurrences and associated footprints, data sets or simulations are necessary, which have a high temporal and spatial resolution, cover reality as best as possible, and are able to predict wind or gust speeds for future climate conditions. In order to meet these requirements, this study combines data from General Circulation Models (GCMs), reanalyses, Regional Climate Models (RCMs), and observations with respect to the individual advantages.

The first part relates large-scale reanalysis wind speeds and regional gust speeds simulated with the COSMO-CLM RCM by multiple linear regression models. These models are trained with a sample of 100 historical windstorms, which had a large influence on European onshore areas. By applying the obtained transfer functions to other large-scale data (GCM simulations), this kind of statistical-dynamical downscaling enables to estimate high-resolution gust speed footprints for Europe in a computationally cost-efficient way. A validation against observations of German weather stations shows that both the results for the combined downscaling approach and for pure dynamical downscaling with an RCM are in congruence with measurements and have similar deviations. The deviations from observations are caused by model biases due to local effects, which cannot be parameterized by the RCM. Thus, the second part aims at adjusting RCM simulations to observations. For this purpose, wind observations of 173 selected test sites and gust observations of 111 selected test sites of the German Weather Service as well as COSMO-CLM simulations are fitted by Weibull distributions. The observation-based distribution parameters are interpolated to the RCM grid, where they are related to the parameters of the simulations by probability mapping. This enables to correct the simulations while retaining the regular grid. Validation with grid points and nearby test sites shows an improvement of about 84 % and 64 % of the sites for wind and gust, respectively. Averaged over all test sites, for wind, 99 of the 100 selected events are improved in terms of more realistic simulations, and 88 events are improved for gusts.

In the third part, the introduced statistical-dynamical downscaling is applied to a large ensemble of decadal hindcasts simulated with the earth system model of the Max-Plack-Institue (MPI-ESM-LR, baseline 1). The decadal

predictability of peak wind speeds over Europe is analyzed using ten different realizations of yearly initialized decades between 1979 and 2010. Comparing original COSMO-CLM footprints and statistical-dynamically downscaled footprints of all days within the investigation period with respect to selected quantiles shows that the approach is appropriate for this large ensemble. The methodology is also able to identify periods with enhanced windstorm activity as exemplary shown for the years 1990 - 1993. The validation against uninitialized simulations using skill scores indicates that both the original hindcasts and the downscaled hindcasts are able to predict wind speeds and peak wind speeds for Europe on decadal scales. The performance is best for high quantiles equal or above 75 % and for the first years (1 - 4) after initialization.

It is shown that the combination of the different data sets enables to increase the data resolution in a computationally inexpensive way, while small-scale features parameterized by the RCM are still included. This is important for large ensembles like given for decadal hindcasts and predictions. Additionally, the approach has the advantage of estimating peak winds as proxy for gusts, whereas most large-scale data sets only provide wind speeds. For wind speed, it is recommendable to adjust the simulations to observations by quantile mapping. The same technique delivers for gust speeds improvements only in some areas of the German investigation area. In general, adding or omitting parts of the approach introduced here is easy to implement as all techniques are applicable stand-alone and joined together. This enables to use the methodology also for other parameters.

Zusammenfassung

Der Winter 2013 / 14 hat einmal mehr gezeigt, dass Stürme der mittleren Breiten einen großen Einfluss auf Europa haben, da sie durch Böen und indirekt durch Sturmfluten große, teils versicherte, Schäden verursachen. Zur Untersuchung von Stürmen, ihrem Auftreten und damit verbundenen Wind- und Böensignaturen, sind geeignete Datensätze nötig. Diese sollten eine große zeitliche und räumliche Auflösung haben, die Realität so gut wie möglich widerspiegeln und in der Lage sein, Wind- oder Böengeschwindigkeiten unter zukünftigen Klimabedingungen zu simulieren. Um diesen Anforderungen gerecht zu werden, zeigt diese Arbeit eine Möglichkeit Daten von globalen Klimamodellen, Reanalysen, Regionalmodellen und Beobachtungen unter Berücksichtigung der individuellen Vorteile zu kombinieren.

Der erste Teil setzt Windgeschwindigkeiten aus Reanalysen und Böengeschwindigkeiten, die mit dem Regionalmodell COSMO-CLM simuliert wurden, in Beziehung. Dazu werden lineare Regressionsmodelle mit einer Stichprobe von 100 Stürmen, die einen großen Einfluss auf das Europäische Festland hatten, trainiert. Die ermittelten Transferfunktionen können anschließend auf andere großskalige Daten (Klimamodelle) angewandt werden. Durch diese Art der statistisch-dynamischen Regionalisierung ist es möglich, hoch aufgelöste Böensignaturen für Europa mit geringem Rechenaufwand zu schätzen. Eine Validierung gegenüber Beobachtungen Deutscher Wetterstationen zeigt sowohl für die Ergebnisse des kombinierten Ansatzes als auch für die Ergebnisse der rein dynamische Regionalisierung mit einem Regionalmodell gut Übereinstimmungen mit Messungen und ähnliche Abweichungen. Die Abweichungen zu den Beobachtungen werden dabei durch lokale Effekte verursacht, die nicht durch das Regionalmodell parameterisiert werden können. Aus diesem Grund zielt der zweite Teil der Arbeit auf die Anpassung von Regionalmodellsimulationen an Beobachtungen. Dafür werden Weibull Verteilungen an Windbeobachtungen 173 ausgewählter Stationen, Böenbeobachtungen 111 ausgewählter Stationen und COSMO-CLM Simulationen angepasst. Die beobachtungsbasierten Verteilungsparameter werden anschließend auf das Regionalmodellgitter interpoliert, wo sie durch "Probability Mapping" mit den Parametern der Simulationen verknüpft werden. Dadurch können die Simulationen korrigiert werden, während das regelmäßige Gitter beibehalten wird. Eine Validierung mit Gitterpunkten und benachbarten Stationen zeigt eine Verbesserung der Simulationen in Richtung der Beobach-

tungen an 84 % der Stationen für Wind und an 64 % der Stationen für Böen. Gemittelt über alle Stationen können für Wind 99 der 100 ausgewählten Ereignisse verbessert werden und für Böen 88 Ereignisse.

Im dritten Teil wird die statistisch-dynamische Regionalisierung auf ein großes Ensemble dekadischer "Hindcasts" des Erdsystemmodells des Max-Planck-Institus (MPI-ESM-LR, baseline 1) angewandt. Die dekadische Vorhersagbarkeit von Spitzenwindgeschwindigkeiten über Europe wird mit Hilfe von zehn unterschiedlichen Realisierungen jährlich initialisierter Dakaden zwischen 1979 und 2010 untersucht. Vergleicht man ausgewählte Quantile der originalen COSMO-CLM Signaturen und der statistisch-dynamisch regionalisierten Signaturen, zeigt sich, dass der Ansatz für dieses große Ensemble geeignet ist. Die Methode kann außerdem zur Identifizierung von Zeiträumen mit erhöhter Sturmaktivität genutzt werden, wie beispielhaft an den Jahren 1990 - 1993 gezeigt wird. Der Vergleich zu uninitialisierten Simulationen liefert Qualitätsmaße, die darauf hinweisen, dass sowohl die "Hindcasts", als auch die regionalisierten Simulationen geeignet sind, um Windgeschwindigkeiten bzw. Spitzenwindgeschwindigkeiten für Europa auf dekadischen Skalen vorherzusagen. Das Ergebnis ist dabei am besten für hohe Quantile größer oder gleich 75 % und für die ersten Jahre (1 - 4) nach der Initialisierung.

Es wurde gezeigt, dass die Kombination der verschiedenen Datensätze dazu führt, dass die Auflösung der Daten ohne großen Rechenaufwand erhöht werden kann, während die durch das Regionalmodell parameterisierten kleinskaligen Eigenschaften erhalten bleiben. Des Weiteren hat die Methodik den Vorteil, dass Spitzenwinde als Näherung von Böen geschätzt werden können, wohingegen die meisten großskaligen Datensätze nur Windgeschwindigkeiten liefern. Für Windgeschwindigkeiten ist es empfehlenswert, die Simulationen an die Beobachtungen durch "Quantile Mapping" anzupassen. Für Böen liefert die gleiche Technik nur in machen Gebieten Deutschlands eine Verbesserung. Im Allgemeinen ist es jedoch einfach, einzelne Teile der Methodik hinzuzufügen oder wegzulassen, da alle Techniken sowohl alleine als auch zusammenhängend anwendbar sind. Dies erlaubt auch eine einfache Anpassung für andere Parameter.

1 Introduction

1.1 Motivation

Windstorms are typical weather phenomena affecting Europe, which occur mostly in fall and winter. They are associated to intense low-pressure systems (cyclones) forming over the North Atlantic and propagating eastwards to western Europe. Intense low-pressure systems like Christian in October 2013 and Xaver in December 2013 show that windstorms and related gusts have a strong impact on Europe. With peak gusts of $191\,\mathrm{km/h}$ [1] ($53\,\mathrm{m/s}$) in coastal areas and $168\,\mathrm{km/h}$ [1] ($47\,\mathrm{m/s}$) in the low land, windstorm Christian caused an interruption of transportation and shipping, as well as electric power outages in several countries. Even though the low-pressure system was well predicted, there were 14 fatalities in Europe. Windstorm Xaver had similar gust speeds, but a comparatively broad wind signature. Especially the German coast was affected by a storm tide, but due to early warnings, damage could be minimized with appropriate flood protection measures. The windstorm season of the winter 2013 / 14 was particularly distinct, as several windstorms, partly grouped to cyclone families, show along with the October event Christian and the December event Xaver. Around Christmas 2013, the cyclones Christian, Dirk and Erich brought intense squalls to Europe. In the first days of January 2014, Europe was hit again by a windstorm series consisting of Anne, Christina, Dagmar, and Elfride II. The later windstorms, like Petra, Qumaira, Ruth, and Tini during the first half of February caused severe damages particularly by storm surges at the British Isles. Similarly pronounced windstorm seasons affected Europe also during the 1990s. For this decade, the years 1990, 1993, and 1999 were particularly outstanding. Also the cyclones Kyrill and Xynthia of the years 2007 and 2010 showed that windstorms are one of the most important and devastating natural hazards affecting Europe. Such severe windstorm events do not only affect the social sector, but also economics, e. g. in terms of insurance claims. In order to investigate how far the occurrence of these extreme events and series of intense windstorms is influenced by climate change, it is fundamental to analyze

---

[1]Peak gusts from: www.unwetterzentrale.de/uwz/819.html

impacts of windstorms under current and future climate conditions. This involves sufficiently large ensembles of reliable high-resolution predictions of wind and gust speeds. For this purpose, techniques are needed, which deliver high-resolution simulations without producing high computational costs. The information are needed on different temporal scales to adjust planning strategies concerning climate change adaption. For most sectors, e. g. politics or economy, time frames of about ten years are important to react adequately and thus decadal predictions are in high demand.

In this study, methods are developed to obtain according simulations and predictions. The following introduction will first give a short overview of the meteorological background. Afterwards, demands for the analysis of windstorms are further explained and state-of-the-art methodologies are introduced. The last subsection outlines the structure of the statistical-dynamical downscaling model, potential optimization opportunities, and its applicability for decadal hindcasts. The next chapters include three published / submitted journal articles and material on additional investigations. The thesis closes with a summary and conclusions chapter.

1.2 Meteorological background

The atmospheric circulation is an aspect of meteorology, which has been investigated since several centuries (see e. g. Davis, 1899) and is recorded in various textbooks like Schönwiese (1994). The general factors leading to movement of air mass within the atmosphere are compensatory processes. Due to a positive net radiation at the equator and a negative net radiation at the poles, warm air masses are transported from the equator to the poles and cold air masses are transported from the poles to the equator. This general circulation is influenced by the Coriolis force, which leads to a deviation to the right at the Northern Hemisphere (NH) and to the left at the Southern Hemisphere (SH). In reality, several local influencing factors lead to a more complex circulation scheme. Close to the equator, northeast (at the NH) and southeast (at the SH) trade winds, induced by the Hadley cell (Hadley, 1735), flow together in the inner tropical convergence zone. The subtropics are characterized by a zone of high pressure including e. g. the Azores High on the NH. The relatively warm air masses of the subtropics and the relatively cold air masses of the polar regions are separated by the polar front. Corresponding to the Azores High, the Icelandic Low builds a semi-permanent low pressure system within this region of the NH. The polar regions themselves are influenced by thermal induced high pressure systems.

For the genesis of extratropical cyclones leading to intense windstorms over Europe, the predominantly westerly flow over the North Atlantic, in-

fluenced by location and intensity of the Azores High and Icelandic Low, and baroclinic instability over the Mid-latitudes are important (theory after Charney, 1947). This baroclinic zone is prone to small perturbations caused by changes in the temperature gradient. Such wave disturbances intensify and build frontal systems during the development of a cyclone. Cold air is advected to the south and warm air to the north, building a warm sector between the warm front and the cold front (Bjerknes and Solberg, 1922). In a three-dimensional view, a cyclone is characterized by divergence at the upper levels, rising air masses, and convergence at the surface, leading to decreasing pressure and a cyclonic circulation. During its lifetime, the low pressure system propagates eastwards with the general westerly flow and intensifies further until it is occluded. At this stage the pressure is lowest and the cyclone leads to strong wind speeds in particular south of the center where the cyclonic movement is added to the westerly flow. As the westerlies are strongest in fall and winter due to the steeper temperature gradient, severe windstorms mostly occur during these seasons. After the occlusion, the core pressure increases, especially after hitting land. There, the increased friction leads to a larger deviation of the wind and a faster cyclolysis than over the sea (Adamson et al., 2006). Thus, low pressure systems propagating over the North Atlantic to Europe typically disperse after a few days.

An important factor influencing the mean wind speed is friction: the air flow in the boundary layer is, especially next to the ground, characterized by turbulence, which can either be induced by friction or by thermal effects. The intensity of turbulence is also named gustiness. Gusts are short-time exceedances of the mean wind speed and are often joint with changes in the wind direction. The German Weather Service ("Deutscher Wetterdienst", DWD) defines a gust as exceedance of the 10-minute-mean of wind speed of minimum $5\,\mathrm{m/s}$ lasting for 3 to 20 seconds [2]. Wind gusts and peak wind speeds are one of the main factors leading to damages during windstorms. Therefore several loss models are based on a relationship to gust speeds or maximum wind speeds (Della-Marta et al., 2009; Klawa and Ulbrich, 2003).

1.3   Analysis of windstorms

For the analysis of European windstorms, there are mainly three available groups of data sets: observations, Regional Climate Model (RCM) simulations, and General Circulation Model (GCM) simulations. Concerning observations for Germany, the DWD provides a dense network of stations observing wind and gust speeds. These and other measurements deliver the best opportunity to draw an image of reality, at least at the measurement

---

[2]Definition from: www.deutscher-wetterdienst.de/lexikon/index.htm?ID=B&DAT=Boe

sites. However, the observations are limited in time by the length of the time series and limited in space by the points of observations. This disadvantage appears in particular for gust speeds, for which the density of observations is even lower than for wind speeds. Furthermore, wind and particularly gust speeds are clearly more heterogeneous than other meteorological parameters like temperature. Thus, for area-wide analyses, RCMs, which dynamically downscale the desired parameters, are more appropriate. These models can use boundary conditions e.g. from reanalysis data initialized with observations from different sources. One potential data set is the ERA-Interim reanalysis (Dee et al., 2011) from the European Centre for Medium-Range Weather Forecasts (ECMWF). In order to resolve sub-grid scale processes like gusts, clouds, land surface changes or convection, physical parameterizations can be implemented (e.g. Noilhan and Planton, 1989; Hack, 1994). In recent years, several approaches have been developed to parameterize gust speeds in addition to simulations of wind speed (e.g. Goyette et al., 2003). However, although the model physics are continually improved, there are still model biases, since not all local-scale factors can be covered perfectly. Additionally, the parameterizations and the increased resolution result in high computational costs, so that RCMs are only applicable for selected regions and time periods of interest and not for global investigations or large ensembles. For this purpose, GCMs are a commonly used tool to analyze the climate system and its physical processes on different spatial and temporal scales. They can be used to create simulations representing past, present or future climate conditions. An example is the atmospheric GCM ECHAM6, which is based on the global numerical weather prediction system of the ECMWF and further developed at the Max Planck Institute for Meteorology in Hamburg (see Stevens et al., 2013, for details). An example for the application of GCMs and quite new field of research is the investigation of decadal predictability using present climate hindcasts and future climate predictions (Mieruch et al., 2013). A drawback of all GCM simulations is the coarse spatial resolution, which allows for a global assessment but does not allow for studies on regional or local scale. In case of windstorms this also means that only wind speeds can be simulated, as local factors influencing gust speeds (e.g. roughness length) are typically below the resolved mesh size of the model grid. One possibility to estimate future climate wind and gust speeds is to use GCM simulations instead of reanalysis data as boundary conditions within RCMs. However, this is only applicable for a small ensemble.

As shown, none of the introduced data sets seems to be the optimal solution for a detailed investigation of windstorms and related wind and gust speeds. Therefore, the question arises, whether there is an opportunity to take the best attributes of each dataset and to minimize the disadvantages. The resulting aim of this study is to develop, validate and apply appropriate techniques to combine wind and/or gust speeds in different resolutions to optimize the prediction of European windstorms and gust speeds.

1.4 State-of-the-art methodologies

1.4.1 Downscaling and model output statistics

Several different methods for the downscaling and post processing of climatological data have been developed (Maraun et al., 2010, for review). Amongst European research institutions, the RCM of the Consortium for Small-scale MOdelling in CLimate Mode (COSMO-CLM, hereafter CCLM, Rockel et al., 2008) is commonly used for downscaling. The model is designed for different time scales and spatial resolutions of 1 km to 50 km. Beside dynamical downscaling by an RCM like the CCLM, statistical downscaling techniques relating large-scale predictors, such as GCM data or reanalyses, and local-scale predictands exist (Wilby et al., 2004, for review). The three main groups of statistical downscaling are weather classification, regression models, and weather generators, which can be used stand-alone or in combination.Compared to dynamical downscaling, the computational costs can be considerably reduced by these methods. In order to maintain the advantages of dynamical downscaling like gust parameterizations, combined statistical-dynamical approaches have been developed (e. g. Boé et al., 2006; Fuentes and Heimann, 2000). However, dynamical as well as statistical and statistical-dynamical downscaling techniques have weaknesses in producing realistic wind and gust estimations, in particular for complex terrain. Hence, the downscaling results should be post processed to bring them closer to observations. For this purpose, the perfect prog approach and Model Output Statistics (MOS) have been developed (Klein and Glahn, 1974). For the former, observed predictors and predictands are related; for the latter, observations are connected with simulations. The resulting transfer functions of both approaches can be applied on model output. However, most perfect prog and MOS approaches deliver corrected values only at specific locations and not on a regular grid.

1.4.2 Decadal predictions

The analysis of decadal predictability is one potential field of application of GCMs. Hindcasts and predictions should be able to reproduce natural and anthropogenic variability. Several coupled ocean atmosphere models and earth system models have been compared within the Coupled Model Intercomparison Project Phase 5 (CMIP5), stating that the results are promising for surface temperature, sea surface temperature and circulation patterns, especially over the North Atlantic (Taylor et al., 2012). For other parameters like precipitation it is found that there is still potential for improvement. A current European project is MiKlip ("Mittelfristige Klimaprogno-

sen", decadal predictions), where the goal is to build a model system for different parameters, which is suitable for decadal climate predictions on the large scale and also on the regional scale (Mieruch et al., 2013). Within this project, simulations of the Earth System Model of the Max-Planck-Institute (MPI-ESM) including the Ocean Model MPIOM and the atmospheric model ECHAM6 are investigated. The simulations consist of different realizations of yearly initialized decades between 1960 and 2011. So far, two systems are are available, baseline0 and baseline1, which differ mainly in the number of ensemble members (three against ten realizations) and the initialization (ocean against combined ocean atmosphere initialization). PRODEF (PRObabilistic DEcadal Forecast for central and western Europe) is one of the subprojects that aim at increasing the spatial resolution of decadal hindcasts and predictions by regionalization. The analysis of wind and gust speeds in terms of energy supply and windstorm impacts is one of the foci of PRODEF.

Up to a few years ago, studies dealing with wind and / or gusts and providing Europe-wide high-resolution products are limited. This work thus offers an important contribution of research and fills the gap between different scales. On the one hand, the spatial resolution can be increased by a statistical-dynamical downscaling model; on the other hand, the applicability for large ensemble e. g. on decadal scales is given.

1.5 The statistical-dynamical downscaling model and its application

The methodologies illustrated in Section 1.4 are adopted and adjusted in order to combine the advantages of different wind and gust data sets. First, a statistical-dynamical downscaling approach is developed. For this purpose, gust footprints simulated with an RCM on a high-resolution grid are related to large-scale wind speeds of a reanalysis data set by transfer functions. Here, the CCLM is used as RCM (marked in blue in Figure 1.1). For each CCLM grid point, the surrounding 16 ERA-Interim reanalysis wind speeds are considered as large-scale predictors (marked in red in Figure 1.1). By Multiple Linear Regression (MLR) the 16 grid points are weighted with regression coefficients. Once calculated, these regression coefficients can be (re-)applied on large-scale data like GCMs (marked in green in Figure 1.1), which need to have the same grid as the ERA-Interim training data set. Therewith, the transfer functions can be validated and new statistical-dynamically downscaled gust speeds can be estimated. Here, the transfer functions are reapplied on ERA-Interim reanalysis data to reproduce dynamically downscaled footprints. The reproduced gust values are validated against the original CCLM simulations using Root Mean Squared Errors (RMSEs).
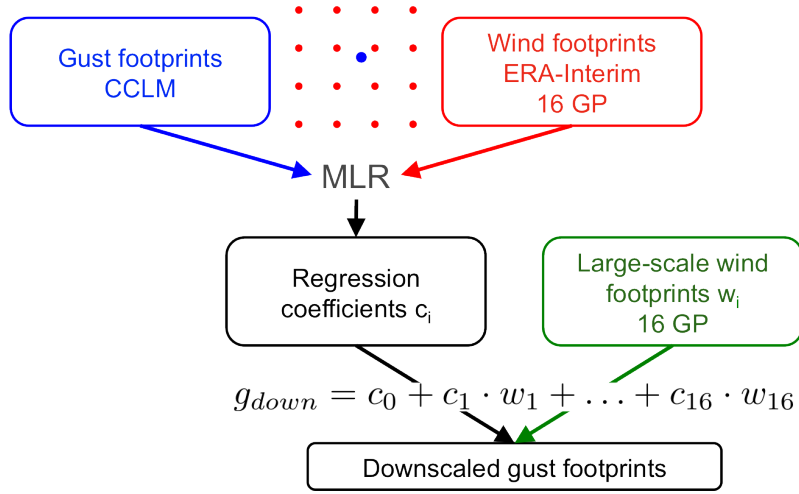
Figure 1.1: Schematic chart of the statistical-dynamical downscaling method relating large-scale wind speeds and regional-scale gust speeds.

In order to bring the CCLM simulations closer to observations, an approach based on MOS is tested for practicability regarding wind and gust speeds. For this study, the investigation area is reduced to Germany, to ensure consistent measurements with a sufficient spatial and temporal distribution. Here, the observed wind and gust speeds were provided by the DWD. For the methodology, a probabilistic approach has been chosen, i.e. simulated wind or gust speeds (CCLM; marked in blue in Figure 1.2) and observed wind or gust speeds (marked in red in Figure 1.2) are each fitted by a theoretical distribution - here the Weibull distribution. In order to allow for a comparison of both data sets, the distribution parameters of the observations are interpolated onto the CCLM grid. On this grid, the simulated wind or gust speeds can be corrected by quantile mapping. In contrast, most previous studies only deliver an adjustment of simulations at measurement sites. A potential enlargement of the gust data set is given by a wind-gust model. The idea is to estimate gust speeds from wind speeds considering statistical relations between the distributions of both parameters. The approach is further developed in Seregina (2012) and published in Seregina et al. (2014). Details to the development and the outcomes are presented in a supplementary part of this work (Chapter 4).
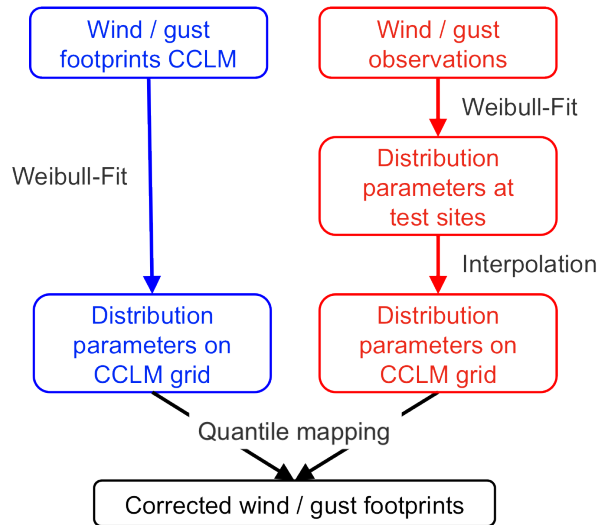
Figure 1.2: Schematic chart of model output statistics combining observations and regional climate model data.

The last part of this work deals with the application of the statistical-dynamical downscaling approach developed in the first part in order to demonstrate the advantages. For this purpose, decadal hindcasts and predictions of MPI-ESM in its lower resolution of the baseline1 system (MPI-ESM-LR) are investigated. The simulated ensemble members are initialized using different time steps of an assimilation run leading to a large ensemble of daily values from different realizations. For comparison purposes, the same model is used to calculate an uninitialized historical run. By comparing initialized and uninitialized values, RMSE-based skill scores can be calculated to proof the added value of initialization. For regional-scale investigations, both historical runs and hindcasts have to be downscaled. However, this amount of data including daily values between 1960 and 2011 is too large for downscaling with a classical RCM. Hence, the statistical-dynamical approach is perfectly suitable for this aim. Applying the statistical-dynamical downscaling approach involves amongst other things to identify periods with enhanced windstorm activity. Additionally, it delivers the opportunity to calculate skill scores not only for large-scale wind, but also for regional-scale peak winds as an estimation for gust speeds.

The statistical-dynamical downscaling approach developed with 100 selected windstorms over Europe and its validation are published in the first scientific paper (Chapter 2). In the second publication (Chapter 3), the relationship between CCLM simulations and measurements is analyzed. Because of different country specific measurement densities and thresholds for storing gust data, the investigation is delimitated to Germany. Chapter 4 contains additional work on the relationship between wind and gusts, resulting in

a wind-gust model. The third publication (Chapter 5) deals with the application of the methodology introduced in Chapter 2 on a large ensemble of large-scale simulations to investigate decadal predictability of wind and peak wind speeds. Finally, Chapter 6 gives a summary and discussion of the results.

2 Downscaling of windstorms

Published journal article:

Haas, R., and J. G. Pinto (2012), A combined statistical and dynamical approach for downscaling large-scale footprints of European windstorms, *Geophysical Research Letters*, 39, L23804, doi:10.1029/2012GL054014.

A combined statistical and dynamical approach for downscaling large-scale footprints of European windstorms

R. Haas[1] and J. G. Pinto[1]

[1]   The occurrence of mid-latitude windstorms is related to strong socio-economic effects. For detailed and reliable regional impact studies, large datasets of high-resolution wind fields are required. In this study, a statistical downscaling approach in combination with dynamical downscaling is introduced to derive storm related gust speeds on a high-resolution grid over Europe. Multiple linear regression models are trained using reanalysis data and wind gusts from regional climate model simulations for a sample of 100 top ranking windstorm events. The method is computationally inexpensive and reproduces individual windstorm footprints adequately. Compared to observations, the results for Germany are at least as good as pure dynamical downscaling. This new tool can be easily applied to large ensembles of general circulation model simulations and thus contribute to a better understanding of the regional impact of windstorms based on decadal and climate change projections. **Citation:** Haas, R., and J. G. Pinto (2012), A combined statistical and dynamical approach for downscaling large-scale footprints of European windstorms, *Geophys. Res. Lett.*, *39*, L23804, doi:10.1029/2012GL054014.

1. Introduction

[2]   Windstorms are the main natural hazards affecting Europe, with a large impact on the societal and economic sectors [e.g., *Fink et al.*, 2009]. Their occurrence over Western Europe may increase under future climate conditions [e.g., *Della-Marta and Pinto*, 2009]. Studies quantifying impacts on regional scales [e.g., *Della-Marta et al.*, 2010; *Schwierz et al.*, 2010] typically use a combination of large-scale data like reanalysis datasets or General Circulation Model (GCM) simulations, and Regional Climate Model (RCM) simulations. The high resolutions of RCMs (typically 10–50 km) involve high computational costs. Thus, they only focus on a region of interest and their applicability to multi-model ensembles is limited [cf. *Kjellström et al.*, 2011].

[3]   A computational inexpensive alternative is statistical downscaling, which relates large-scale predictors and local predictands by transfer functions. Different statistical downscaling techniques have been developed for various atmospheric parameters (e.g., *Maraun et al.* [2010] for a review). In recent years, some studies also concentrated on the regionalization of wind data. For example, *Bernardin et al.* [2009] applied a system of stochastic differential equations on numerical weather prediction model data for wind refinement. A physical-statistical approach was introduced by *De Rooy and Kok* [2004], decomposing the total error between model and observation into small-scale representation mismatch and large-scale model error. *Pryor et al.* [2005] focused on wind energy applications and downscaled near-surface wind speed empirically using GCM data. Nevertheless, the research on statistical downscaling is still very limited for wind applications and none of the previous studies focused specifically on mid-latitude windstorms.

[4]   The objective of this work is to develop and validate an approach suitable to reproduce dynamical downscaled RCM gust speeds in a cost-efficient way. This is important for building a storm catalog of many thousands of events, required for decadal projections, climate change investigations or insurance applications. We propose a new statistical downscaling tool, which is able to generate gust speeds on a high-resolution grid over Europe by Multiple Linear Regression (MLR) using RCM output for training purposes.

2. Data

2.1. Reanalysis Data

[5]   In this study, ERA-Interim reanalysis data [*Dee et al.*, 2011] from the European Centre for Medium-Range Weather Forecasts (ECMWF) is used as large-scale forcing for both dynamical and statistical downscaling. The dataset has a horizontal resolution of T255 ($0.75° \times 0.75°$) and covers the period from 1989 until the end of 2010. 6-hourly instantaneous wind speeds are used to establish a ranking of historical windstorms (details in Section 3.1.). For each storm, ERA-Interim data with original resolution within the investigation area ($-14.7656°$E to $34.4531°$E, $32.6315°$N to $66.3155°$N; Figure S1 in the auxiliary material) is compared to dynamically downscaled high-resolution data.[1]

2.2. Regional Climate Model Data

[6]   The selected historical storms are dynamically downscaled with the COSMO-CLM (RCM of the COnsortium for Small-scale MOdelling in CLimate Mode, hereafter CCLM [*Rockel et al.*, 2008]). A resolution of 7 km ($0.0625°$) is reached by two step nesting using ERA-Interim as initial and boundary conditions. Wind gusts are estimated with an approach using friction velocity as a predictor for turbulence [*Schulz*, 2008]. For more details on RCM validation against

---
[1]Institute for Geophysics and Meteorology, University of Cologne, Cologne, Germany.

Corresponding author: R. Haas, Institute for Geophysics and Meteorology, University of Cologne, Kerpener Str. 13, DE-50937 Cologne, Germany. (rhaas@meteo.uni-koeln.de)

---
[1]Auxiliary materials are available in the HTML. doi:10.1029/2012GL054014.

observations and other gust estimation approaches, see *Born et al.* [2012]. Each simulation consists of at least 4 days.

3. Methods

3.1. Selection of Events

[7] Several methods have been developed to estimate the potential impact associated with windstorms based on wind or gust speeds [e.g., *Klawa and Ulbrich*, 2003]. Here, we consider a Meteorological Index (MI) to estimate potential losses, defined as spatially aggregated cubic exceedances of the local 98th gust percentile [see *Pinto et al.*, 2012, equation 3]. This variable is a proxy for the impact of a storm purely associated with its meteorological characteristics, without considering exposure or vulnerability. MI is computed over Europe ($-9.8438°$E to $34.4531°$E; $35.4385°$N to $64.912°$N; Figure S1), but only for land grid points. The 100 top-ranked days in the ERA-Interim period are derived according to MI (see Table S1). For training and validation of the statistical downscaling approach, events are defined as the storm date plus one day before and after. Several well known historical storms are included [cf. *Fink et al.*, 2009]. Note that some consecutive days may be often attributed to the same storm (e.g., 20070118 and 20070119 for Kyrill). However, in order to maintain a consistent database on a daily basis, those dates are kept separated. A windstorm footprint (wind signature) for the full extension of a storm like Kyrill can be obtained by considering the maximum gust on both days at each grid point.

3.2. Multiple Linear Regression

[8] The statistical approach relates CCLM simulations and ERA-Interim data. We estimate a transfer function via MLR. One regression model is build per CCLM grid point:

$$y_i = c_0 + c_1 x_{i1} + \dots + c_k x_{ik} + \epsilon_i \quad i = 1, \dots, e \quad k = 1, \dots, 16 \quad (1)$$

The model includes CCLM daily maximum gust speed (vmax) values as predictands y_i. The event set has been enlarged to a 300-day-list by adding one day before and after each event. Due to consecutive days in the 100-day-list (see Table S1), the 300-day-list includes duplication of calender days. These days have been excluded, thus $e = 240$. The predictors x_{ik} consist of the wind speeds at the 16 ERA-Interim grid points next to the CCLM grid point. The vector of regression coefficients $\hat{c} = c_k$ can be estimated by the method of least squares:

$$\hat{\mathbf{c}} = (\mathbf{X}^T \mathbf{X})^{-1} \mathbf{X}^T \mathbf{y} \quad (2)$$

with X = matrix of predictors and y = the vector of predictands. This transfer function is here reapplied on reanalysis data for cross-validation (see Section 3.3). However, the regression coefficients can be easily applied to other datasets (e.g., GCM).

3.3. Validation

[9] The effectiveness of the methodology is evaluated by cross-validation. Two distinct validation approaches are performed. First, the ability to reproduce the wind signature of a single storm with a transfer function estimated from the other 99 events (leave-one-out validation) is analysed.

Second, the list is separated into training and validation datasets according to dates and rank of MI. The separation can be performed with sequential (first and second 50 values) or disordered (even and odd entry numbers) lists. For both validation approaches, three-day-signatures are used.

[10] The root mean squared error (*RMSE*) and the relative root mean squared error (*RMSE$_{rel}$*) are calculated per event and per grid point as a measure of skill:

$$RMSE = \sqrt{\frac{\sum_{i=1}^{n}(\hat{x}-x)^2}{n}} \qquad RMSE_{rel} = \frac{\sqrt{\frac{\sum_{i=1}^{n}(\hat{x}-x)^2}{n}}}{\frac{\sum_{i=1}^{n}x}{n}} \quad (3)$$

with x = dynamically downscaled CCLM gusts and $\hat{x}$ = statistically downscaled gusts. For *RMSE* and *RMSE$_{rel}$* per event, n = number of grid points. For *RMSE* and *RMSE$_{rel}$* per grid point, n = number of events = 100.

4. Results

[11] The performance of the statistical downscaling is now compared with dynamical downscaling and forcing ERA-Interim data (Figure 1). The leave-one-out validation of the statistically downscaled wind signatures shows that the method performs best for strong events with a broad wind signature associated with a typical cyclone propagating eastwards over the North and/or Baltic Sea (cf. example of storm Wiebke; Figure 1a). Larger deviations between dynamical and statistical downscaling are found for uncommon weather situations, e.g., days with multiple footprints (cf. Xynthia; Figure 1d) or footprints affecting areas where severe windstorms are unusual (e.g., Southwestern Europe, cf. Martin; Figure 1b). Due to the low number of such events, the MLR model has difficulties to reproduce them adequately. A mismatch also occurs if the CCLM footprints do not follow the ERA-Interim footprints tightly, as our method follows the large-scale input (cf. wind speeds West of Norway for Xynthia; Figure 1d).

[12] The absolute RMSE per event, i.e., the sum over all grid points, is 2 to 5 ms^{-1} (not shown). Summed over all events, the range is 1 to 6 ms^{-1} at most grid points (Figure 2a). The results are depicted except for the border of the model area, where the CCLM produces spurious values (compare, e.g., Figure 1c at the Northern and Eastern border). The statistical method performs best over most European onshore areas from Portugal to Belarus and results are biased by the number of events affecting each area. To take this into account, the number of events per grid point, where vmax exceeds 20 ms^{-1} (corresponding to 8 Bft, a common threshold used by insurance companies [cf. *Klawa and Ulbrich*, 2003]) is analyzed (Figure 2b). As a visible relation between the number of events and the absolute RMSE is revealed, a subset of grid points where less than one third of the events (33) reached this threshold is excluded, thus ensuring a reasonable sample size. Further, grid points above 2000 m are excluded to avoid deviations associated with underestimation of the model topography and unrealistic high dynamically downscaled gusts which are not in congruence with the large-scale forcing. As the absolute RMSE is larger in areas where the gust speeds are generally higher, Figure 2c displays *RMSE$_{rel}$* with excluded grid points shaded in grey. Over those areas the relative errors amount to 20–40 %, except over a small area over Southeastern France with up to 70 %. Better results are achieved over the colored area with a 5–30 % range.
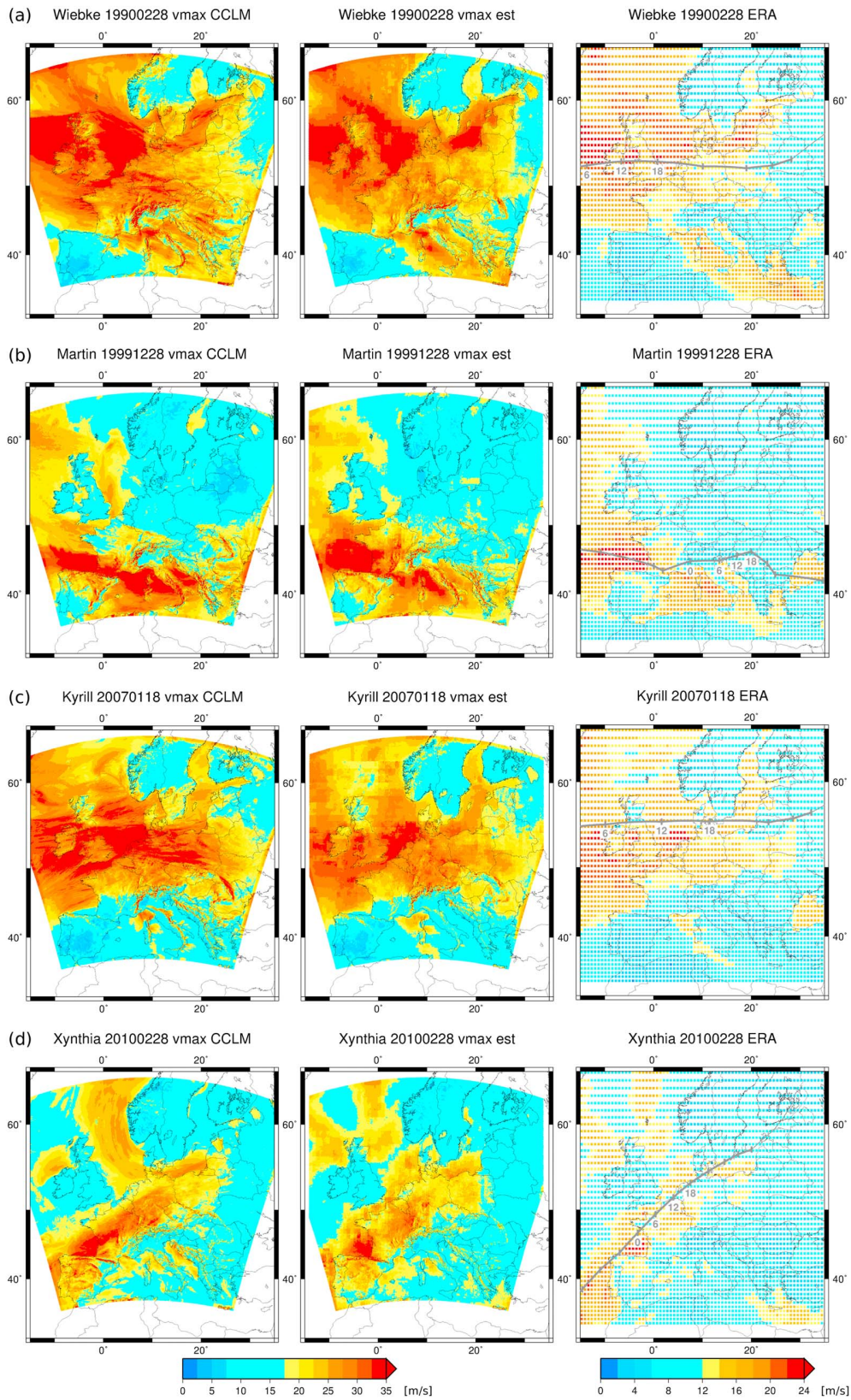
Figure 1. Three-day-signatures of the leave-one-out validation for selected events: (a) Wiebke, (b) Martin, (c) Kyrill, and (d) Xynthia. Dates are labeled as YYYYMMDD. (left) Original CCLM simulated gusts vmax. (middle) Estimated statistically downscaled gusts vmax est. (right) ERA-Interim wind speeds and 6-hourly positions of the associated cyclone tracks, marked as thick lines for the event days and thin lines for following days. UTC is only given for day two of the 3-day-signature.
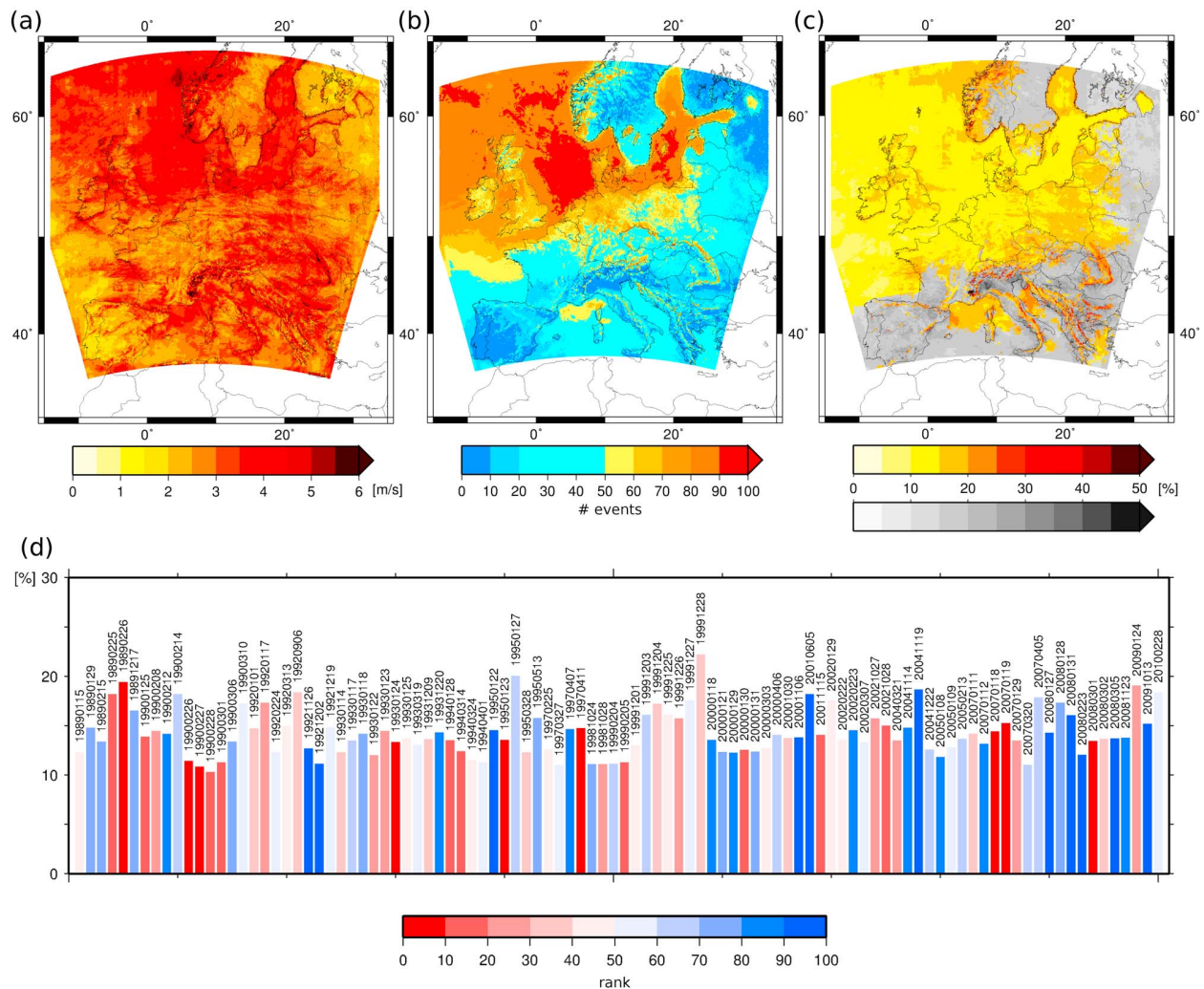
Figure 2. (a) Absolute RMSE of leave-one-out validation summed over events in ms^{-1}. (b) Number of events per grid point with gust speeds greater equal 20 ms^{-1}. (c) Relative RMSE of leave-one-out validation summed over all events in %. Colored grid points have a model height below 2000 m and are hit by gust speeds greater or equal 20 ms^{-1} on at least 33 of the 100 events. All other grid points are shaded in gray. (d) Relative RMSE of leave-one-out validation summed over the colored grid points in %. Bars are colored according to the rank of MI of each event (red is top rank; blue is low rank). Dates are given above each bar (YYYYMMDD).

[13] The 100 events have relative errors of 10–20 % averaged over the colored area (Figure 2d). These deviations are randomly distributed, which means they are not correlated to MI or rank according to MI (compare colors of bars). A detailed analysis of the wind signatures (Figure 1) indicates that the location of the footprint plays indeed an important role for the skill of the technique. In fact, $RMSE_{rel}$ averaged over all events and grid points decreases from 16 % to 14 % by the selection of colored areas in Figure 2c.

[14] A second validation approach is to split the dataset into training and validation period. The periods are separated sequentially by dates (first and second 50 days) or by MI rank (more severe events and less severe events). Additionally, the original dataset is split disordered according to even and odd entry numbers of the dates or of the MI ranks, thus each second value will be used for validation. The results are similar as for the leave-one-out validation: The selection of colored areas (Figure 2c) brings a slight improvement

of about 2 % for both sequential and disordered periods (Table 1). Regarding sequential periods, the difference between choosing higher or lower MIs as training period is marginal. The separation by dates shows slightly better results for the estimation of the earlier period than for the later period. This could be associated with an enhanced number of difficult cases (e.g., uncommon footprints or multiple footprints per event) during this later period.

[15] Finally, the quality of the results of the statistical downscaling is compared exemplary to those of pure dynamical downscaling against observations in Germany, as here the dataset of measurements is sufficiently large and quality-proofed unlike other countries. 39 test sites are selected according to the best data availability (Table S2). For each test site, the maximum wind gust observation (1-day- or 3-day-maxima) is compared to downscaled gusts at the nearest CCLM grid point. The scattering of the values of both downscaling methods around the optimal diagonal is similar

Table 1. $RMSE_{rel}$ in % for Cross-Validation With Training and Validation Periods[a]

Validation Period	Training Period	Sequential All Grid Points	Disordered All Grid Points	Sequential Selected Grid Points	Disordered Selected Grid Points
dates 1	dates 2	16.56	15.66	14.42	13.84
dates 2	dates 1	17.39	16.12	15.67	14.18
MIs 1	MIs 2	16.37	15.95	14.58	14.08
MIs 2	MIs 1	16.90	16.00	14.77	14.08

[a]Dates 1 are for the sequential case the first 50 days and dates 2 the 50 later ones. MIs 1 are for the sequential case the more severe events and MIs 2 the less severe ones. Selected grid points have (i) a model height under 2000 m and (ii) gust speeds reaching 20 ms^{-1} on at least on 33 of the 100 events.

(see Figure 3a for 3-day-maxima). In fact, the RMSE is slightly better for the statistical than for the dynamical downscaling (4.30 ms^{-1} vs. 4.51 ms^{-1}). This tendency is also found for the mean deviations summed over all events (Figure 3b). Thus, the results of the statistical approach are at least as good as the original CCLM values. This demonstrates the ability of the statistical downscaling to reproduce reliable gust speeds on a high-resolution grid. As Germany features a wide range of landscapes from lowland coastal areas to high alpine regions, the results are assumed to be representative for other European countries.

5. Summary and Conclusions

[16] We have introduced and validated a new statistical downscaling tool to derive wind or gust speeds on a small-scale grid over Europe using CCLM simulations as training data. ERA-Interim data and CCLM output of 100 selected windstorm events are related by a MLR model. The cross-validation shows that the statistical MLR model is able to reproduce dynamically downscaled wind signatures well, with relative errors of 10–20 % per event, and is thus a cost-efficient alternative. Larger deviations are obtained for

high altitudes [cf. also *Bernardin et al.*, 2009], for events with multiple footprints or events affecting locations rarely hit by windstorms. The windstorms associated with untypical weather situations, which are currently not well captured by the training dataset of dynamical downscaled footprints, could be improved by a larger set of events. Compared to observations, the results of this statistical approach are in Germany at least as good as the dynamical downscaling.

[17] The proposed combination of statistical and dynamical downscaling permits to apply once obtained regression coefficients to large datasets to produce a wide sample of high-resolution wind signatures. This is a clear advantage to pure dynamical downscaling that is limited by its prohibitive computational costs. On the other hand, the use of dynamical downscaled wind gusts for training the method enables to overcome the obvious handicaps of a purely statistical approach, e.g., regarding the representation of smaller scale effects like flow deviation and channeling due to orographic features. These effects are included here, provided they are represented in the RCM simulations. A better representation of such effects might be obtained by considering RCM simulations at higher spatial resolution. Compared to other statistical downscaling techniques applied on wind or
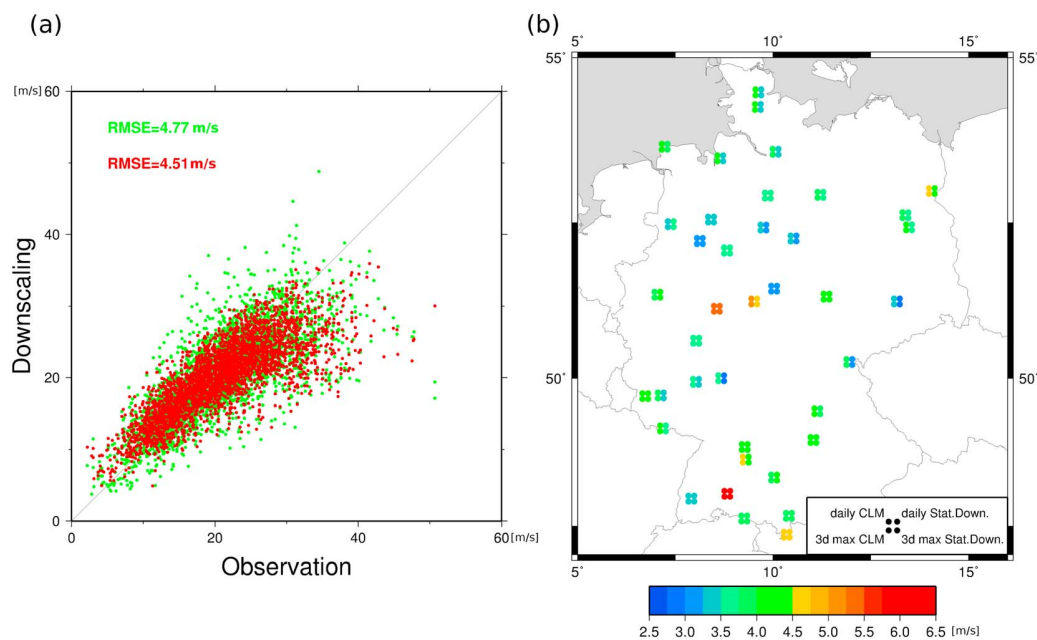
Figure 3. (a) Observations of 100 events and 39 test sites against dynamically downscaled values (green) and statistically downscaled values (red). All values are the maxima of three days. For the calculation of the RMSE $n = 390$, $\hat{x} =$ observations, and $x =$ downscaled values. (b) RMSE of dynamical downscaling (left points) and statistical downscaling (right points) for daily values (top points) and for 3-day-maxima (bottom points). The errors are calculated as for Figure 3a.

gusts, this method is quite straightforward to apply on other datasets and model domains.

[18] The intention of this study was to reproduce the dynamically downscaled wind signatures. Future investigations will focus on model output statistics to calibrate the downscaled wind signatures to observations. The probability distributions of simulations and observations may be related by probability mapping [e.g., *Haas and Born*, 2011]. This would enable to correct the footprints and apply the approach on pre-adjusted gust speeds.

References

Bernardin, F., M. Bossy, C. Chauvin, P. Drobinski, A. Rousseau, and T. Salameh (2009), Stochastic downscaling method: Application to wind refinement, *Stochastic Environ. Res. Risk Assess.*, 23, 851–859.
Born, K., P. Ludwig, and J. G. Pinto (2012), Wind gust estimation for mid-European winter storms: Towards a probabilistic view, *Tellus, Ser. A*, 64, 17471, doi:10.3402/tellusa.v64i0.17471.
Dee, D. P., et al. (2011), The ERA-Interim reanalysis: Configuration and performance of the data assimilation system, *Q. J. R. Meteorol. Soc.*, 137, 553–597.
Della-Marta, P. M., and J. G. Pinto (2009), Statistical uncertainty of changes in winter storms over the North Atlantic and Europe in an ensemble of transient climate simulations, *Geophys. Res. Lett.*, 36, L14703, doi:10.1029/2009GL038557.
Della-Marta, P. M., M. A. Liniger, C. Appenzeller, D. N. Bresch, P. Köllner-Heck, and V. Muccione (2010), Improved estimates of the European winter windstorm climate and the risk of reinsurance loss using climate model data, *J. Appl. Meteorol. Climatol.*, 49, 2092–2120.
De Rooy, W. C., and K. Kok (2004), A combined physical-statistical approach for the downscaling of model wind speed, *Weather Forecast.*, 19, 485–495.
Fink, A. H., T. Brücher, V. Ermert, A. Krüger, and J. G. Pinto (2009), The European storm Kyrill in January 2007: Synoptic evolution, meteorological impacts and some considerations with respect to climate change, *Nat. Hazards Earth Syst. Sci.*, 9, 405–423.
Haas, R., and K. Born (2011), Probabilistic downscaling of precipitation data in a subtropical mountain area: A two-step approach, *Nonlinear Processes Geophys.*, 18, 223–234.
Kjellström, E., G. Nikulin, U. Hansson, G. Strandberg, and A. Ullerstig (2011), 21st century changes in the European climate: Uncertainties derived from an ensemble of regional climate model simulations, *Tellus, Ser. A*, 63, 24–40.
Klawa, M., and U. Ulbrich (2003), A model for the estimation of storm losses and the identification of severe winter storms in Germany, *Nat. Hazards Earth Syst. Sci.*, 3, 725–732.
Maraun, D., et al. (2010), Precipitation downscaling under climate change: Recent developments to bridge the gap between dynamical models and the end user, *Rev. Geophys.*, 48, RG3003, doi:10.1029/2009RG000314.
Pinto, J. G., M. K. Karremann, K. Born, P. M. Della-Marta, and M. Klawa (2012), Loss potentials associated with European windstorms under future climate conditions, *Clim. Res.*, 54, 1–20.
Pryor, S. C., J. T. Schoof, and R. J. Barthelmie (2005), Empirical downscaling of wind speed probability distributions, *J. Geophys. Res.*, 110, D19109, doi:10.1029/2005JD005899.
Rockel, B., A. Will, and A. Hense (2008), The regional climate model COSMO-CLM (CCLM), *Meteorol. Z.*, 17, 347–348.
Schulz, J. P. (2008), Revision of the turbulent gust diagnostics in the COSMO model, *COSMO Newsl.*, 8, 17–22.
Schwierz, C., P. Köllner-Heck, E. Zenklusen Mutter, D. N. Bresch, P.-L. Vidale, M. Wild, and C. Schär (2010), Modelling European winter wind storm losses in current and future climate, *Clim. Change*, 101, 485–514.

Supplementary material
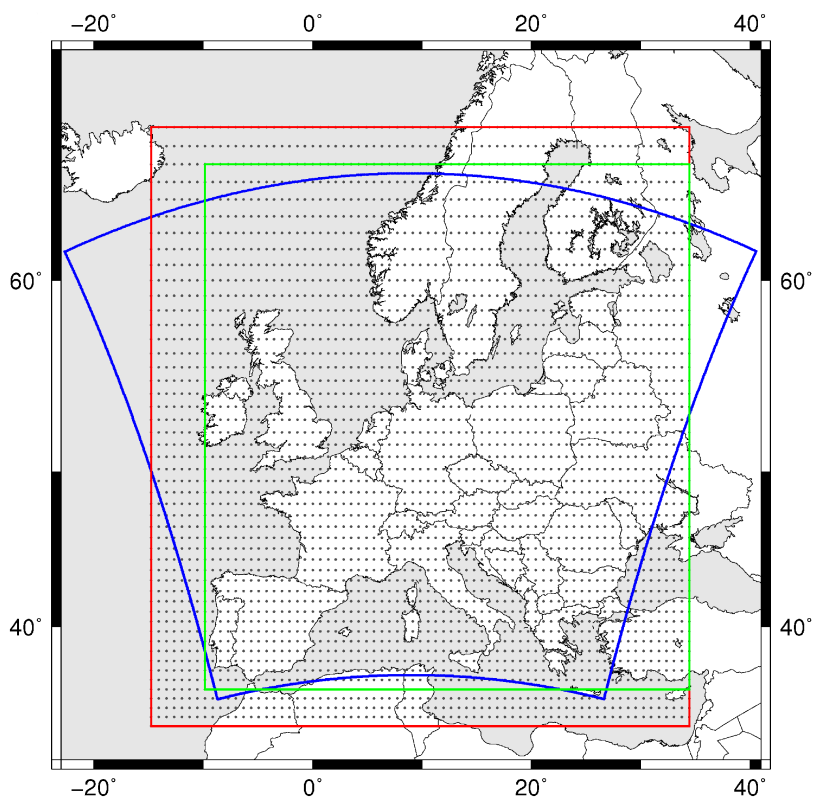
Figure S1: Investigation area. CCLM is simulated with 0.0625° resolution within blue area; ERA-Interim data is used with 0.7° resolution for the statistical downscaling within red area, and for MI calculation within green area.

Table S1: 100 Days with highest *MI* between 1989 and 2010 in chronological order. MI is computed using daily maximum of ERA-Interim surface wind speeds for each grid point. The cubic exceedances of the local 98th percentile are aggregated over land within green area in Figure 1a (-9.8438°E to 34.4531°E, 35.4385°N to 64.912°N).

Date	MI	Rank	Date	MI	Rank
19890115	284.1512	43	19990205	448.1312	13
19890129	224.8765	74	19991201	293.425	41
19890215	222.4623	79	19991203	233.2323	64
19890225	414.3149	16	19991204	298.1472	39
19890226	533.812	5	19991225	282.9562	45
19891217	226.6007	70	19991226	376.3548	20
19900125	400.3774	18	19991227	249.6054	56

19900208	352.1099	24	19991228	339.1889	31
19900212	219.3445	87	20000118	219.596	84
19900214	231.6447	65	20000121	225.3398	73
19900226	647.7467	2	20000129	220.7681	81
19900227	812.5004	1	20000130	427.668	14
19900228	468.9158	10	20000131	222.6852	77
19900301	426.4633	15	20000303	279.1825	46
19900306	224.2552	75	20000406	238.1307	60
19900310	264.1957	51	20001030	335.1147	32
19920101	331.9634	34	20001106	211.2333	93
19920117	343.8363	27	20010605	207.2603	99
19920224	256.163	53	20011115	458.3886	11
19920313	292.8794	42	20020129	293.883	40
19920906	326.7523	36	20020222	266.8806	49
19921126	208.9968	95	20020223	216.4567	88
19921202	211.3982	92	20020307	251.2844	54
19921219	241.972	59	20021027	342.3214	29
19930114	310.9885	37	20021028	450.3947	12
19930117	234.2697	62	20040321	348.731	25
19930118	226.3903	71	20041114	219.5183	85
19930122	369.4093	21	20041119	214.6404	90
19930123	363.7773	23	20041222	229.9375	68
19930124	506.141	7	20050108	220.9854	80
19930125	283.432	44	20050109	250.7358	55
19930319	242.7713	58	20050213	231.2205	67
19931209	339.8903	30	20070111	329.6783	35
19931220	220.5499	82	20070112	219.436	86
19940128	411.3488	17	20070118	584.8074	3
19940314	383.7234	19	20070119	491.8994	8
19940324	272.2186	47	20070129	344.4809	26
19940401	258.6016	52	20070320	231.6341	66
19950122	209.8251	94	20070405	235.7918	61
19950123	488.5009	9	20080127	207.3255	98
19950127	227.775	69	20080128	222.4852	78
19950328	302.8398	38	20080131	206.7533	100
19950513	226.0232	72	20080223	211.5456	91
19970225	271.1239	48	20080301	574.3024	4
19970327	246.0028	57	20080302	332.8554	33
19970407	216.0787	89	20080305	208.3307	96
19970411	514.6126	6	20081123	219.6692	83
19981024	223.8985	76	20090124	343.356	28
19981028	366.3806	22	20091013	207.9343	97
19990204	233.9155	63	20100228	264.3112	50

Table S3: 39 test sites in Germany providing three gust observations for all events (day of the highest MI plus one day before and after).

WMO No.	Name	Longitude	Latitude	Height
102910	Angermünde	13.9931	53.0331	54
104600	Artern	11.2931	51.3756	164
103820	Berlin Tegel	13.3108	52.5656	36
103840	Berlin Tempelhof	13.4039	52.4686	48
103480	Braunschweig	10.4486	52.2928	81
101290	Bremerhaven	8.5772	53.5347	7
106150	Deuselbach	7.0556	49.7631	481
103210	Diepholz	8.3431	52.5897	39
104100	Essen	6.9686	51.4056	150
106370	Frankfurt/Main	8.5986	50.0464	112
108030	Freiburg	7.8353	48.0242	236
106280	Geisenheim	7.9547	49.985	110
104440	Göttingen	9.9528	51.5017	167
101470	Hamburg Fuhlsbüttel	9.99	53.635	11
103380	Hannover	9.6797	52.4658	55
106850	Hof	11.8775	50.3133	565
100380	Hohn	9.5394	54.3128	10
104270	Kahler Asten	8.49	51.1817	839
104380	Kassel	9.4436	51.2978	231
109460	Kempten	10.3364	47.7244	705
108180	Klippeneck	8.7558	48.1064	973
109290	Konstanz	9.1911	47.6783	443
103050	Lingen	7.3089	52.5194	22
102530	Lüchow	11.1392	52.9739	17
105260	Bad Marienberg	7.9597	50.6633	547
101130	Norderney	7.1525	53.7139	11
107630	Nürnberg	11.0569	49.5044	314
109480	Oberstdorf	10.2769	47.3989	806
104800	Oschatz	13.0947	51.2972	150
103170	Osnabrück	8.0544	52.2572	95
107080	Saarbrücken Ensheim	7.1083	49.2142	320
103250	Bad Salzuflen	8.7531	52.1056	135
100265	Schleswig	9.5494	54.5289	43
102350	Soltau	9.7942	52.9619	76
107390	Stuttgart Schnarrenberg	9.2011	48.8292	314
107380	Stuttgart Echterdingen	9.2253	48.6892	371
106090	Trier Petrisberg	6.6592	49.7492	265
108380	Ulm	9.9539	48.3847	567
107610	Weißenburg	10.9617	49.0203	422

3 Improvement of footprints

Published journal article:

Haas, R, J. G. Pinto, and K. Born (2014), Can dynamically downscaled windstorm footprints be improved by observations through a probabilistic approach? *Journal of Geophysical Research*, 119, 713–725, doi: 10.1002/2013JD020882.

RESEARCH ARTICLE

Key Points:
- We introduced an approach to adjust RCM windstorm footprints to observations
- The method is generally able to enhance the results of dynamical downscaling
- The application of the approach produces better results for wind than for gusts

Supporting Information:
- Readme
- Figure S1
- Figure S2
- Figure S3
- Figure S4

Correspondence to:
R. Haas,
rhaas@meteo.uni-koeln.de

Can dynamically downscaled windstorm footprints be improved by observations through a probabilistic approach?

Rabea Haas[1], Joaquim G. Pinto[1,2], and Kai Born[1,3]

[1]Institute for Geophysics and Meteorology, University of Cologne, Cologne, Germany, [2]Department of Meteorology, University of Reading, Reading, UK, [3]TÜV Rheinland Energie und Umwelt GmbH, Cologne, Germany

Abstract Windstorms are a main feature of the European climate and exert strong socioeconomic impacts. Large effort has been made in developing and enhancing models to simulate the intensification of windstorms, resulting footprints, and associated impacts. Simulated wind or gust speeds usually differ from observations, as regional climate models have biases and cannot capture all local effects. An approach to adjust regional climate model (RCM) simulations of wind and wind gust toward observations is introduced. For this purpose, 100 windstorms are selected and observations of 173 (111) test sites of the German Weather Service are considered for wind (gust) speed. Theoretical Weibull distributions are fitted to observed and simulated wind and gust speeds, and the distribution parameters of the observations are interpolated onto the RCM computational grid. A probability mapping approach is applied to relate the distributions and to correct the modeled footprints. The results are not only achieved for single test sites but for an area-wide regular grid. The approach is validated using root-mean-square errors on event and site basis, documenting that the method is generally able to adjust the RCM output toward observations. For gust speeds, an improvement on 88 of 100 events and at about 64% of the test sites is reached. For wind, 99 of 100 improved events and ~84% improved sites can be obtained. This gives confidence on the potential of the introduced approach for many applications, in particular those considering wind data.

1. Introduction

In recent decades, global circulation models (GCMs) have become commonly used tools to understand physical processes in the climate system [e.g., *Meehl et al.*, 2007]. They allow for an assessment of possible representations of past, present, and future climate conditions for different spatial scales and a wide range of temporal scales. However, due to their comparatively coarse resolution, GCMs show deficiencies in representing regional and local climate conditions adequately. To overcome this shortcoming, several downscaling techniques have been developed, which can be roughly grouped into dynamical and statistical methods, or a combination of both (for review see, e.g., *Giorgi and Mearns* [1991], *Hewitson and Crane* [1996], *Wilby and Wigley* [1997], and *Maraun et al.* [2010]). For statistical downscaling, large-scale variables (predictors) are related to local variables (predictands) via statistical transfer functions [e.g., *Wilby et al.*, 1998; *Hanssen-Bauer et al.*, 2005]. For dynamical downscaling, large-scale reanalyses or GCM data are combined with regional climate models (RCMs) resulting in high-resolution simulations (5–50 km) over a region of interest [*Meehl et al.*, 2007; *Christensen et al.*, 2007]. Statistical-dynamical downscaling usually combines a weather-typing approach with regional climate model (RCM) modeling [e.g., *Fuentes and Heimann*, 2000; *Pinto et al.*, 2010]. These techniques can be used both for the purpose of numerical weather prediction and to determine the response of climate change on local- and regional-scale variables.

A large suite of methods has been developed in recent decades, particularly focusing on temperature and precipitation [e.g., *Wilby and Wigley*, 1997]. Less attention has been paid to other variables like 10 m wind speed and—even less often—to wind gusts, although 10 m wind speed is one of the standard meteorological variables reported by weather stations [*World Meteorological Organization*, 2008]. Research on wind speeds and wind gusts at regional and local scales has focused, e.g., on the development and enhancement of methodologies to estimate gust speeds from wind observations [e.g., *Wieringa*, 1973; *Verkaik*, 2000; *De Rooy and Kok*, 2004]. Not only absolute values but also probability distributions of wind speeds can be estimated by empirical downscaling [e.g., *Pryor et al.*, 2005; *Pryor and Barthelmie*, 2010]. Further, modeling approaches including wind

gust parameterizations have been developed to obtain wind gust speeds and windstorm footprints comparable to observations [e.g., *Brasseur*, 2001; *Goyette et al.*, 2001; *Ágústsson and Ólafsson*, 2009; *Pinto et al.*, 2009; *Born et al.*, 2012]. However, dynamically downscaled wind or gust speeds do not necessarily match to observations perfectly due to local-scale factors that can affect the measurements and which cannot be captured by the RCMs [e.g., *Goyette et al.*, 2003; *Born et al.*, 2012].

To bridge this gap, methods to adjust the RCM output toward local observations have been developed. The statistical estimation of the local distribution of a climate variable, when only its large-scale value is given, is known as the climate inversion problem [*Kim et al.*, 1984]. Classical approaches usually correct model output at test site locations and were first used in the context of weather forecasts [*Glahn and Lowry*, 1972]. With this aim, the basic methodologies are the "perfect prog" approach and the Model Output Statistics (MOS) approach, which differ in the way of establishing the relationships between the variables [*Klein and Glahn*, 1974]. In the perfect prog approach, the relationship is built between observed predictands and predictors, while in the MOS approach it is built between the predictands and numerical model output. In both approaches, the resulting statistical function is applied to the simulated output.

Although approaches have been developed to obtain results on a regular grid using MOS [e.g., *Glahn et al.*, 2009], most MOS applications on wind aim for information only at specific locations [e.g., *Thorarinsdottir and Gneiting*, 2010]. By contrast, this study aims at correcting RCM output on a high-resolution grid by probability mapping. The method is applied not only for grid points where observations are available but also for all grid points in the investigation area. Here we focus on Germany, where the German Weather Service provided a dense network of wind and gust measurements. With this aim, the following three-step procedure is proposed: First, theoretical distributions are fitted to observed and simulated wind and gust speeds. Second, the distribution parameters of the observations are interpolated onto the RCM grid. Finally, the distributions of RCM variables are compared to interpolated distributions of observations by probability mapping. This enables an adjustment of the simulated wind and gust speeds toward the measurements. The results are evaluated using standard root-mean-square error (RMSE) skill scores, which also enable the interpretation of the effectiveness of the procedure for wind and gust speeds event based (i.e., errors averaged over all sites for each event) and site based (i.e., errors averaged over all events for each site).

Details on data sources and preparation are given in section 2. In section 3 methods to fit and to interpolate the data, as well as to validate the results, are explained. This section also includes an introduction to circulation weather types, which are used to analyze the potential influence of large-scale atmospheric circulation on the methodology. The results are presented in section 4, in which a difference is made between results on events and results at test sites. The paper finishes with discussion and conclusion.

2. Data

2.1. Selection of Events

The basic data set is a sample of 100 windstorm events with a strong impact on Europe as selected in *Haas and Pinto* [2012]. The selection of these storms resulted from the calculation of a loss-related meteorological index (MI) after *Pinto et al.* [2012]. The index is computed using ERA-Interim reanalysis data [*Dee et al.*, 2011] with a resolution of T225 (0.75°× 0.75°). Six-hourly instantaneous wind speeds over Europe (−14.7657°E to 34.4531°E, 32.6315°N to 66.3155°N) are considered. At each grid point, the cubic exceedance of the local 98th gust percentile is calculated (following *Klawa and Ulbrich* [2003]) and afterward the sum over all land grid points within this area is built. All days during the period 1989 to 2010 are ranked according to the MI. Hundred days with the highest MI are selected as set of events, which are represented by 3 day periods around the event. The detailed event list can be found in Table S1 (supporting information). Although the focus of the present study lies only on Germany, the selection of events was kept on a pan-European basis (a) for consistency with *Haas and Pinto* [2012] and (b) as the ultimate aim is the application of the method on the larger investigation area. As there is a very strong overlapping of the top-ranking storms between Europe and Germany (78% for Top 50 and 61% for Top 100), the results would be comparable if the event selection was performed for Germany alone. This results from the fact that most of the selected 100 storms also affect Germany, due to its geographical location in the center of the chosen Europe domain [see *Haas and Pinto*, 2012, Figure S1].
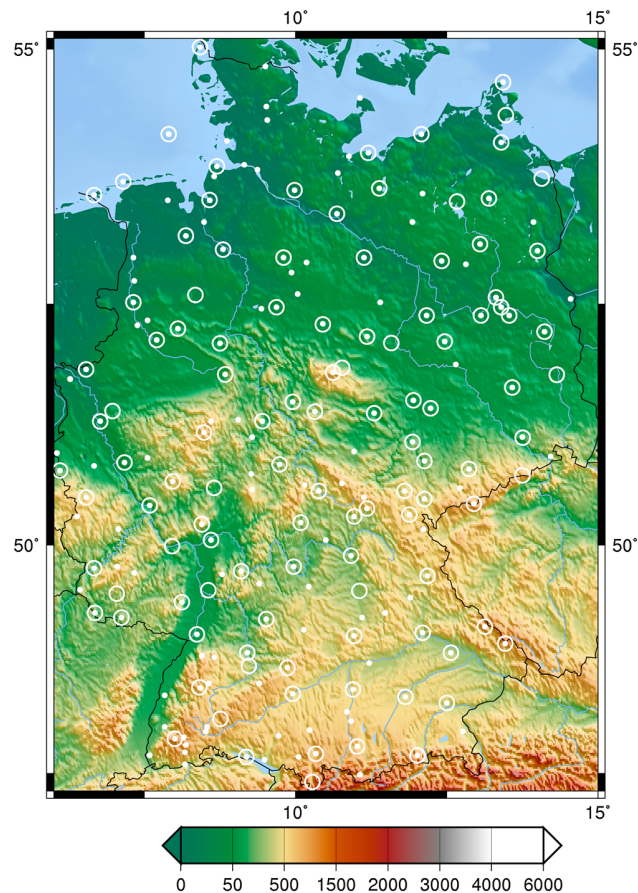
Figure 1. Orography of Germany and locations of test sites, with circles denoting gust measurements and points denoting wind measurements.

2.2. Regional Climate Model

The dynamically downscaled windstorm footprints used in this study are simulations of the COSMO-CLM (RCM of the Consortium for Small-scale Modeling in Climate Mode version 4.8., hereafter CCLM [*Rockel et al.*, 2008]). ERA-Interim reanalysis data are also used as initial and boundary conditions for the simulations of historical storms. By a two-step nesting approach, a resolution of 7 km (0.0625°) is reached. Gust speeds are computed by an approach using friction velocity as estimator for turbulence [*Schulz*, 2008]. A comparison with other wind gust estimation approaches and observations can be found in *Born et al.* [2012]. Both wind and gust speeds are available as RCM output on an hourly basis. Wind speeds are instantaneous values on the hour, while gust speeds are the maxima of all model time steps within the last hour. For the purpose of this study, daily maxima of both parameters are extracted for each RCM grid point. As region of interest, we chose all grid points within the area 5.5°E to 15°E and 47.2°N to 55.1°N (domain including Germany, Figure 1).

2.3. Observations

Wind and gust speed measurements of the observational network of the German Weather Service (DWD) are used. Gust speeds are available as daily maximum and wind speed as hourly mean values, which are aggregated to daily maximum wind speeds if more than 12-hourly values per day are reported. The DWD provides 434 sites measuring wind speed and 299 sites measuring gust speed. However, not all of these sites deliver observations for all of the selected events. For our analyses, 228 sites reported a sufficient amount of wind speed data and 151 sites of gust speed data (reports at minimum 70 of the 100 events). In this context, at least one of the 3 days should have an observation to count the event. Selected test sites should be representative for the surrounding area. Thus, in a second selection step, sites with large outliers differing clearly from neighboring sites are removed resulting in a set of 173 and 111 sites for wind and gusts, respectively

(Figure 1). There is an overlap of 94 test sites measuring both wind and gust speeds (marked with dots and circles in Figure 1). Outliers in observations may originate from steep gradients between two nearby test sites (e.g., the sites around the mountain Brocken; 10.62°E, 51.8°N) or at locations influenced by, e.g., channeling effects or in coastal areas. A distinct increase of the RMSE (>5%) is identified when applying the MOS on the first selection of sites (228 and 151 for wind and gust, respectively).

3. Methodology

In this section, the used methods for data preparation and evaluation are presented. First, the wind data are fitted by theoretical Weibull distributions to determine the parameters. The estimated parameters of observations are interpolated to the RCM grid and related to the parameters of the simulations by a probability mapping. Finally, the results are validated by RMSEs and interpreted using circulation weather types.

3.1. Weibull Fit

For the following calculations, theoretical Weibull distributions are fitted to observed and simulated wind and gust speeds. We consider observations and simulations of the selected events (3 days each, at maximum 300 values in total) to fit the distribution parameters. Several previous studies on wind suggest adopting the Weibull distribution for this purpose (following *Justus et al.* [1978]). The scale parameter α and the shape parameter β can be easily estimated using the cumulative distribution function (CDF) form

$$F(x) = 1 - \exp\left(-\alpha x^{\beta}\right) \tag{1}$$

by replacing α and β with slope m and axis intercept b of a regression line through the wind and gust speeds of each test site or grid point:

$$\ln(-\ln(1 - F(x))) = \ln(\alpha) + \beta \cdot \ln(x) = b + m \cdot \ln(x) \tag{2}$$

Four pairs of parameters are estimated: One pair for wind observations ($m_{Obs,Wind}$, $b_{Obs,Wind}$), one pair for gust observations ($m_{Obs,Gust}$, $b_{Obs,Gust}$), one pair for wind simulations ($m_{Sim,Wind}$, $b_{Sim,Wind}$), and one pair for gust simulations ($m_{Sim,Gust}$, $b_{Sim,Gust}$). The correlation between the empirical values and the values resulting from the regression line is on average very high (0.98). Therefore, the uncertainty of the fit is negligible and not further considered. The small deviation of the observations and simulations from the regression line confirms the Weibull distribution to be an appropriate fit. Figure S1 shows an example of transformed wind and gust observations and the regression lines for site Bamberg (Southern Germany).

3.2. Interpolation

To compare observations and simulations, distribution parameters of observations are interpolated to CCLM grid points. Here we use distance-weighted interpolation taking into account the nearest 20 sites to each grid point. The choice of 20 sites was found to be a reasonable compromise between regions with high and low station density. Each of the 20 sites is weighted by a factor w_i, which is calculated using the longitudinal and latitudinal distances in kilometers ($d\text{lon}_i$ and $d\text{lat}_i$) between grid point and sites:

$$w_i = \frac{\exp\left(-\dfrac{\sqrt{d\text{lon}_i^2 + d\text{lat}_i^2}}{c}\right)}{\sum_{j=1}^{20} \exp\left(-\dfrac{\sqrt{d\text{lon}_j^2 + d\text{lat}_j^2}}{c}\right)} \tag{3}$$

Here we use a correlation length c of 15 km. This radius has been tested empirically and delivers a good compromise between extreme smoothing and too much details resulting in a patchy interpolated field. The parameters for wind observations ($m_{Obs,Wind}$, $b_{Obs,Wind}$) and for gust observations ($m_{Obs,Gust}$, $b_{Obs,Gust}$) estimated as stated in the previous section are interpolated using equation (3). In the following, $m_{Obs,Wind}$, $b_{Obs,Wind}$, $m_{Obs,Gust}$, and $b_{Obs,Gust}$ denote the interpolated parameters, which are needed for the probability mapping.

3.3. Probability Mapping

To adjust the simulated wind and gust speeds (x_{Sim}) to observations (x_{Obs}), a probability mapping is carried out following the quantile-matching method described in *Michelangeli et al.* [2009]. A transfer function is obtained by equalizing the theoretical distributions of observations F_{Obs} and simulations F_{Sim}:

$$F_{Obs}(x_{Obs}) = F_{Sim}(x_{Sim}) \tag{4}$$

As the corrected simulations of wind or gust speeds $x_{Sim,corr}$ are estimations (denoted with the hat) of the observations x_{Obs}, they can be calculated using the inverse distribution of the observations F_{Obs}^{-1} and the distribution of simulations F_{Sim}:

$$x_{Sim,corr} = \widehat{x_{Obs}} = f_{Obs}^{-1}(F_{Sim}(x_{Sim})) = \left(\frac{\ln(1 - (1 - \exp(-\exp(b_{Sim} \cdot x^{m_{Sim}}))))}{-\exp(b_{Obs})} \right)^{\frac{1}{m_{Obs}}} \tag{5}$$

With m_{Obs}, m_{Sim}, b_{Obs}, and b_{Sim} being the estimated slope and axis intercept of the observations and simulations, respectively. The equation can be used for the correction of wind and gust speeds by inserting the according parameters m (slope) and b (intercept).

3.4. Validation

To validate the approach, we compare observed wind and gust speeds x_{Obs} of each event at each site to the uncorrected and corrected simulations x_{Sim} and $x_{Sim,corr}$ of the nearest grid point next to this site. The squared deviations $(x_{Sim} - x_{Obs})^2$ and $(x_{Sim,corr} - x_{Obs})^2$ are each averaged over all events or over all test sites to the root-mean-square error (RMSE) and are normalized with the according means of the observations x_{Obs}. Thus, the relative RMSEs that we use for the following analyses are

$$\text{RMSE}_{CCLM} = \frac{\sqrt{\frac{\sum_{i=1}^{n}(x_{Sim} - x_{Obs})^2}{n}}}{\frac{\sum_{i=1}^{n} x_{Obs}}{n}} \tag{6a}$$

$$\text{RMSE}_{MOS} = \frac{\sqrt{\frac{\sum_{i=1}^{n}(x_{Sim,corr} - x_{Obs})^2}{n}}}{\frac{\sum_{i=1}^{n} x_{Obs}}{n}} \tag{6b}$$

Here the number of stations is $n = 173$ for wind speeds and $n = 111$ for gust speeds to evaluate the RMSE score with respect to events. For an evaluation per test site, the score is calculated using n = number of days with observations (with a maximum of 300, 3 days times 100 events).

3.5. Circulation Weather Types

In order to assess the possible influence of large-scale atmospheric circulation on the performance of the methodology, circulation weather types (CWTs) after *Jones et al.* [1993] are calculated. This method is based on the manual Lamb weather types, which were originally used to classify circulation patterns over the British Isles [*Lamb*, 1972; *Jenkinson and Collinson*, 1977], and has been used for many climate variability and climate change studies [e.g., *Buishand and Brandsma*, 1997; *Trigo and DaCamara*, 2000; *Jones et al.*, 2012]. CWTs are determined from geostrophic wind direction and speed using large-scale data of mean sea level pressure (MSLP) at a central point and of 16 surrounding grid points (Figure S2). With this aim, ERA-Interim reanalysis data were interpolated to a 2.5° × 2.5° grid. A central point over Germany (50°N; 10°E) is selected for computations, and the 12 UTC MSLP field is used as representative for the large-scale atmospheric circulation of each day. Following *Jones et al.* [1993], westerly flow, southerly flow, resultant flow, westerly shear vorticity, southerly shear vorticity, and total shear vorticity are determined. Therewith all days are grouped into eight directional types defined as 45° sectors (Figure S3): northeast (NE), east (E), southeast (SE), south (S), southwest (SW), west (W), northwest (NW), and north (N). Additionally, there are two circulation types: cyclonic (C) and anticyclonic (A). If neither rotational nor directional flow dominates, the day is attributed a hybrid CWT (e.g., anticyclonic west). In addition, we also consider the resultant flow parameter *f* (a measure of
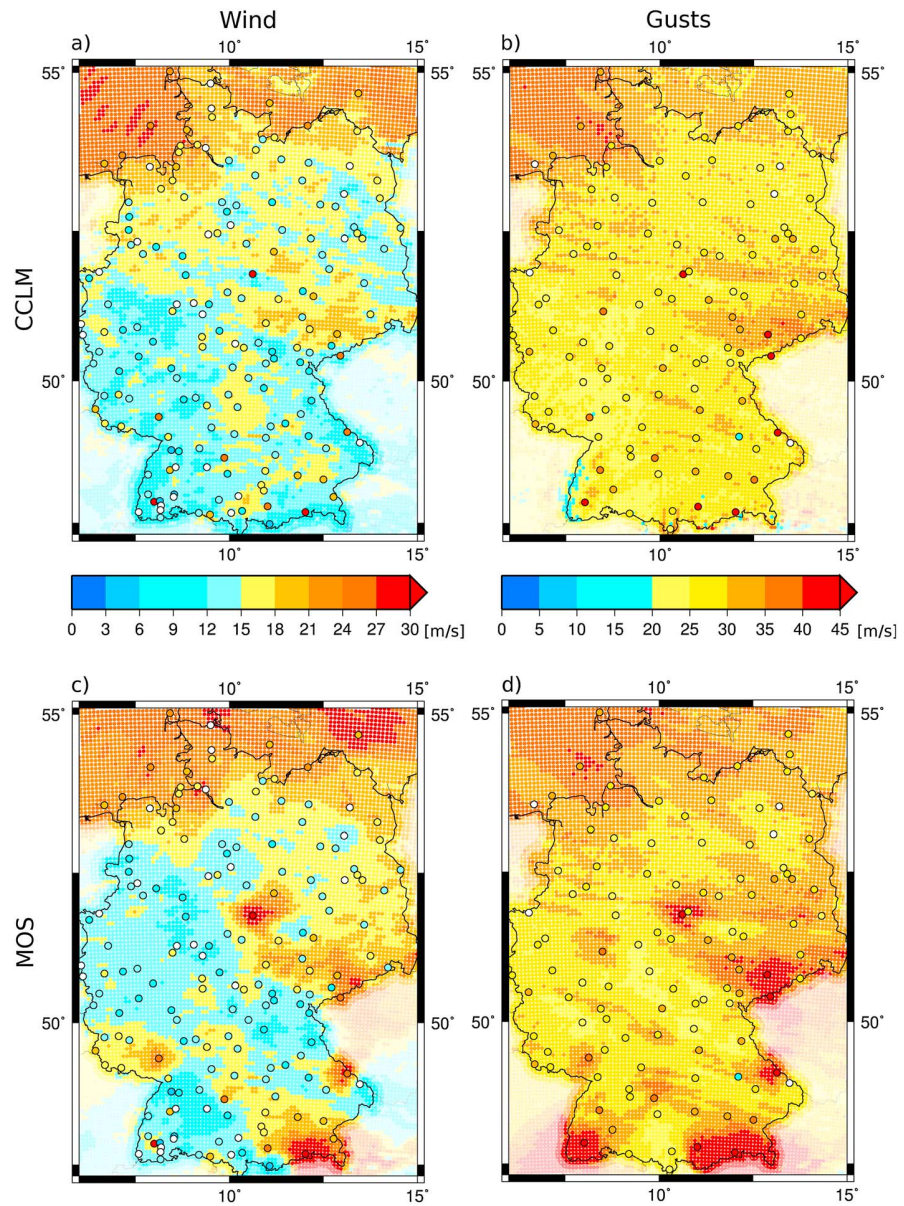
Figure 2. (a and b) Example of originally simulated and (c and d) MOS-corrected footprints. One day signatures of wind (Figures 2a and 2c) and gust speeds (Figures 2b and 2d) for storm Emma (1 March 2008). The black-rimmed dots are the selected test sites, marked in white for missing observations on this date. Neighboring states of Germany are faded out, as no test sites are used in these regions.

intensity of geostrophic wind, calculated from westerly and southerly flow), and its potential influence on the performance of the MOS approach.

4. Results

4.1. Results on Events

In this section, wind and wind gusts derived by the RCM are compared to observations. In particular, their potential improvement by the application of MOS is investigated. The simulated wind and gust speeds are not always congruent with observations, as exemplary shown in Figures 2a and 2b for windstorm Emma (29 February to 2 March 2008). It is apparent that some test sites are overestimated (mainly costal test sites), whereas others are underestimated (mainly at higher altitudes). To reduce this mismatch, the simulated values at the CCLM grid points are corrected according to the transformation equation introduced in section 3.3. After the correction, the
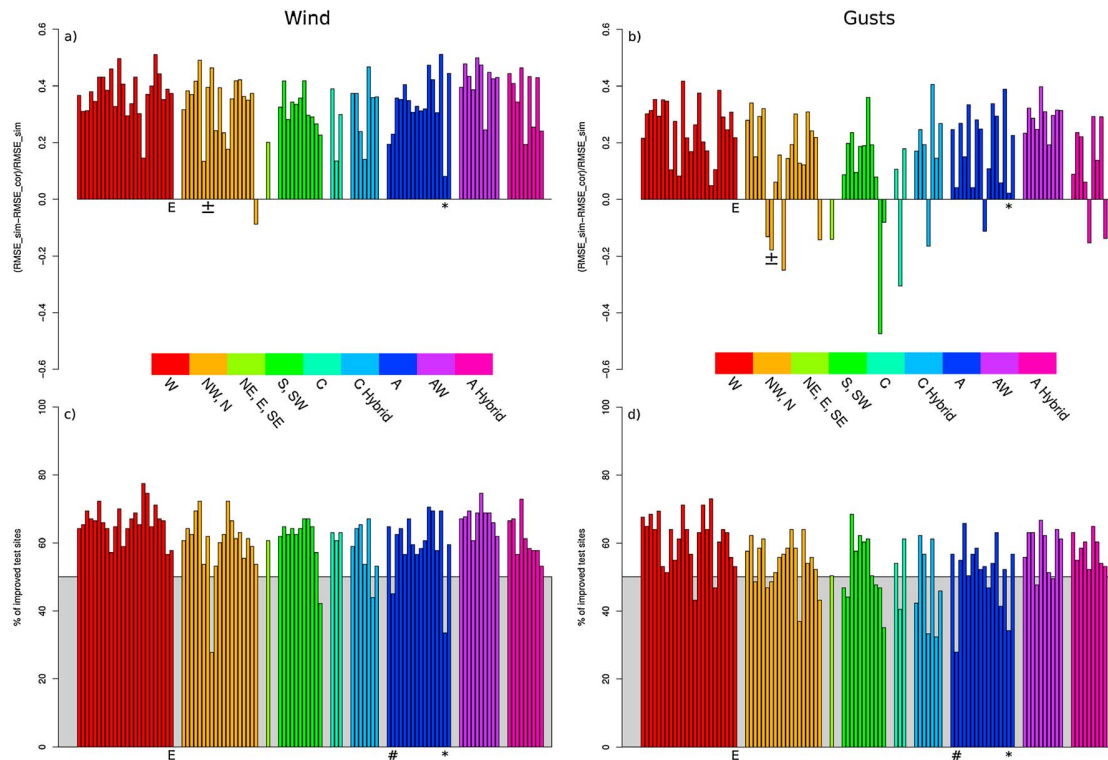
Figure 3. Difference between RMSE$_{CCLM}$ and RMSE$_{MOS}$ for (a) wind and (b) gusts on event basis, with positive values denoting an improvement (decrease of RMSE). Asterisk (5 April 2007) is an example for low improvement without worsening; plus-minus sign (28 March 1995) denotes an example for diverging behavior for wind and gust speeds. Percentage of improved test sites per event regarding (c) wind and (d) gusts: sharp sign (29 January 1989) and asterisk (5 April 2007) denote examples for little number of improved test sites for wind and gust speeds. Bars outside the grey box denote events with more than 50% improved test sites. Events are grouped in CWTs and in chronological order within these groups. Windstorm Emma (1 March 2008) is marked with "E."

spatial patterns of the resulting footprints are in better agreement with observations (Figures 2c and 2d) than the direct RCM output (Figures 2a and 2b). Nevertheless, a small worsening is identified for certain areas, meaning that the MOS correction leads to values further away from observations (overcorrection). This can, e.g., be the case if the original CCLM simulations are already in a very good agreement with the observations.

To give an objective measure of this improvement, the observations are compared to simulations. For each test site, the corresponding nearest neighbor RCM grid point is considered. The deviations at all test sites are summed to calculate two RMSE per event, one for the original simulations (RMSE$_{CCLM}$) and one for the corrected simulations (RMSE$_{MOS}$). For wind speed, the RMSE can be improved on 99 of the 100 events (RMSE$_{CCLM}$ > RMSE$_{MOS}$, Figure 3a). The analysis with gust speeds evidences an improvement on 88 events (Figure 3b). The example of Emma shows a good improvement for both parameters, i.e., the RMSE$_{CCLM}$ summed over all test sites is reduced by the application of the MOS (marked with E in Figure 3). For other events, the approach does not impair the footprints and also does not affect both wind and gust considerably as, e.g., event on 5 April 2007 (denoted with asterisk in Figures 3a and 3b). This small improvement results from quite large event-specific RMSE$_{CCLM}$ (0.4751 for wind and 0.2122 for gusts) that cannot be improved significantly. Compared to Emma, this windstorm produced weaker wind gusts over Germany and caused little damage. This leads to the assumption that the correction may be more effective for higher wind and gust speeds. On the other hand, there are also events, which show a mixed response: while wind speeds are explicitly improved, gust speeds experience a worsening (e.g., event on 28 March 1995, denoted with plus-minus sign in Figures 3a and 3b). As the simulated gusts are already quite good compared to wind speeds, there is a limited potential for improvement, but the risk of an overcorrection. This shows that the change of the RMSE of wind speeds and gusts is not always in agreement.

The influence of the large-scale atmospheric flow conditions on the performance of the methodology is analyzed by assigning CWTs to the 100 windstorm events. With this aim, the CWT type attributed to the middle day of each 3 day period per event is considered. The bars in Figure 3 are colored according to the CWTs, with infrequent types merged together into groups (compare Table 1). In general terms, the improvement due

Table 1. $RMSE_{CCLM}$ and $RMSE_{MOS}$ per CWT[a]

| CWT | Number of Days | $RMSE_{CCLM}$ | | $RMSE_{MOS}$ | | $(RMSE_{CCLM} - RMSE_{MOS})/RMSE_{CCLM}$ | |
		Wind	Gust	Wind	Gust	Wind	Gust
West	71	0.3664	0.2580	0.2379	0.2022	**0.3507**	**0.2164**
Northwest, Nord	50	0.3782	0.2549	0.2509	0.2315	0.3366	0.0918
Northeast, east, southeast	3	0.4440	0.2737	0.3395	0.2691	<u>0.2354</u>	<u>0.0168</u>
South, southwest	28	0.3948	0.2603	0.2632	0.2233	0.3335	0.1419
Cyclonic	11	0.4490	0.2986	0.3530	0.3032	<u>0.2137</u>	<u>−0.0157</u>
Cyclonic hybrid	17	0.4303	0.3071	0.3285	0.2910	<u>0.2365</u>	<u>0.0523</u>
Anticyclonic	55	0.4389	0.2882	0.3073	0.2554	0.2999	0.1136
Anticyclonic west	35	0.3727	0.2420	0.2295	0.1849	**0.3843**	**0.2357**
Anticyclonic hybrid (excluding anticyclonic west)	30	0.3896	0.2384	0.2448	0.2018	**0.3715**	0.1537
All	300	0.3930	0.2661	0.2620	0.2252	0.3333	0.1535

[a]Outstanding low and large improvements for wind (below 25% and above 35%) and gusts (below 10% and above 20%) are underlined and marked in bold, respectively.

to MOS is somewhat dependent on the CWT. Exceptions are events occurring during infrequent CWTs (NE/E/S; C; C hybrid), for which the improvement of the RMSE is small in the case of wind and gust speed. These improvements below 10% for gusts and 25% for wind are marked as underlined values in Table 1. On the other hand, the best improvements (>20%, bold values in Table 1) for gust speeds are found for west or anticyclonic west CWT events. This is in line with the above statement that the MOS has a stronger influence on larger gust speeds, as intense windstorms are often associated with westerly weather situations [*Donat et al.*, 2010]. The same CWTs contribute to the best RMSE improvements regarding wind speed, with the anticyclonic hybrid type additionally featuring improvements above 35%. The overall view points to a better behavior of the methodology for wind than for gusts with an averaged enhancement of ~33% and ~15%, respectively.

In addition to the RMSE, Figures 3c and 3d depict the percentage of improved test sites per event. The percentage of improved test sites for wind speed (Figure 3c) is generally higher than for gust speeds (Figure 3d). For wind speed, almost all events (95 of 100) show an improvement for more than 50% of the test sites. On the other hand, the application of the MOS on gust speeds does not deliver such clear results (77 of 100 events above 50%). For some events, the percentage of improved test sides falls below the 50% line in both data sets (e.g., 29 January 1989 or 5 April 2007; marked with sharp sign and asterisk in Figures 3c and 3d). These events are characterized by comparatively weak wind and gust speeds over Germany, so this finding corroborates the idea that the applied MOS improvement performs better on stronger events.

4.2. Results at Test Sites

We now consider how far the MOS application leads to an improvement of the results at individual test sites. When summing up the deviations over all events, for 145 of the 173 test sites (83.82%), $RMSE_{MOS}$ is smaller than $RMSE_{CCLM}$. These improved test sites have a homogeneous spatial distribution over Germany without any clear spots or highlighted regions (Figure 4a). Figure 4c shows that for most of the test sites, where the MOS application increases the RMSE, the change is only marginal with negative values close to zero. For gust speeds, the $RMSE_{CCLM}$ is reduced at 71 of 111 test sites, which corresponds to 63.96%. The spatial pattern is comparable to the one of the wind speeds (Figure 4b), but with a tendency to smaller RMSE changes with a clear peak in the histogram around zero (Figure 4d). The outliers (<-0.3), both in the wind and the gusts histograms (Figures 4c and 4d), can be attributed to local effects like steep topographical gradients.

A detailed analysis at each of the test sites leads to the conclusion that they can be separated into three categories: At test sites of the first category, most events are improved by the MOS, if CCLM wind and gust speeds are larger than observed values (Figures 5a–5d). This is the case if most of the cumulative distribution function (CDF) of the simulations lies below the CDF of the observations (Figures 5e and 5f). These test sites can be identified by

$$\mu + 0.5 \cdot \sigma < x \ \wedge \ m_{Obs} < m_{CCLM} \ \wedge \ b_{Obs} > b_{CCLM},$$
$$\text{or} \quad \mu - 0.5 \cdot \sigma > x \ \wedge \ m_{Obs} > m_{CCLM}.$$

with x being the intersection of the two CDFs with the distribution parameters m_{Obs}, m_{CCLM}, b_{Obs}, and b_{CCLM}, μ is the mean of the observations of the 100 events and σ is the corresponding standard deviation. The interval $[\mu - 0.5 \cdot \sigma; \mu + 0.5]$ has been selected after empirical tests.
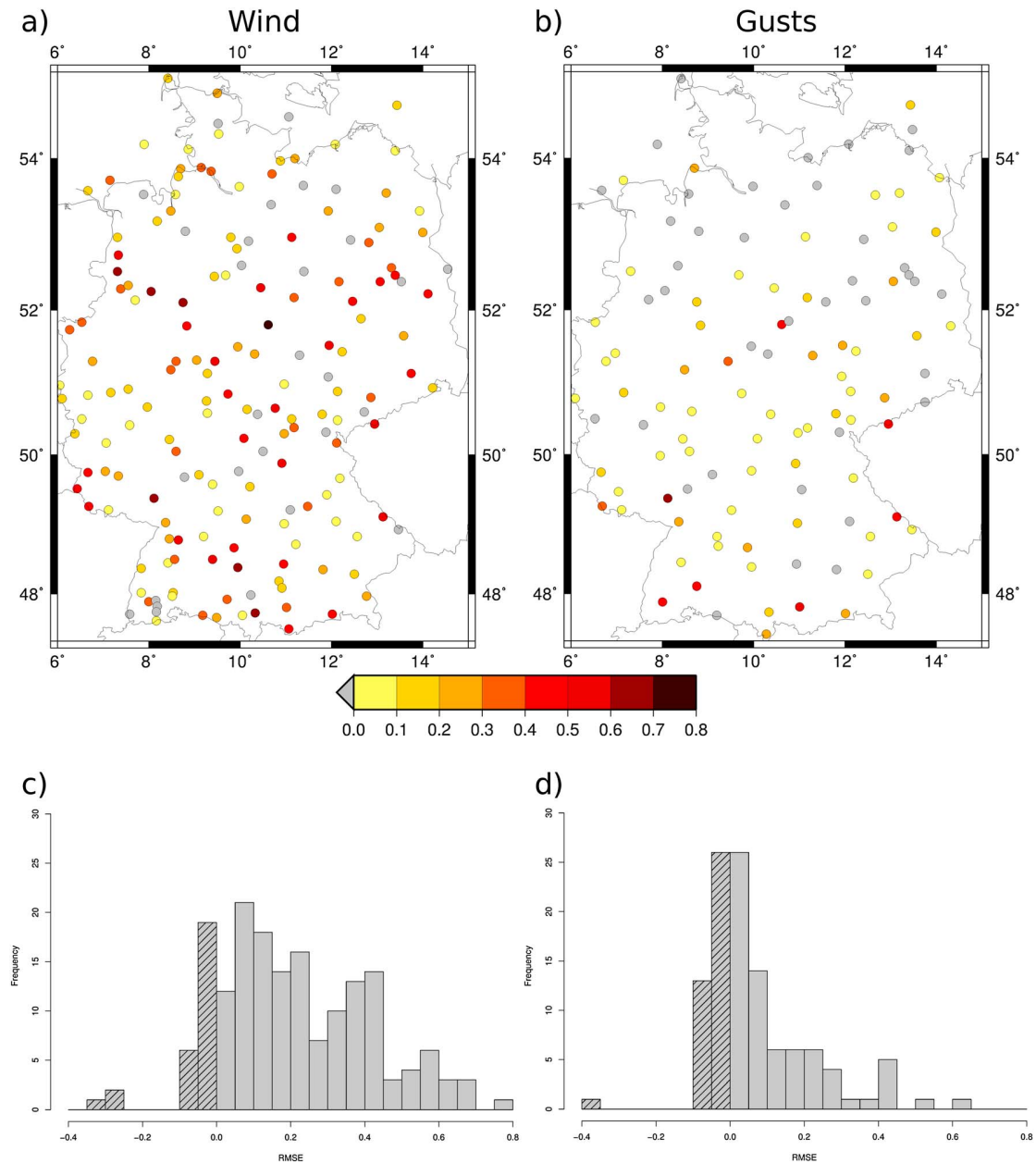
Figure 4. Spatial distribution of (a) 173 test sites selected for wind and (b) 111 test sites selected for gusts. Colors according to change in RMSE between original and corrected simulation normalized with the RMSE of the original simulation. Histogram of improvement (positive values) and disimprovement (negative values, shaded, corresponding to grey dots in Figures 4a and 4b) test sites for (c) wind and (d) gusts.

For category 2, the MOS improves events with simulated wind or gust speeds being smaller than the observed (Figures 6a–6d). These test sites can be identified by a CDF of CCLM values above the CDF of measurements (Figures 6e and 6f). An objective identification scheme would be

$$\mu + 0.5 \cdot \sigma < x \ \wedge \ m_{Obs} > m_{CCLM} \ \wedge \ b_{Obs} < b_{CCLM},$$
$$\text{or } \mu - 0.5 \cdot \sigma > x \ \wedge \ m_{Obs} < m_{CCLM}.$$

For the third category, it is difficult to apply the MOS, because the events are widely scattered (rare category, Figure S4). This category is characterized by intersecting CDFs near the mean of the observations ($\mu - 0.5 \cdot \sigma < x < \mu + 0.5 \cdot \sigma$). Ninety-four test sites report wind and wind gusts (marked with dots and circles in Figure 1), whereof at 64 sites the sorting lead to the same category regarding wind or gusts.
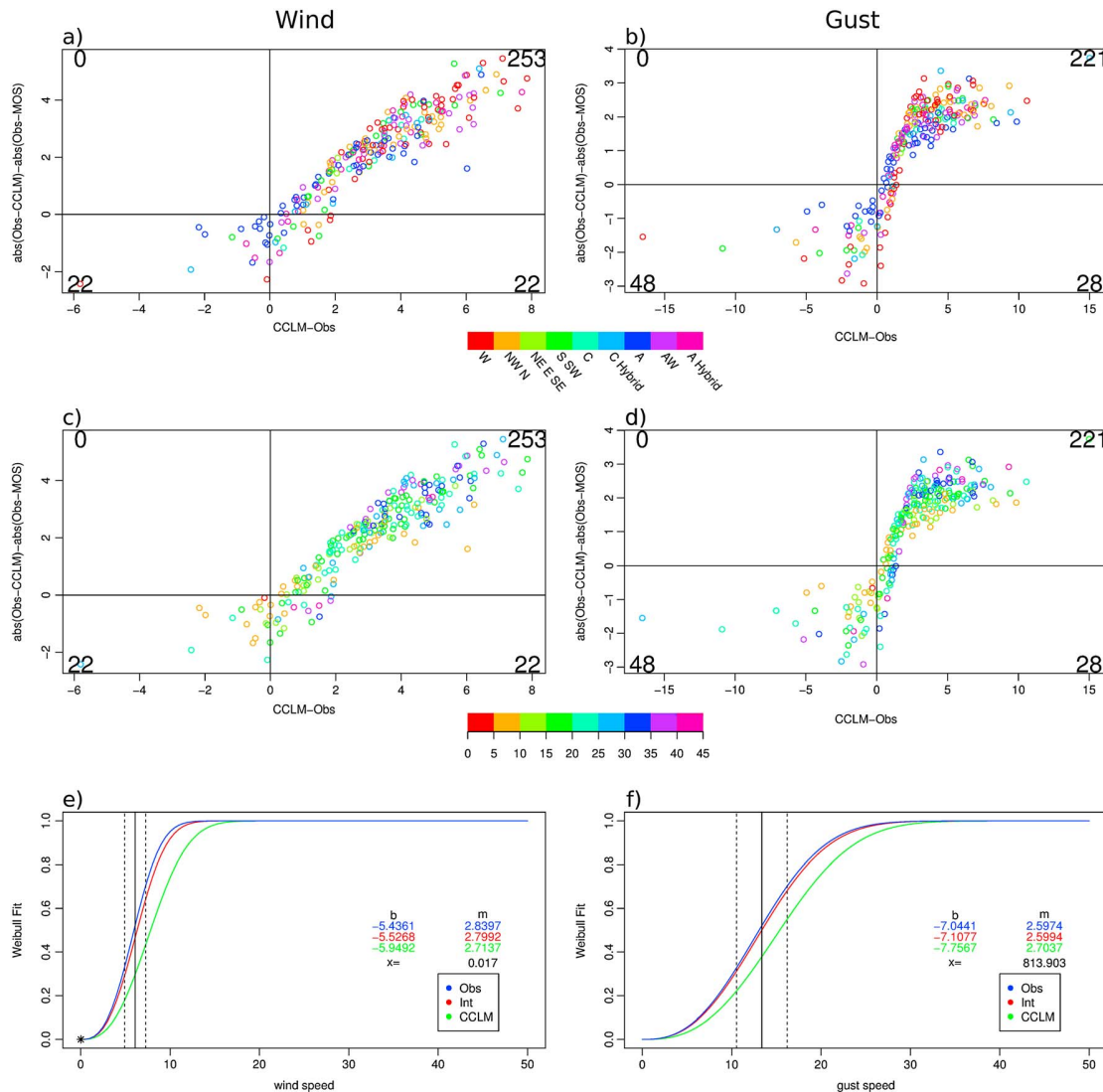
Figure 5. Category 1: Events are improved if CCLM > observation. (Dis)improvement of the simulations by the MOS against difference between original simulation and observation. Colors are according to (a and b) CWTs and (c and d) f parameter. The numbers denote the number of events in each corner (maximal sum = 300). (e and f) Distribution of observations (blue), interpolated distribution of observations (red), and distribution of simulations (green). Solid vertical line is the mean (μ) of the observations, and dashed vertical lines build the interval $[\mu - 0.5 \cdot \sigma; \mu + 0.5 \cdot \sigma]$ with the standard deviation σ. (left) Wind and (right) gusts.

On the one hand, observations could be interpolated to grid points as absolute values to identify whether the simulated gust or wind speed is greater than the observation on grid point basis. On the other hand, this would result in large uncertainties. In order to find an alternative method to identify the events for which $RMSE_{MOS}$ is larger than $RMSE_{CCLM}$, the dependence on the CWT of each event is examined. The dots in Figures 5a, 5b, 6a, and 6b are colored according to the CWT for each event. For the shown categories 1 and 2, there is apparently little correlation between CWT and an improvement of the $RMSE_{CCLM}$. Especially for gusts, at most category 3 test sites (Figure S4), the events with an anticyclonic CWT are distributed like events at category 1 test sites, i.e., scattered around a diagonal from bottom left to top right (c.f. Figures 5a–5d). They are corrected, if the CCLM value is larger than the observation. In contrast, the distribution of events with a westerly CWT tends to be more comparable to events at category 2 test sites, as they are improved if the CCLM value is smaller than the observation, corresponding to a diagonal from top left to bottom right (c.f. Figures 6a–6d). Thus, the consideration of the CWT can potentially help to interpret the scattering of the events and to refine the classification of categories. Nevertheless, further considerations would be necessary to effectively use the CWT information in practical terms.
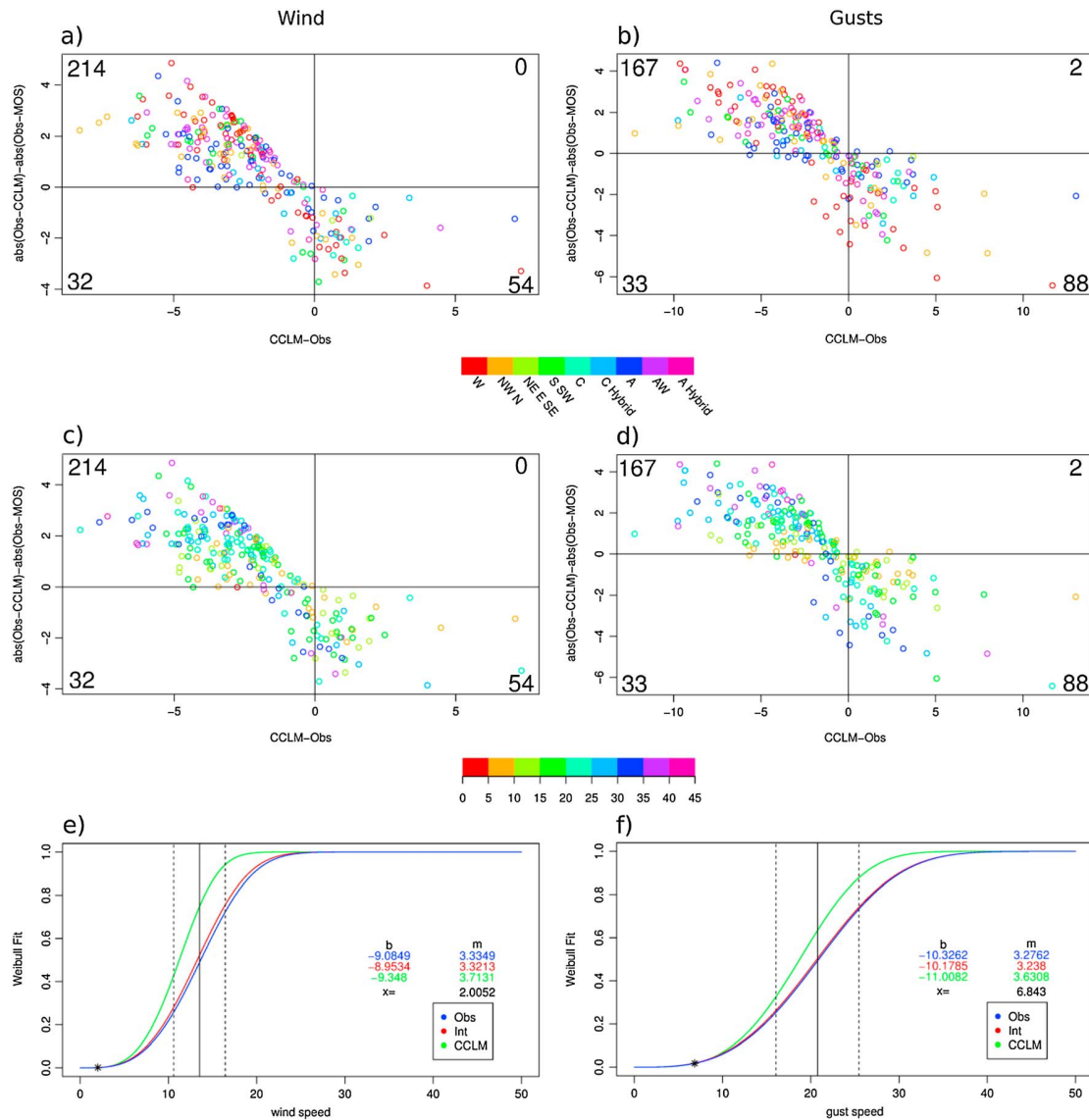
Figure 6. Category 2: Events are improved if CCLM < observation. As in Figure 5.

The CWT classification not only reflects the direction of the large-scale circulation but also provides f as measure of the total geostrophic flow intensity induced by the synoptic situation. The dots in Figures 5c, 5d, 6c, and 6d are colored according to this parameter. At category 1 and 2 test sites, the events with small f parameters tend to be little affected by the MOS, while events with large f parameters show a clear adjustment either in positive or negative direction. This is attributed to the fact that high wind and gust speeds can be attributed to large f values, thus having more potential to be adjusted by the approach. At category 3 test sites, events with small f values tend to behave as events at category 1 test sites, thus being corrected if the CCLM value is larger than the observation (analogue to category 3 and CWT types). Accordingly, events with large f values tend to behave as events at category 2 test sites, thus being improved if the CCLM value is smaller than the observation.

In general, a reasonable improvement of wind speeds by the use of the MOS approach is found. The RMSE summed over all events and test sites is decreased by 33% (Table 1). The application on gusts also brings an overall improvement (15%, Table 1) but has more outliers for specific events or test sites.

5. Discussion and Conclusions

In this study, we introduced an approach to adjust dynamically downscaled windstorm footprints to observations. For this purpose, we selected 100 storm events, which had a large impact on Europe and compared wind and gust speeds simulated by the CCLM with according observations of 173 (111) DWD test sites. At each grid point and each test site the theoretical Weibull distribution is fitted to wind and gust speeds. The distributions of observations are interpolated to the CCLM grid points to use both distributions in a probability mapping approach to correct the simulated values. Unlike most previous studies dealing with MOS applied on wind data, we developed and applied the method not only for specific locations as, e.g., wind farms, but for producing an area-wide output on a grid. It has been shown that this method is generally able to enhance the results of dynamical downscaling toward observations. Nevertheless, when considering gust speeds, there are still some events and test sites that are not improved, or in some cases even worsened. By contrast, the application of the approach on wind speeds clearly produces better results, both event and site based.

The analysis of events indicated an improvement of 99% for wind speed and 88% for gust speed. Thereby, events having a pronounced wind signature with high wind or gust speeds have a larger potential to be corrected by the introduced MOS approach. However, we found that the change in RMSE for wind and the change in RMSE for gusts are not always congruent. The analysis of test sites also delivers better results for wind speeds (~84% improved sites) than for gust speeds (~64% improved sites). The quality of the MOS application on test site basis can be quantified by an objective scheme regarding the deviation between observations and simulations of the closest grid point. To get the information at each grid point, such an identification of categories could also be based on the CDF of the interpolated distribution parameters.

In general terms, an application of this methodology to wind speed can be recommended due to the promising improvement of the wind fields. On the other hand, the methodology should be further improved before it can generally be applied to wind gust data, as currently less improvement is found. The generally better performance of the approach applied on wind speed in comparison to gust speed can be attributed to several reasons. First, it is presumably due to the strong temporal variability of gusts and the local differences. This also involves more extremes and outliers in the gust data. Second, the larger data sets for hourly wind speed may play a determinant role on the enhanced performance of the approach. Longer time series of gust speeds with a sufficient number of observations at more sites would potentially bring the results for gust closer to the ones for wind.

Future investigations should focus on a larger domain (Europe) to be able to adjust the full downscaling model introduced in *Haas and Pinto* [2012], provided an adequate set of measurement data is available. Eventually, the interpolation scheme needs to be adapted to be applicable on a larger set of test sites. This could, e.g., be done by adjusting the weighting factors or by embedding local characteristics like topography to avoid too steep gradients in the interpolated field. The effective use of the CWT information to identify events or test sites with a large or small potential of correction still needs further considerations. The use of historical data delivers the opportunity to apply an event-based MOS or the objective identification scheme introduced in section 4.2 to enhance the results for gust speeds. Such an identification of generally good or worse performing events or test sites is, due to the obvious nonexistence of observations for the future, not applicable for future climate investigations. Nevertheless, without this identification, the MOS approach itself can be applied for future climate investigations, if the transfer functions for wind and gust speed are assumed to be stationary in time. This assumption of stationarity should be proofed in future studies. Regarding the promising results for wind speed, a clear potential for application on GCM simulations is evident. The approach could, e.g., be applied in combination with the downscaling method introduced in *Haas and Pinto* [2012]. This enables the analysis of decadal predictability and climate change projections considering large ensembles. The methodology could also be applied to other variables like temperature, for which much better data coverage exists.

References

Ágústsson, H., and H. Ólafsson (2009), Forecasting wind gusts in complex terrain, *Meteorol. Atmos. Phys.*, *103*, 173–185.
Born, K., P. Ludwig, and J. G. Pinto (2012), Wind gust estimation for Mid-European winter storms: Towards a probabilistic view, *Tellus A*, *64*, 17,471, doi:10.3402/tellusa.v64i0.17471.
Brasseur, O. (2001), Development and application of a physical approach to estimating wind gusts, *Mon. Weather Rev.*, *129*, 5–25.

Buishand, A., and T. Brandsma (1997), Comparison of circulation classification schemes for predicting temperature and precipitation in the Netherlands, *Int. J. Climatol.*, *17*, 875–889.

Christensen, J., et al. (2007), Regional climate projections, in *Climate Change, 2007: The Physical Science Basis, Contribution of Working Group I to the Fourth Assessment Report of the Intergovernmental Panel on Climate Change*, chap. 11, pp. 847–940, Cambridge Univ. Press, Cambridge.

De Rooy, W. C., and K. Kok (2004), A combined physical-statistical approach for the downscaling of model wind speed, *Wea. Forecast.*, *19*, 485–495.

Dee, D. P., et al. (2011), The ERA-Interim reanalysis: Configuration and performance of the data assimilation system, *Q. J. R. Meteorol. Soc.*, *137*, 553–597.

Donat, M. G., G. C. Leckebusch, J. G. Pinto, and U. Ulbrich (2010), Examination of wind storms over Central Europe with respect to circulation weather types and NAO phases, *Int. J. Climatol.*, *30*, 1289–1300, doi:10.1002/joc.1982.

Fuentes, U., and D. Heimann (2000), An improved statistical-dynamical downscaling scheme and its application to the alpine precipitation climatology, *Theor. Appl. Climatol.*, *65*, 119–135.

Giorgi, F., and L. O. Mearns (1991), Approaches to the simulation of regional climate changes: A review, *Rev. Geophys.*, *29*, 191–216.

Glahn, H. R., and D. A. Lowry (1972), The use of Model Output Statistics (MOS) in objective weather forecasting, *J. Appl. Meteorol.*, *11*, 1203–1211.

Glahn, B., K. Gilbert, R. Cosgrove, D. P. Ruth, and K. Sheets (2009), The gridding of MOS, *Wea. Forecast.*, *24*, 520–529.

Goyette, S., M. Beniston, D. Caya, J. P. R. Laprise, and P. Jungo (2001), Numerical investigation of an extreme storm with the Canadian Regional Climate Model: The case study of windstorm VIVIAN, Switzerland, February 27, 1990, *Clim. Dyn.*, *18*, 145–178, doi:10.1007/s003820100166.

Goyette, S., O. Brasseur, and M. Beniston (2003), Application of a new wind gust parameterization: Multiscale case studies performed with the Canadian regional climate model, *J. Geophys. Res.*, *108*(D134374), doi:10.1029/2002JD002646.

Haas, R., and J. G. Pinto (2012), A combined statistical and dynamical approach for downscaling large-scale footprints of European windstorms, *Geophys. Res. Lett.*, *39*, L23804, doi:10.1029/2012GL054014.

Hanssen-Bauer, I., C. Achberger, R. E. Benestad, D. Chen, and E. J. Førland (2005), Statistical downscaling of climate scenarios over Scandinavia, *Clim. Res.*, *29*, 255–268.

Hewitson, B. C., and R. G. Crane (1996), Climate downscaling: Techniques and application, *Clim. Res.*, *7*, 85–95.

Jenkinson, A. F., and F. P. Collinson (1977), An initial climatology of gales over the North Sea, Synoptic Climatology Branch Memorandum, 62, Met. Office, Bracknell, U. K.

Jones, P. D., M. Hulme, and K. R. Briffa (1993), A comparison of Lamb circulation types with an objective classification scheme, *Int. J. Climatol.*, *13*, 655–663, doi:10.1002/joc.3370130606.

Jones, P. D., C. Harpham, and K. R. Briffa (2012), Lamb weather types derived from reanalysis products, *Int. J. Climatol.*, *33*, 1129–1139, doi:10.1002/joc.3498.

Justus, C. G., W. R. Hargraves, A. Mikhail, and D. Graber (1978), Methods for estimating wind speed distributions, *J. Appl. Meteorol.*, *17*, 350–353.

Kim, J.-W., J.-T. Chang, N. L. Baker, D. S. Wilks, and W. L. Gates (1984), The statistical problem of climate inversion: Determination of the relationship between local and large-scale climate, *Mon. Weather Rev.*, *112*, 2069–2077.

Klawa, M., and U. Ulbrich (2003), A model for the estimation of storm losses and the identification of severe winter storms in Germany, *Nat. Hazards Earth Syst. Sci.*, *3*, 725–732.

Klein, W. H., and H. R. Glahn (1974), Forecasting local weather by means of Model Output Statistics, *Bull. Am. Meteorol. Soc.*, *55*, 1217–1227.

Lamb, H. H. (1972), *British Isles Weather Types and a Register of the Daily Sequence of Circulation Patterns 1981–1971*, Geophys. Mem., vol. 116, p. 85, HMSO, London.

Maraun, D., et al. (2010), Precipitation downscaling under climate change: Recent developments to bridge the gap between dynamical models and the end user, *Rev. Geophys.*, *48*, RG3003, doi:10.1029/2009RG000314.

Meehl, G. A., et al. (2007), Global climate projections, in *Climate Change 2007: The Physical Science Basis. Contribution of Working Group I to the Fourth Assessment Report of the Intergovernmental Panel on Climate Change*, pp. 747–845, Cambridge Univ. Press, U. K.

Michelangeli, P.-A., M. Vrac, and H. Loukos (2009), Probabilistic downscaling approaches: Application to wind cumulative distribution functions, *Geophys. Res. Lett.*, *36*, L11708, doi:10.1029/2009GL038401.

Pinto, J. G., C. P. Neuhaus, A. Krüger, and M. Kerschgens (2009), Assessment of the wind gust estimates method in mesoscale modelling of storm events over West Germany, *Meteorol. Z.*, *18*, 495–506.

Pinto, J. G., C. P. Neuhaus, G. C. Leckebusch, M. Reyers, and M. Kerschgens (2010), Estimation of wind storm impacts over West Germany under future climate conditions using a statistical-dynamical downscaling approach, *Tellus A*, *62*, 188–201.

Pinto, J. G., M. K. Karremann, K. Born, P. M. Della-Marta, and M. Klawa (2012), Loss potentials associated with European windstorms under future climate conditions, *Clim. Res.*, *54*, 1–20.

Pryor, S. C., and R. J. Barthelmie (2010), Climate change impacts on wind energy: A review, *Renew. Sust. Energy Rev.*, *14*, 430–437.

Pryor, S. C., J. T. Schoof, and R. J. Barthelmie (2005), Empirical downscaling of wind speed probability distributions, *J. Geophys. Res.*, *110*, D19109, doi:10.1029/2005JD005899.

Rockel, B., A. Will, and A. Hense (2008), The regional climate model COSMO-CLM (CCLM), *Meteorol. Z.*, *17*, 347–348.

Schulz, J. P. (2008), Revision of the turbulent gust diagnostics in the COSMO model, *COSMO Newsl.*, *8*, 17–22.

Thorarinsdottir, T. L., and T. Gneiting (2010), Probabilistic forecasts of wind speed: Ensemble Model Output Statistics by using heteroscedastic censored regression, *J. R. Statist. Soc. Series A*, *173*, 371–388.

Trigo, R. M., and C. C. DaCamara (2000), Circulation weather types and their influence on the precipitation regime in Portugal, *Int. J. Climatol.*, *20*, 1559–1581.

Verkaik, J. W. (2000), Evaluation of two gustiness models for exposure correction calculations, *J. Appl. Meteorol.*, *39*, 1613–1626.

Wieringa, J. (1973), Gust factors over open water and built-up country, *Boundary Layer Meteorol.*, *3*, 424–441.

Wilby, R. L., and T. M. L. Wigley (1997), Downscaling general circulation model output: A review of methods and limitations, *Prog. Phys. Geogr.*, *21*, 530–548.

Wilby, R. L., T. M. L. Wigley, D. Conway, P. D. Jones, B. C. Hewitson, and D. S. Wilks (1998), Statistical downscaling of GCM output: A comparison of methods, *Water Resour. Res.*, *34*, 2995–3008.

World Meteorological Organization (WMO) (2008), Guide to meteorological instruments and methods of observation, WMO-No. 8, WMO, Geneva, Switzerland.

Supplementary material
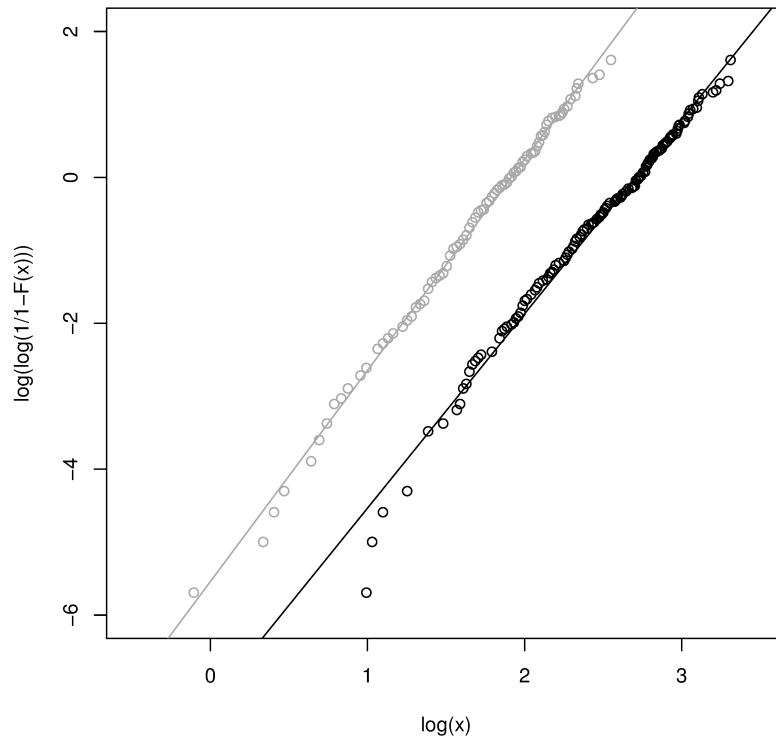
Figure S1: Example for estimation of Weibull distribution parameters at site Bamberg in Bavaria (49.8753°E, 10.9219°N, height: 240m, c.f. Figure 4). Transformed wind speeds (grey) and gust speeds (black) of the three days of all 100 events are fitted by regression lines resulting in the estimated Weibull parameters.
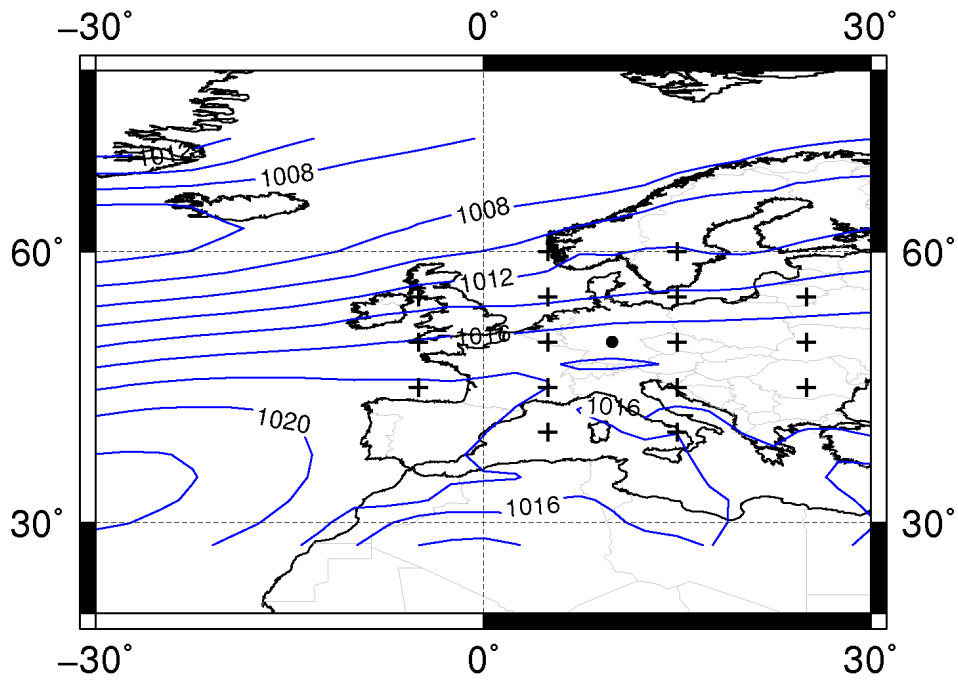
Figure S2: Averaged mean sea level pressure field during 1989 to 2010 and grid points used to calculate the CWTs.
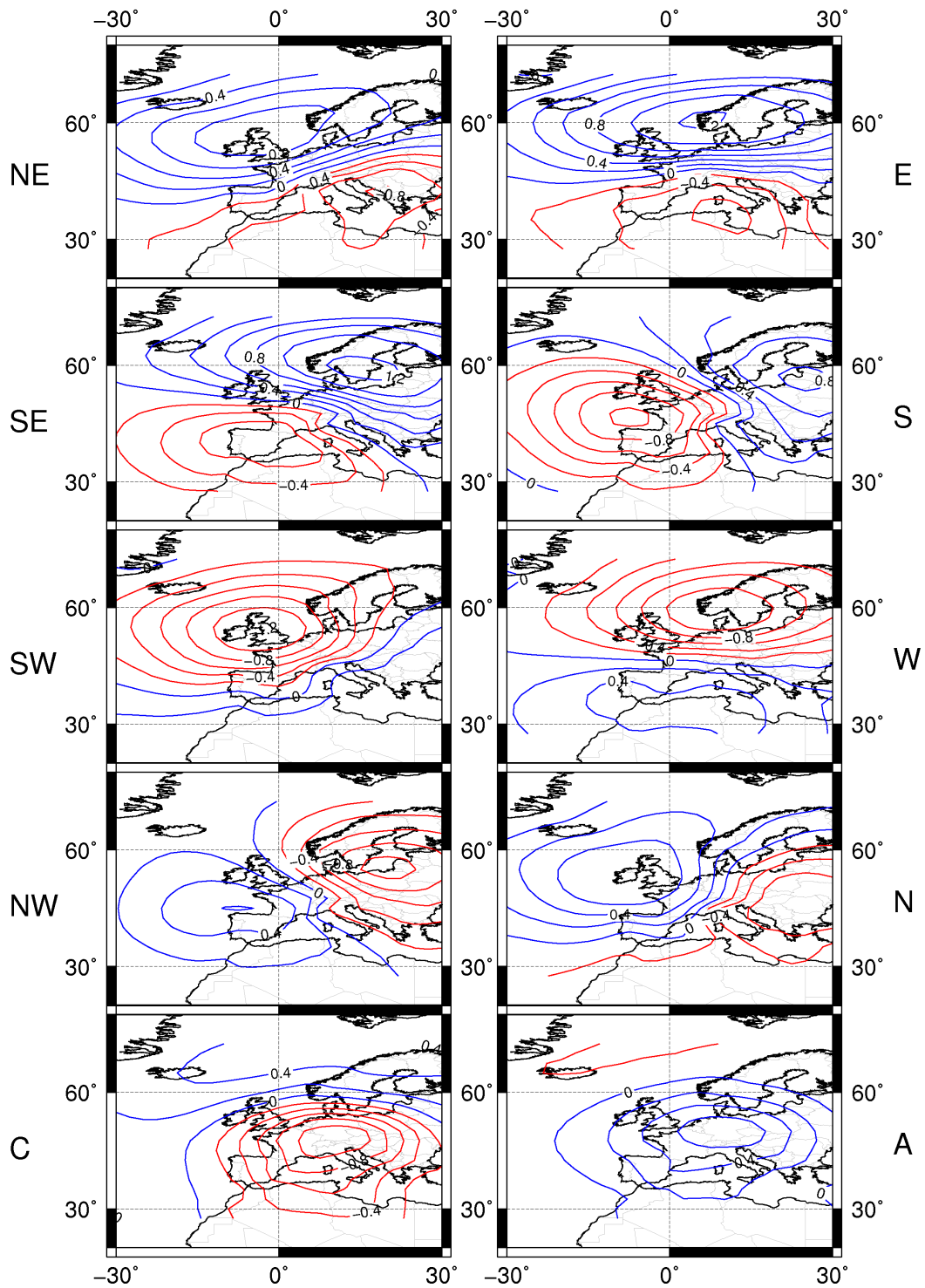
Figure S3: Anomalies from averaged mean sea level pressure field per CWT.
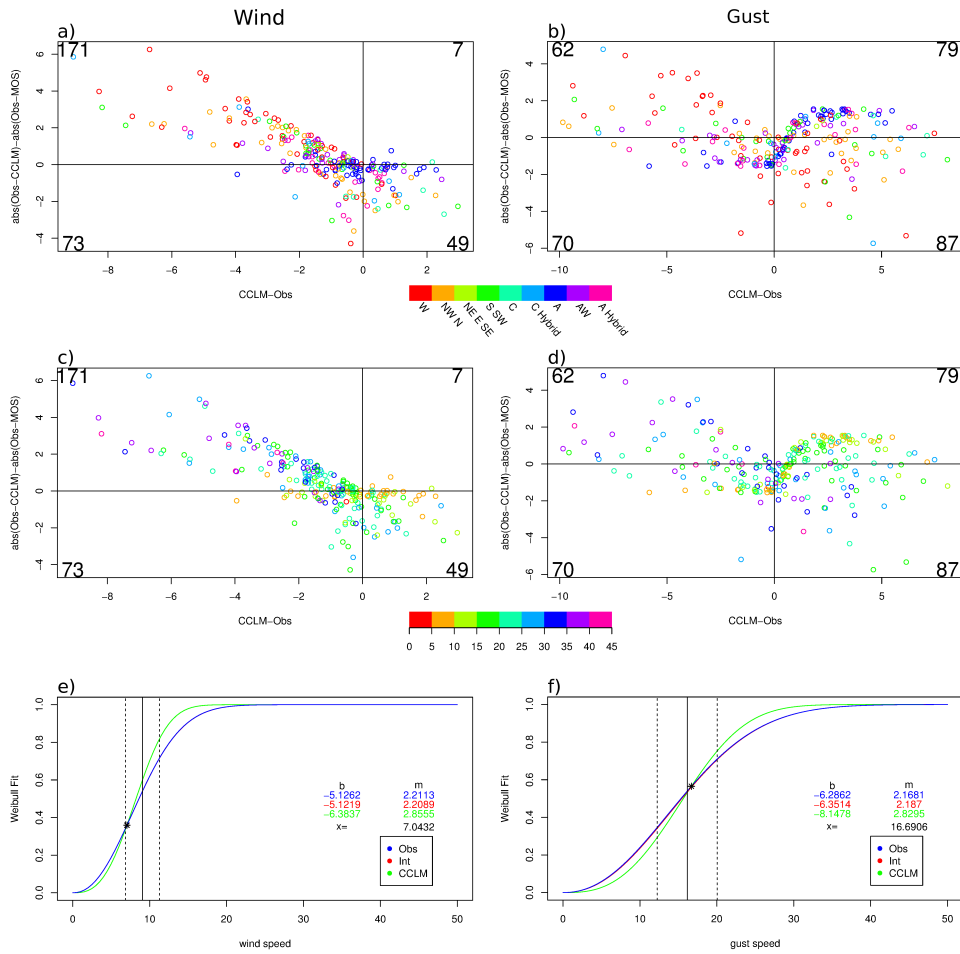
Figure S4: Category 3 characterized by intersecting CDFs near the mean of the observations. (Dis)improvement of the simulations by the MOS against difference between original simulation and observation. Colors are according to CWTs (a,b) and f parameter (c,d). The numbers denote the number of events in each corner (maximal sum = 300). (e,f): Distribution of observations (blue), interpolated distribution of observations (red) and distribution of simulations (green). Solid vertical line is the mean (μ) of the observations and dashed vertical lines build the interval with the standard deviation σ. Left: wind, right: gusts.

Table S1: 100 events in chronological order, selected according to MI. The numbers in the last column contains information of the CWTs with 11 = northeast, 12 = east, 13= southeast, 14 = south, 15 = southwest, 16 = west, 17 = northwest, 18 = north, 32 = cyclonic and 33 = anticyclonic. Hybrid types are marked with two numbers.

Date	MI	Rank	CWT	Date	MI	Rank	CWT
19890115	284.151	43	33	19990205	448.131	13	17
19890129 #	224.877	74	33	19991201	293.425	41	16
19890215	222.462	79	33	19991203	233.232	64	17
19890225	414.315	16	32	19991204	298.147	39	17
19890226	533.812	5	16	19991225	282.956	45	16
19891217	226.601	70	16	19991226	376.355	20	32,16
19900125	400.377	18	16	19991227	249.605	56	32
19900208	352.110	24	16	19991228	339.189	31	18
19900212	219.345	87	15	20000118	219.596	84	33,18
19900214	231.645	65	17	20000121	225.340	73	33
19900226	647.747	2	16	20000129	220.768	81	17
19900227	812.500	1	17	20000130	427.668	14	16
19900228	468.916	10	32,16	20000131	222.685	77	33,16
19900301	426.463	15	17	20000303	279.183	46	17
19900306	224.255	75	33,17	20000406	238.131	60	33
19900310	264.196	51	33,17	20001030	335.115	32	15
19920101	331.963	34	33,16	20001106	211.233	93	32
19920117	343.836	27	33	20010605	207.260	99	33,15
19920224	256.163	53	33	20011115	458.389	11	33
19920313	292.879	42	16	20020129	293.883	40	33,16
19920906	326.752	36	33	20020222	266.881	49	16
19921126	208.997	95	33,17	20020223	216.457	88	16
19921202	211.398	92	16	20020307	251.284	54	33,17
19921219	241.972	59	15	20021027	342.321	29	17
19930114	310.989	37	33	20021028	450.395	12	33
19930117	234.270	62	33,16	20040321	348.731	25	16
19930118	226.390	71	33	20041114	219.518	85	33
19930122	369.409	21	17	20041119	214.640	90	32,16
19930123	363.777	23	16	20041222	229.938	68	16
19930124	506.141	7	16	20050108	220.985	80	33,16
19930125	283.432	44	16	20050109	250.736	55	33,15
19930319	242.771	58	33	20050213	231.221	67	32,18
19931209	339.890	30	17	20070111	329.678	35	17
19931220	220.550	82	16	20070112	219.436	86	33,16
19940128	411.349	17	17	20070118	584.807	3	17
19940314	383.723	19	17	20070119	491.899	8	33,16
19940324	272.219	47	33,16	20070129	344.481	26	33

19940401	258.602	52	16	20070320	231.634	66	32,11
19950122	209.825	94	16	20070405 *	235.792	61	33
19950123	488.501	9	16	20080127	207.326	98	33
19950127	227.775	69	15	20080128	222.485	78	33
19950328 ±	302.840	38	32	20080131	206.753	100	33,17
19950513	226.023	72	18	20080223	211.546	91	33,17
19970225	271.124	48	16	20080301 E	574.302	4	17
19970327	246.003	57	16	20080302	332.855	33	17
19970407	216.079	89	33	20080305	208.331	96	33
19970411	514.613	6	33,18	20081123	219.669	83	32,15
19981024	223.899	76	15	20090124	343.356	28	33
19981028	366.381	22	16	20091013	207.934	97	33
19990204	233.916	63	17	20100228	264.311	50	17

Unpublished supplementary material

These figures do not belong to the published material of Haas et al. (2014a). They arose during the review process based on a reviewers comment concerning stationarity of the transfer functions. In the present published manuscript, stationarity is only discussed in general terms. A detailed discussion with respect to the following figures is given in Chapter 6.
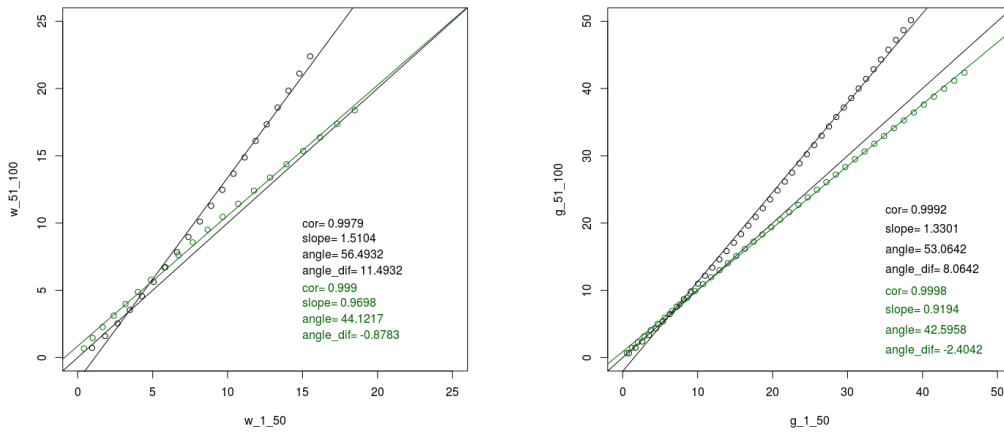
Figure S5: Transfer functions are build for two periods consisting of the first and the second 50 events for wind ($T_{1,50,wind}$ and $T_{51,100,wind}$) and gusts ($T_{1,50,gust}$ and $T_{51,100,gust}$). For wind speed (left), exemplary values between $1\,\text{m/s}$ and $20\,\text{m/s}$ are inserted to obtain corrected $w_{1,50}$ and $w_{51,100}$. For gust speed (right), exemplary values between $1\,\text{m/s}$ and $40\,\text{m/s}$ are inserted to obtain corrected $g_{1,50}$ and $g_{51,100}$. The resulting values are plotted for two example grid points (green and black) and regression lines are fitted.
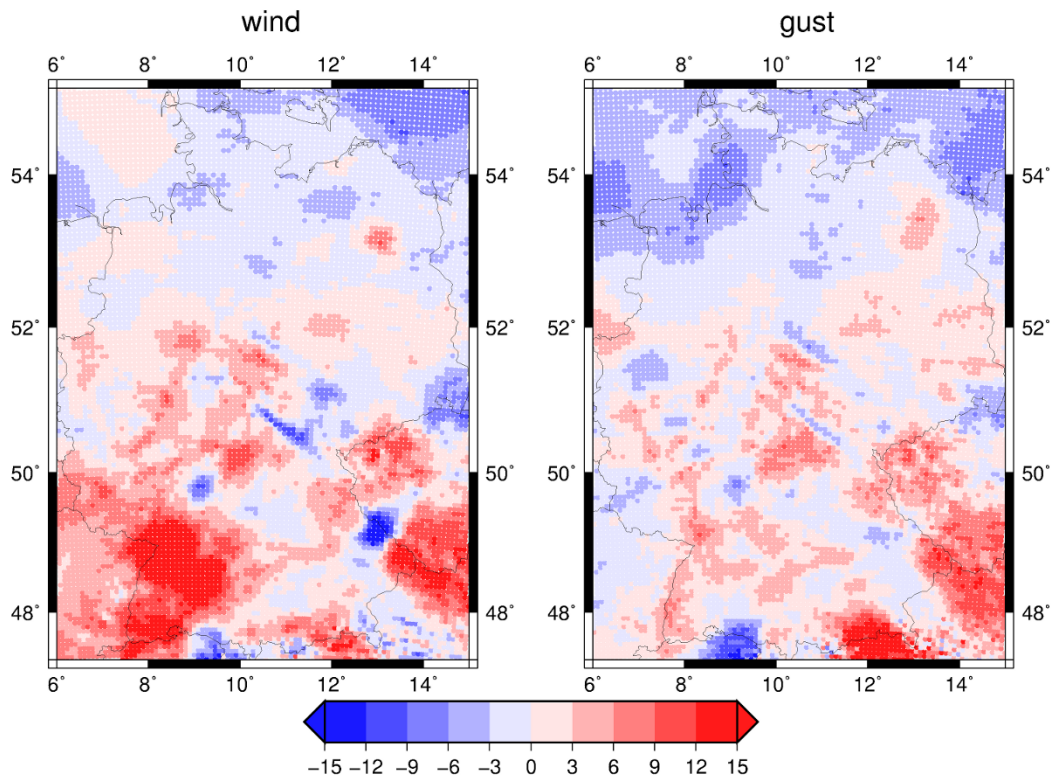
Figure S6: Differences of regression line angles from the identity line. Left: regression lines resulting from corrected wind speeds. Right: regression lines resulting from corrected gust speeds.

4 Wind-gust model

Extreme wind speeds or gusts are one of the main factors leading to damages during windstorms. Therefore, it is important to investigate not only wind speeds but also gust speeds. Due to the lack of gust observations in comparison to wind observations, it is desirable to enhance the gust database. One possibility is to estimate synthetic gusts by the relation between both parameters. In Haas et al. (2014a), observed wind and gust speeds are each fitted by theoretical Weibull distributions (Chapter 3, Equation 1). The according distribution parameters α and β are estimated for measurements at different DWD test site in Germany (c. f. Chapter 3, Figure 1). After a transformation following Equation 2 in Chapter 3, these distribution parameters can be approximated by the linear regression parameters m and b (c. f. Chapter 3, Figure S1). Plotting m and b against each other for wind (blue dots in Figure 4.1) and gusts (green dots in Figure 4.1) shows that both parameters are not independent and have a negative correlation.

In general, an increased probability for high wind or gust speeds is either be reflected in lower m or b values than for small wind or gust speeds. However, the curves are more sensitive to m as it influences the shape of the cumulative density function (CDF). This is reflected in a wider range of b values, which are responsible for the scale of the CDF. Additionally, the lower gust parameters are in line with gust speeds generally exceeding wind speeds. Regression lines through the points of both data sets (Figure 4.1) show this by similar slopes (-0.25 and -0.26) but a lower intercept of gust values (0.71) compared to wind values (1.10). The different number of blue and green points in Figure 4.1 reflects the fact that less measurement sites provide gust observations with a sufficient quantity of data. The preparation of the daily wind and gust measurements for Haas et al. (2014a) presented in Chapter 3 reveals that some of the DWD test sites are not appropriate for probabilistic approaches. Since some test sites had too short time series or large gaps within the time series, and others were moved during the investigation period or have other inhomogeneities, wind observations of 173 sites and gust observations of only 111 sites were selected. In order to enlarge the amount of gust measurements, the estimation of synthetic gust speeds from measured wind speeds would be helpful. For this purpose, the relation
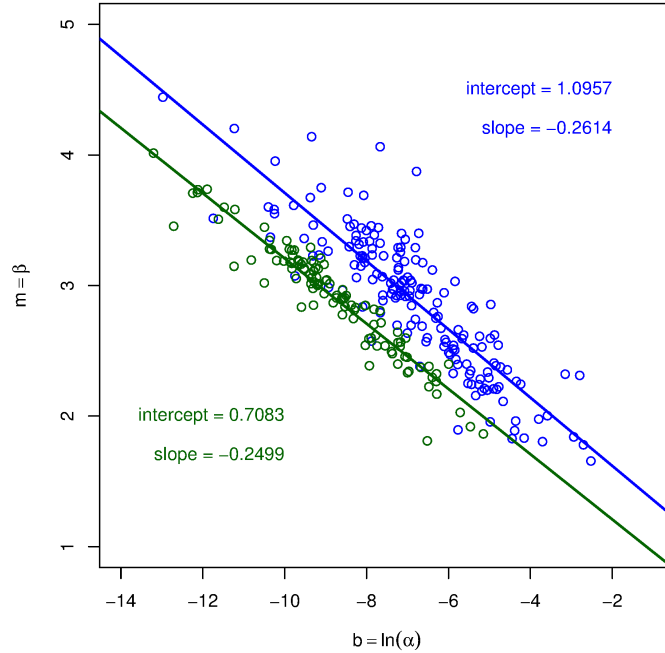
Figure 4.1: Fitted Weibull parameters m and b for wind (blue) and gust (green) at different measurement sites in Germany and linear regression lines through all sites with slope and axis intercept.

between the two shown regression lines can e.g. be used to build a transfer function between wind and gust speeds. Therewith it would be possible to model gust speed distributions for test sites where only wind speed or few gust observations are given.

This concept has been further developed in Seregina (2012) and Seregina et al. (2014). Other than in Haas et al. (2014a), for these studies, hourly observations from the DWD were considered instead of daily data. These are even more prone to inhomogeneities and had to be proven carefully. Only data between 2001 and 2012 has been used to avoid conflicts with a threshold of 12.5 m/s concerning the report and storage of hourly gust data (standard before 2001). In order to reduce influences of topography and other local conditions on the wind measurements, a roughness length based exposure correction has been performed. The gust speeds and corrected wind speeds have been afterwards used to build wind-gust models using linear relations as described above. The model to estimate gust distribution parameters have been build for four sectors of 90° (N, E, S, W) based on the observed wind direction. A cross-validation has shown that for the west sector originally determined gust distribution parameters and parameters estimated by the transfer function between the regression lines have high correlations of 0.98 (scale parameter, equivalent to b) and 0.91 (shape parameter, equivalent to m). The correlations for the other sectors were similar for the scale parameter but lower for the shape parameter. This can be explained by the larger

amount of data for the west sector, as this is the predominant wind direction over Europe. In a second step, the estimated gust distribution parameters and the known wind distributions have been used within a probability mapping approach to obtain synthetic gust speeds from specific wind speed measurements. These synthetic gusts have been evaluated against measurements by RMSEs. The synthetic gusts were well simulated with errors ranging between $1\,\mathrm{m/s}$ and $2\,\mathrm{m/s}$, whereas higher deviations were only obtained for mountain test sites. During the further utilization of the synthetic gusts, it was identified that the highest gust values are smoothed out and that peaks are underrepresented in the data set of the synthetic gusts. A further finding was that large-scale events like windstorm Kyrill with a broad footprint are better reproduced than local events like caused convective systems. A few summer events could only identified with the original gust data set and not with the estimated gusts.
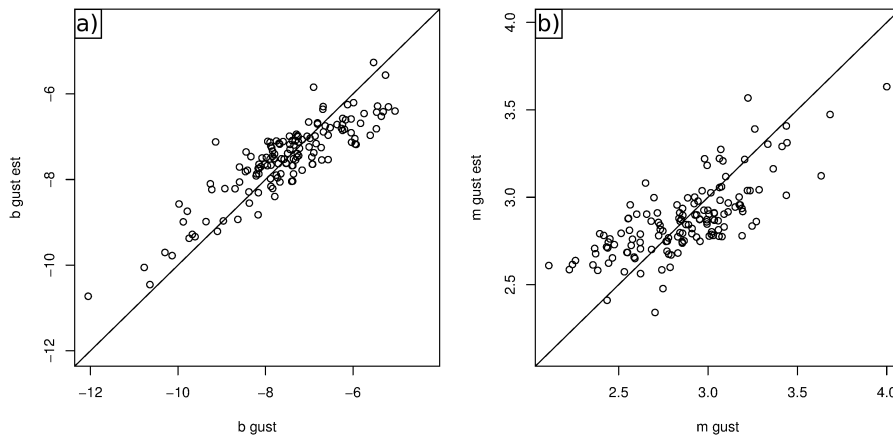
Figure 4.2: Weibull parameters determined from available winter days between 1989 and 2011 for a selection of 141 test sites with sufficient data amount for wind and gust measurements. a) Fitted Weibull parameter b for observed gusts against b estimated with the wind-gust model. b) Same as a) but for m.

Although the wind-gust model can also be applied on daily data, the hourly data including the exposure correction is more suitable. For testing purposes, the gust parameters are here estimated with the wind-gust model based on available daily wind and gust speed observations during the winters of 1989 to 2011. Figure 4.2 shows quite large deviations of these parameters from the parameters derived from the Weibull fit, especially for m. Therefore, the generation of synthetic gust speeds is not assumed to be appropriate with these parameters. On the other hand, the wind-gust model build of hourly data would not have been appropriate for the study presented in Chapter 3, as also windstorms before 2001 should be analyzed, when the hourly data set is limited by the $12.5\,\mathrm{m/s}$ threshold. This means that the model can indeed be

applied on data before 2001, but the transfer function can only be estimated from the later data. This is the case because the Weibull distribution is not suitable for the limited range of gust values before 2001. Nevertheless, the wind-gust model has potential for case studies of specific windstorms and their return periods. Seregina (2012) and Seregina et al. (2014) showed an approach to obtain long return periods as a feasible application. Therewith, maximum return periods considering specific locations and average return periods considering specific events could be estimated. The results were in line with measurements and promising for a wide range of potential further applications.

5   Decadal predictability

Revised journal article:

Haas, R., M. Reyers, and J. G. Pinto, Decadal predictability of regional-scale peak winds over Europe using the Earth System Model of the Max-Planck-Institute for Meteorology, *Meteorologische Zeitschrift*, in review.

Decadal predictability of regional-scale peak winds over Europe using the Earth System Model of the Max-Planck-Institute for Meteorology

Rabea Haas

Institute for Geophysics and Meteorology,
University of Cologne, Germany

Mark Reyers

Institute for Geophysics and Meteorology,
University of Cologne, Germany

Joaquim G. Pinto

Department of Meteorology,
University of Reading, Reading, United Kingdom
and
Institute for Geophysics and Meteorology,
University of Cologne, Cologne, Germany

Abstract

The predictability of high impact weather events on multiple time scales is a crucial issue both in scientific and socio-economic terms. In this study, a statistical-dynamical downscaling (SDD) approach is applied to an ensemble of decadal hindcasts obtained with the Max-Planck-Institute Earth System Model (MPI-ESM) to estimate the decadal predictability of peak wind speeds (as a proxy for gusts) over Europe. Yearly initialized decadal ensemble simulations with ten members are investigated for the period 1979 - 2005. The SDD approach is trained with COSMO-CLM regional climate model simulations and ERA-Interim reanalysis data and applied to the MPI-ESM hindcasts. The simulations for the period 1990 - 1993, which was characterized by several windstorm clusters, are analyzed in detail. The anomalies of the 95 % peak wind quantile of the MPI-ESM hindcasts are in line with the positive anomalies in reanalysis data for this period. To evaluate both the skill of the decadal predictability system and the added value of the downscaling approach, quantile verification skill scores are calculated for both the MPI-ESM large-scale wind speeds and the SDD simulated regional peak winds. Skill scores are predominantly positive for the decadal predictability system, with the highest values for short lead times and for (peak) wind speeds equal or above the 75 % quantile. This provides evidence that the analyzed hindcasts and the downscaling technique are suitable for estimating wind and peak wind speeds over Central Europe on decadal time scales. The skill scores for SDD simulated peak winds are slightly lower than those for large-scale wind speeds. This behavior can be largely attributed to the fact that peak winds are a proxy for gusts, and thus have a higher variability than wind speeds. The introduced cost-efficient downscaling technique has the advantage of estimating not only wind speeds but also estimates peak winds (a proxy for gusts) and can be easily applied to large ensemble datasets like operational decadal prediction systems.

Keywords: decadal predictability, downscaling, wind gusts, MPI-ESM-LR, COSMO-CLM, MiKlip decadal prediction system

1. Introduction

The IPCC Fifth Assessment Report (IPCC, 2013) states that the last three decades have been the warmest since 1850 on global average and for many regions of the globe. The long-term trend of increasing temperature in recent decades is expected to intensify during the present century. For other variables, like precipitation and wind, identified and projected long-term trends are comparatively small, and hidden within the natural variability on interannual to decadal time scales. Short-term climate projections to assess such decadal variations are crucial for decision makers to help developing adaptation strategies for the next decade. This points out the necessity of reliable predictions on interannual to decadal timescales, which should represent both natural climate variability and changes occurring due to increasing greenhouse gas concentrations (e.g. SOLOMON et al., 2011). So-called decadal hindcasts are commonly used to assess decadal predictability (e.g. SMITH et al., 2007). These hindcasts are initialized from an assimilation run, which takes into account sea surface temperatures and salinity anomalies in order to represent the oceans states over the historical period. The hindcasts are used to simulate the development of the atmospheric, oceanic and surface fields within the next decade. For comparison, so-called uninitialized historical runs are used. These runs are started from randomly chosen states of a pre-industrial control simulation and only use observed aerosol and greenhouse gas concentrations as external forcing.

A set of decadal hindcasts (for recent decades) and predictions (for future decades) has been released within the Coupled Model Intercomparison Project Phase 5 (CMIP5; TAYLOR et al., 2012). Commonly, these experiments are conducted using earth system models. A set of ensemble members is created by initializing the simulations at slightly different times of an assimilation run (e.g. MÜLLER et al., 2012). Assimilation runs use observed states of the ocean (e.g. sea surface temperature and salinity), and in some cases information on the states of the atmosphere. The hindcast experiments are usually validated against observations and reanalysis datasets to identify any bias and to estimate their predictive skill. Analyses of CMIP5 models showed that the range of ensemble members is not appropriate to represent the uncertainty arising from the initialization inaccuracies (TAYLOR et al., 2012). A lack of observations and too short time series turned out to be challenging for validation. Another difficulty is the differentiation between naturally occurring and anthropogenically induced decadal variability (e.g. SOLOMON et al., 2011).

Even though decadal prediction is a fairly recent field of research, the number of studies dealing with the validation or the application of decadal hindcasts has increased in recent years. Most publications focus on (sea) surface temperature (e.g. SMITH et al., 2007; MÜLLER et al., 2012; SMITH

et al., 2013), circulation patterns (e. g. MSADEK et al., 2010; TENG et al., 2011) or precipitation (e. g. BOER et al., 2008; VAN OLDENBORGH et al., 2012). Focusing on Central Europe, MIERUCH et al. (2014) for example found the highest predictive skill for temperature, while the results for precipitation are less skillful. On the contrary, studies on wind and/or related parameters are rare. KRUSCHKE et al. (2014) evaluated the predictive skill of cyclone activity over the Northern Hemisphere based on decadal hindcasts of the MPI-ESM. They identified distinct areas over the North Atlantic and the North Pacific with positive skill for intense cyclones. MÜLLER et al. (2012) identified the North Atlantic as "a key region for decadal climate predictions", and they found a predictive skill for different parameters (e. g., mean sea level pressure, sea surface temperature) over this area for all lead times up to 9 years. At present, most investigations focus on features on a very large scale (i. e. global), whereas for stakeholders and planning strategies, information on the regional and local scale is more important.

Within the BMBF-funded project MiKlip ("Mittelfristige Klimaprognosen", decadal predictions), the goal is to create a model system based on the Max-Planck-Institute Earth System Model (MPI-ESM), which enables to meet the above mentioned demands on decadal hindcasts (cf. MÜLLER et al., 2012; MIERUCH et al., 2014). It is important to analyze the skill of such a model system both on the large scale and in particular on the regional scale. This study consists of two parts: First, a statistical-dynamical downscaling approach, which is trained with gust speeds of a regional climate model and estimates regional daily peak winds as a proxy for gusts, is validated. Second, the approach is applied to decadal hindcasts of the MPI-ESM and its predictive skill is evaluated. The decadal predictability is assessed using quantile verification skill scores, which are calculated by comparing initialized simulations and uninitialized historical runs. For the regionalization of large ensembles of decadal hindcasts and predictions, a cost-efficient downscaling approach is required. The combination of statistical and dynamical downscaling generally offers a good alternative to pure dynamical downscaling (e. g. FUENTES and HEIMANN, 2000; PINTO et al., 2010) and can be easily applied for decadal prediction systems. HAAS and PINTO (2012) recently provided evidence that such a combined statistical and dynamical approach is suitable to downscale large-scale footprints of European windstorms using ERA-Interim wind data as predictors. The general concept of the approach is to relate large-scale predictors (explanatory variable) and regional-scale predictands (dependent variable) by transfer functions based on multiple linear regression. The approach has been validated by reproducing purely dynamically downscaled gust speeds for a selection of historical storms. Both downscaling approaches have similar prediction skills in comparison to observed wind gusts (cf. HAAS and PINTO, 2012; their Figure 3).

In the present study, the downscaling approach is applied to the decadal

hindcasts and predictions of MPI-ESM in a low-resolution configuration (MPI-ESM-LR). As the main objective is to analyze changes in the wind speed statistics on interannual to decadal timescales, we have not selected specific extreme events (like in HAAS and PINTO, 2012) but we have considered the whole climatology and thus all daily values of the MPI-ESM-LR ensemble for the period 1979 - 2005. In order to capture the wind and gust speeds ranges and distributions, selected quantiles are considered (mainly 5 %, 50 % and 90 % - 99 %). The decadal predictability of these quantiles is quantified using a suitable skill score.

The structure of the paper is as follows. The used datasets are introduced in Section 2. In Section 3, the method to estimate a transfer function between regional gust speeds and large-scale wind speeds, the used skill score, and the cyclone tracking methodology are explained. The characteristics of the peak winds predicted by the SDD are compared to gust characteristics as derived from regional climate model (RCM) simulations in Section 4. The results of the application of the SDD method to the decadal hindcasts and the quantification of the added value of initialization are described in Section 5. The paper concludes with a summary and conclusions section.

2. Data

A statistical-dynamical downscaling approach (SDD, see Section 3.1) is used to determine regional peak winds as a proxy for wind gusts from the hindcasts of the MPI-ESM-LR. In order to assess the quality of the hindcasts, the predictive skill of large-scale MPI-ESM-LR wind speeds is quantified. Further, the peak winds predicted by the SDD are compared to gusts as derived from RCM simulations. The used datasets for these analyses are introduced in following subsections.

2.1. MPI-ESM-LR

The decadal hindcasts and predictions evaluated in this study have been conducted within the MiKlip project with the MPI-ESM-LR. The MPI-ESM-LR includes the ECHAM6 general circulation model (European Centre Hamburg model generation 6; STEVENS et al., 2013) for the atmospheric part and the MPIOM model (Max-Planck-Institute Ocean Model; JUNGCLAUS et al., 2013) for the ocean component. This earth system model has already been used with a different configuration for CMIP5 (MÜLLER et al., 2012). In this study, the 2nd generation hindcasts (denoted "baseline1" within the MiKlip consortium) are considered. These hindcasts and predictions are initialized yearly on 1st January by nudging the model towards atmospheric and oceanic fields from the reanalysis data. Each of those simulations is named after its

initialization time and covers a period of 10 years (e.g. dec1960 is valid from January 1961 to December 1970). The atmospheric and oceanic conditions for initializing the ensemble of hindcasts are taken from different time steps of an assimilation run to represent uncertainties in the initial states of the climate system. The 2nd generation ensemble of yearly initialized hindcasts comprises ten members each. Sea surface temperatures and salinity anomalies necessary for the assimilation run are taken from the ocean reanalysis system (ORAs4, BALMASEDA et al., 2012) of the European Centre for Medium-Range Weather Forecasts (ECMWF). Technical details as well as a comparison between the results from the 1st and 2nd generation of the ensembles can be found in POHLMANN et al. (2013). In order to identify the added value of initialization for decadal predictability, we additionally consider three ensemble members of the so-called uninitialized historical run for the period 1960‑2005. These simulations are initialized from randomly chosen states of a pre-industrial control simulation and are, unlike the initialized runs, not tuned to the observed ocean and atmospheric states, but use only the observed aerosol and greenhouse gas concentrations as external forcing (1850‑2005; cf. MÜLLER et al., 2012).

In this study, the MPI-ESM-LR ensemble simulations of large-scale wind speeds are used as predictor (explanatory variable) in the SDD (see Section 3.1). These wind speeds are available as 6-hourly output from MPI-ESM simulations on a $1.875\,^{\circ}\,\mathrm{x}\,1.875\,^{\circ}$ grid (T63).

2.2. ERA-Interim

The ERA-Interim reanalysis data (DEE et al., 2011) from the ECMWF is considered for several purposes: first, it is employed as large-scale forcing for the dynamical downscaling (see section 2.3), and the resulting dataset is used to assess the predictive skill of the baseline1 hindcasts on the regional scale. Second, daily wind speeds serve as explanatory variables to train the statistical-dynamical approach (see Section 3). Wind speeds are considered instead of wind gusts since the reanalysis or climate model datasets do not generally provide a wind gust variable derived with a sophisticated gust parameterization (cf. discussion in ROCKEL and WOTH, 2007; BORN et al., 2012). This is also the case for the ERA-interim data (IFS DOCUMENTATION CY40R1, 2013). Third, mean sea level pressure data is used as input for the cyclone tracking method (see Section 3.3). The ECMWF data has a horizontal resolution of $0.75\,^{\circ}\,\mathrm{x}\,0.75\,^{\circ}$ and is available in 6-hourly time steps from 1979 until present. For consistency reasons, the ERA-Interim wind speeds are bilinearly interpolated to the target grid (MPI-ESM-LR) before the transfer function to the RCM data is built.

2.3. COSMO-CLM

The regional-scale wind gust speeds are simulated with the COSMO-CLM (RCM of the COnsortium for Small-scale MOdelling in CLimate Mode version 4.8., hereafter CCLM [ROCKEL et al., 2008]). This dynamical downscaling (DD) approach uses ERA-Interim reanalysis data as initial and boundary conditions for simulations with a horizontal resolution of 25 km x 25 km (0.22 ° x 0.22 °). The simulation area covers Europe including most of the East Atlantic sector. For the following investigations, we consider a section of this area containing all grid points between 13 °W, 40 °E, 25 °N and 71 °N (Figure 1a).
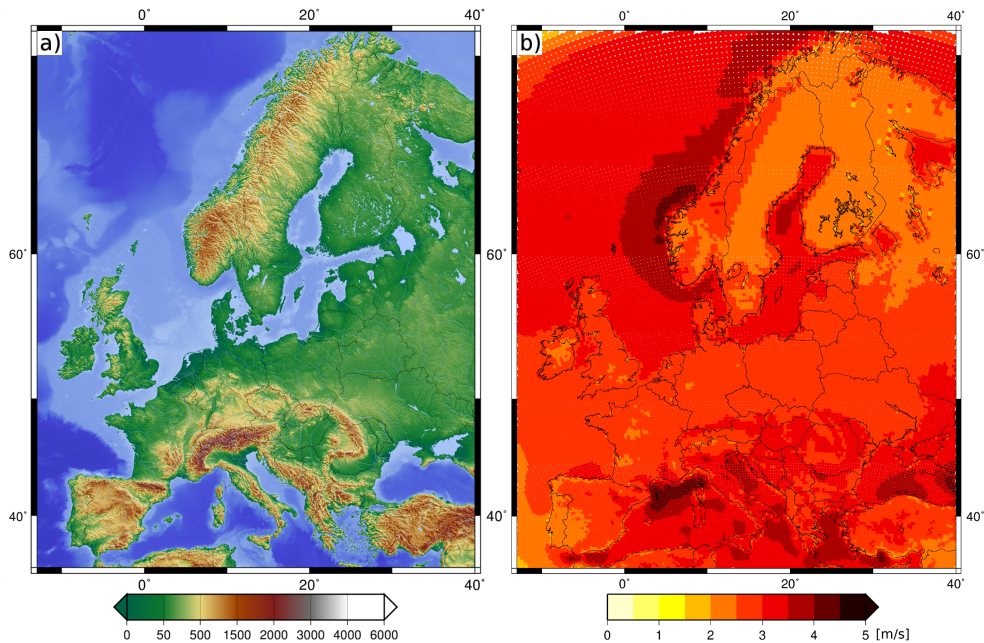
Figure 1: a) Investigation area and topography. b) RMSE between DD gust speeds and SDD peak wind speeds.

For the calculation of gusts, different parameterizations are available in the CCLM (BORN et al., 2012). In this study, we consider wind gusts estimated with the approach from the German Weather Service (DWD), where gusts are computed at 10 m height using friction velocity as estimator for turbulence (SCHULZ, 2008). The DWD gust parameterization distinguishes between convective and dynamical gusts. Here, the maximum of both convective and dynamical is used. BORN et al. (2012) found that wind gust estimates obtained with the DWD-approach correspond well with both other schemes and observations. Further, they concluded that the method is well calibrated for Germany. The wind gust estimation is computed at each step of the RCM and the largest value of the preceding 60 minutes is stored at every hour. Within the context of the present paper, we use the daily maximum of gust speed for every grid point.

3. Methods

3.1. Estimation of a Transfer Function between Regional and Large Scale

To estimate a transfer function between regional-scale gust data and large-scale wind data, we follow the statistical-dynamical downscaling (SDD) methodology introduced in HAAS and PINTO (2012), which is based on multiple linear regression. In general, the SDD is trained by linking daily maximum wind gusts simulated by the CCLM (regional scale) to ERA-Interim reanalysis daily 10m wind speeds (large scale). Hence, the resulting values from the application of the regression model can be seen as a proxy for wind gusts, but should not be named wind gusts as they were obtained without using an explicit wind gust parameterization like in the CCLM. Therefore, the downscaled wind values derived from the SDD approach are hereafter referred to as peak wind speeds, and are a proxy for gust speeds.

As the transfer function is designed for an application on large-scale MPI-ESM-LR runs, which are simulated on a different grid from that of ERA-Interim, the ERA-Interim data ($0.75° \times 0.75°$) is initially bilinearly interpolated to the MPI-ESM-LR grid ($1.875° \times 1.875°$). The regional-scale daily peak wind speed at each CCLM grid point (predictand y) is estimated by the 10m wind speeds (x_k) of the 16 surrounding grid points of the large-scale model. That involves the estimation of one regression model per CCLM grid point:

$$y_i = c_0 + c_1 x_{i1} + \ldots + c_k x_{ik} + \epsilon_i \qquad i = 1, \ldots, e \qquad k = 1, \ldots, 16 \qquad (1)$$

where e is the number of included daily values. The regression coefficients $c_k = \hat{\mathbf{c}}$ are estimated by the method of least squares:

$$\hat{\mathbf{c}} = (\mathbf{X}^T \mathbf{X})^{-1} \mathbf{X}^T \mathbf{y} \qquad (2)$$

where $\mathbf{X}$ is the matrix of large-scale predictors x_{ik} and $\mathbf{y}$ is the vector of predictands y_i. As only the DD includes an explicit gust parameterization, the definitions "DD gust speeds" and "SDD peak wind speeds" are used hereafter.

HAAS and PINTO (2012) demonstrated that the SDD methodology is capable of reproducing DD footprints of extreme windstorms over Europe. Furthermore, a validation against observations provided evidence that the skills of DD and SDD are similar. In Section 4, we test how the methodology performs when using not only extreme events but the whole climatology.

3.2. Quantile Verification Skill Scores

In order to assess the benefit of the initialization of the hindcasts for decadal predictability, both the hindcasts and the uninitialized historical runs are verified against ERA-Interim with the quantile verification score (QVS). For this purpose, all ten ensemble members are used to determine the ensemble mean quantiles per decade. The quantiles are calculated for different lead times after the initialization and cover the period 1979 - 2005, where all datasets are available. The quantiles of the simulated wind speeds in the original MPI-ESM-LR resolution (q_{MPI}) are evaluated against the ERA-Interim wind speed quantiles (q_{ERA}) resulting in the following quantile verification score (QVS, cf. FRIEDERICHS and HENSE, 2007):

$$QVS_{MPI}(\tau) = \sum_{i=1}^{n} \rho_\tau (q_{MPI,i} - q_{ERA,i}) \tag{3}$$

The parameter q indicates the ensemble mean τ-quantile, with τ equal to $\{0.01, 0.05, 0.1, 0.25, 0.5, 0.75, 0.9, 0.95, 0.98, 0.99\}$, specifying the associated probability. The index MPI is equal to *hist* for the historical runs or to *dec* for the decadal hindcasts. The index i refers to the initialized hindcasts and depends on the considered lead time (e. g. hindcast initialized in 1979 to hindcast initialized in 2005 for lead year 1). ρ_τ is the check function for the τ-quantiles where

$$\rho_\tau (x) = \begin{cases} \tau \cdot x & \text{if} \quad x \geq 0 \\ (\tau - 1) \cdot x & \text{if} \quad x < 0 \end{cases} \tag{4}$$

for x equal to the difference between the MPI quantiles and the ERA quantiles. As a consequence, the overestimation ($x > 0$) of high quantiles by the MPI is more penalized than the overestimation of low quantiles, and vice versa in case of an underestimation ($x < 0$).

The quantiles of the peak winds obtained from the SDD approach applied to the MPI-ESM-LR wind speeds ($q_{MPI,SDD}$) are compared against gust quantiles downscaled by DD from the ERA-Interim wind speeds ($q_{ERA,DD}$), resulting in the following QVS:

$$QVS_{MPI,SDD}(\tau) = \sum_{i=1}^{n} \rho_\tau (q_{MPI,SDD,i} - q_{ERA,DD,i}) \tag{5}$$

Following FRIEDERICHS and HENSE (2007), we calculate the quantile verification skill scores (QVSS) based on the above-introduced QVS. For this

purpose, the QVS of initialized decadal hindcasts (dec) are compared to the QVS of the uninitialized historical runs ($hist$) as follows:

$$QVSS = 1 - \frac{QVS_{dec}}{QVS_{hist}} \qquad (6)$$

The same equation is used for the downscaled historical runs ($hist, SDD$) and hindcasts (dec, SDD). A QVSS value of zero indicates that no added value is gained from initialization with observed atmospheric and oceanic states. In case of a positive QVSS the skill of the initialized hindcasts is higher than the skill of the uninitialized historical runs, meaning that the initialization leads to an enhanced decadal predictability.

3.3. Cyclone Tracking

A cyclone identification and tracking method (MURRAY AND SIMMONDS, 1991; PINTO et al., 2005) is applied to 6-hourly ERA-Interim data to obtain complete cyclone life cycles. The Laplacian of the mean sea level pressure is used for cyclone identification as a proxy for the relative geostrophic vorticity (cf. MURRAY AND SIMMONDS, 1991). Trajectories are then built using the tracking algorithm and taking into account the most likely trajectory of a cyclone under the given state of the large-scale circulation. The resulting cyclone tracks include information of the basic properties of the cyclone (e. g. core pressure, propagating velocity) and its changes over time. In this study, the approach is used to quantify cyclone activity in certain time periods.

4. Validation: Estimated Peak Winds versus Simulated Gusts

In order to analyze whether the SDD approach is suitable to quantify the whole range of wind speeds from which the peak wind speeds are recalculated, the estimated transfer function is reapplied to the ERA-Interim data. The SDD transfer function is applied on each calendar day between 1979 and 2010. The resulting peak wind speeds are then compared to the wind gust speeds simulated by CCLM (DD).
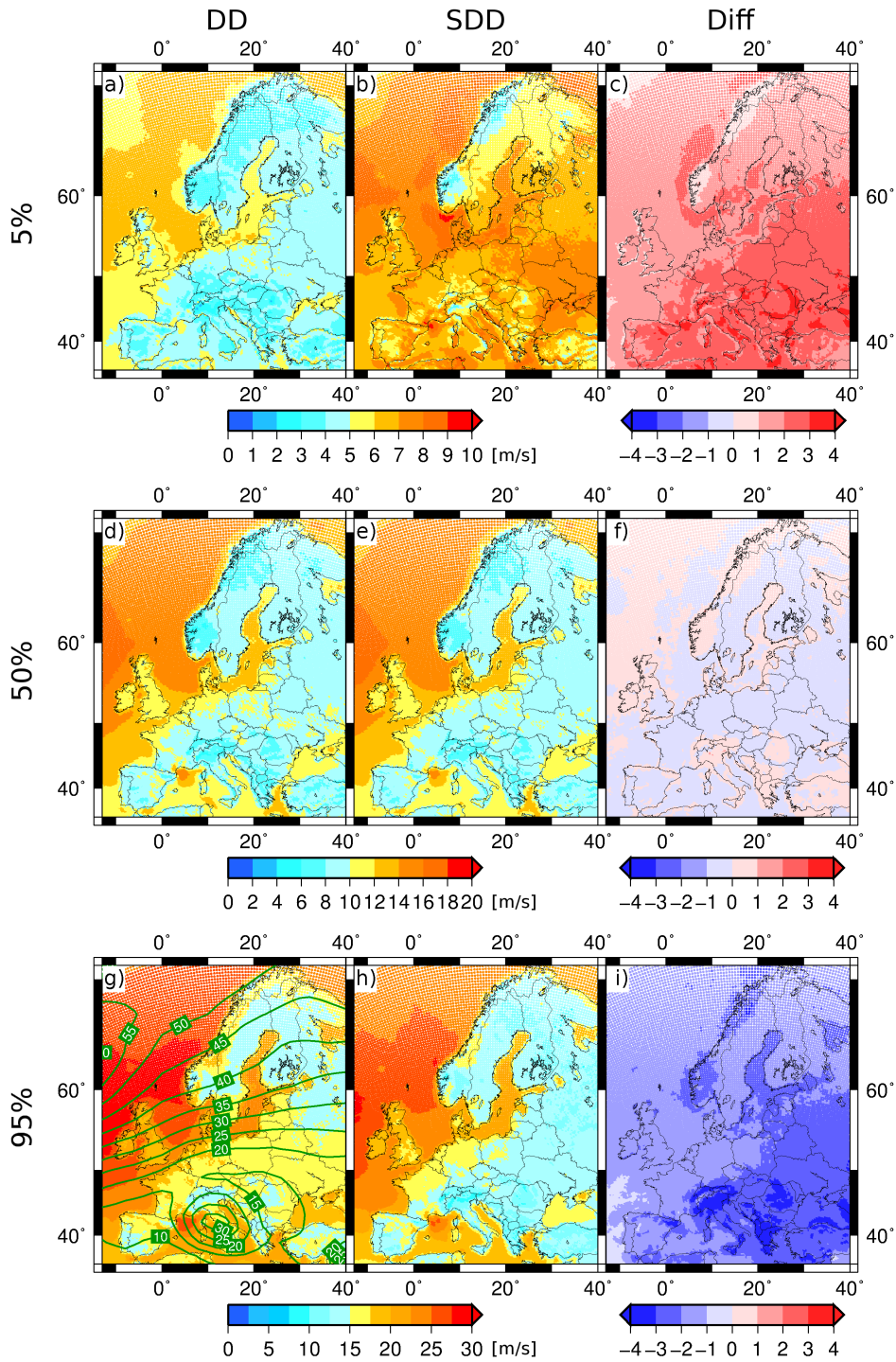
Figure 2: From top to bottom: 5 %, 50 %, and 95 % quantiles of dynamically downscaled gust speeds (left) and statistical-dynamically downscaled peak wind speeds (middle) for years 1979 - 2010 of ERA-Interim. Note the different labeling of color bars. Right: Differences between the quantiles of statistical-dynamical and dynamical downscaling (SDD-DD). Green lines: cyclone track density per year per $(deg.lat.)^2$ for 1979 - 2010 (based on ERA-Interim).

The differences between DD gust speeds and SDD peak wind speeds (proxy for gusts) are accumulated over the investigation period to calculate the RMSE shown in Figure 1b. At most grid points, the RMSE ranges between $2\,\mathrm{ms}^{-1}$ and $3\,\mathrm{ms}^{-1}$, with the lowest values over Eastern Scandinavia. This leads to an overall RMSE of $2.98\,\mathrm{ms}^{-1}$ for the entire investigation area. The highest deviations occur over the Mediterranean at the southeastern coast of France and over the North Sea near the Norwegian coast. While the generally high discrepancies over the North Sea and the North Atlantic are likely related to the variable roughness length over sea surfaces (due to temporal variable wave heights), it is unclear what leads to the particular large deviations near the Norwegian coast. The differences over the Mediterranean are presumably caused by local wind phenomena like the Mistral (canalized wind in the Rhone valley), which are not well reproduced by the SDD approach.

Detailed results of the SDD simulated peak winds, the DD simulated gusts and the differences of both downscaling methods are presented for selected quantiles (5 %, 50 %, and 95 %) in Figure 2. To a first order, the wind values for the low quantiles are overestimated by the SDD (Figure 2c, 5 %), those for the middle quantiles are well reproduced (Figure 2f, 50 %) and those for the high quantiles are underestimated (Figure 2i, 95 %). For the lower quantiles (Figure 2a-c) DD wind gusts are conspicuously higher than for SDD peak wind speeds and the highest differences are apparent in areas close to high orography. For higher quantiles, the deviations between SDD and DD are most pronounced near the Norwegian coast, Mediterranean and Southeastern Europe (Figure 2g-i). Figure 2g documents the good agreement between areas with enhanced cyclone activity and those with high gust speeds, in particular over the North Atlantic and to a lower extent over the Mediterranean Sea, where the area with maximum wind speeds is slightly shifted westwards.

The overestimation (underestimation) of low (high) wind quantiles by the SDD approach leads to steeper cumulative density functions (CDFs) for the SDD values than those for the DD gusts, yielding narrower probability density functions (PDFs). As an example, the CDFs and PDFs for a grid point next to Cologne (Germany; 6.894547 °E, 50.88583 °N are fitted by a Weibull distribution (Figure 3). The figure also reveals that the PDF of the SDD values is not only narrower, but also a bit skewed to the right: the range of gust speeds above the median is wider than the one below the median. This explains the slight tendency to lower SSD medians compared to DD medians (cf. Figure 2f).

Such discrepancies are systematic, and they appear in both the initialized hindcasts and the uninitialized historical runs. As our aim is to compare both simulations to assess the benefit of the initialization for decadal predictability, the impact of the systematic bias on the computed QVSS is assumed to be negligible. Therefore, the transfer function can be applied to the full en-
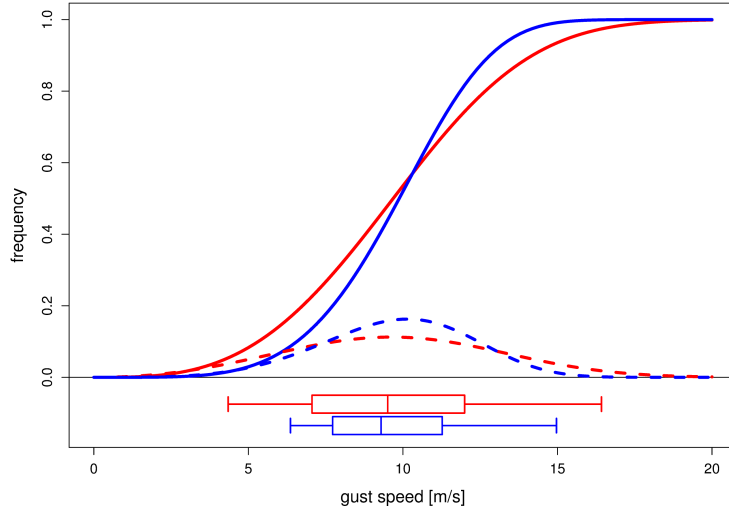
Figure 3: Example cumulative density functions (solid lines) and probabilistic density functions (dashed lines) fitted with a theoretical Weibull distribution at a grid point next to Cologne (Germany; 6.894547 °E, 50.88583 °N). Red denotes dynamically downscaled values and blue statistical-dynamically downscaled values. The box-and-whisker plots show the 5 %, 25 %, 50 %, 75 %, and 95 % quantiles.

semble of MPI-ESM-LR without any adjustments. Nevertheless, for specific applications, e.g. for an operational MiKlip prediction system, a bias correction might be appropriate to rescale the peak wind speeds to the range of simulated wind gust speeds and/or observed wind gusts in order to prevent under- or overestimations.

5. Application: Decadal Hindcasts on Global and Regional Scale

The aim of this section is to assess the decadal predictability of the 2nd generation decadal hindcast ensemble of the MPI-ESM-LR in terms of global and regional wind characteristics. For this assessment, we first examine whether the hindcasts are able to capture (peak) wind speed quantiles during the extraordinary stormy period 1990 - 1993. Further, the predictive skill of the initialized hindcasts compared to the historical uninitialized runs is determined for different wind quantiles. The dependency of the skill on the forecast time, as well as the spread within the MPI-ESM-LR ensemble is quantified. Most analyses are performed for both MPI-ESM-LR large-scale wind speeds and SDD regional-scale peak wind speeds.

The early 1990s are characterized by winters with above-average stormi-
ness over Europe (e.g., ALEXANDERSSON et al., 2000; FESER et al., 2014).
In particular, the 1990 and 1993 seasons featured clusters of windstorms
reaching over Western Europe in rapid succession, embedded in an intensified
and extended eddy driven jet (PINTO et al., 2014). The following analyses
focus on the period 1990 - 1993, which are compared to the climatology of the
years 1979 - 2005. Figure 4a depicts the 95 % quantiles of ERA-Interim wind
speeds for 1990 - 1993, whose positive anomalies are in agreement with the ob-
served enhanced windstorm activity, especially over the North Atlantic, the
North Sea and Central Europe. For other regions like the Mediterranean, the
95 % quantiles of the ERA-Interim wind speeds are lower during 1990 - 1993
compared to the climatology (negative deviation, blue colors). A similar pic-
ture is found for SDD simulated regional-scale peak wind speeds (Figure 4e).
Only the differences in the south of the investigation area are around zero
over land. Both positive and negative deviations are in agreement with the
anomalies of the number of cyclone tracks per year (green lines in Figure 4e).
The positive anomalies of the 95 % quantiles are in line with the enhanced
number of cyclones over the northern and central parts of the investigation
area, as the most intense near surface wind speeds associated with a cyclone
crossing over this area are typically located a few hundreds of kilometers
south of the cyclone core (e.g. PFAHL, 2014, their Figure 8a). Further, the
negative deviations over Southern Europe agree with weak cyclone anomalies
(around zero) over this area.

In order to verify whether the hindcasts are able to capture the wind
characteristics of this anomalous stormy period, the 95 % quantiles of daily
maximum wind speeds are calculated for the initialized MPI-ESM-LR runs
for the period 1990 - 1993. This four-year period is taken from hindcasts
with different initializing dates to analyze the dependency on the lead time
after initialization. We consider the ensemble means of all ten realizations
for the years 1 - 4 of the hindcast ensemble valid from January 1990, years
2 - 5 of the ensemble valid from January 1989, and years 6 - 9 of the ensemble
valid from January 1985. The quantiles for 1990 - 1993 are compared to
the quantiles of the climatology (1979 - 2005) derived from the uninitialized
historical runs. Figure 4b-d shows that the large-scale wind anomalies in the
hindcasts for this period (1990 - 1993) are similar to those in ERA-Interim
in terms of the sign of the anomalies, although characterized by a smaller
magnitude (Figure 4a). Only for years 6 - 9 (Figure 4d), some discrepancies
against ERA-Interim are noticeable. The same results can be found for the
SDD regional-scale peak winds (Figure 4f-h). For years 1 - 4, the patterns
of the downscaled MPI-ESM-LR runs agree best with the downscaled ERA-
Interim quantiles, in spite of the different magnitudes (Figure 4e,f). This
result suggests that the initialization enhances the predictive skill mainly for
short lead times.
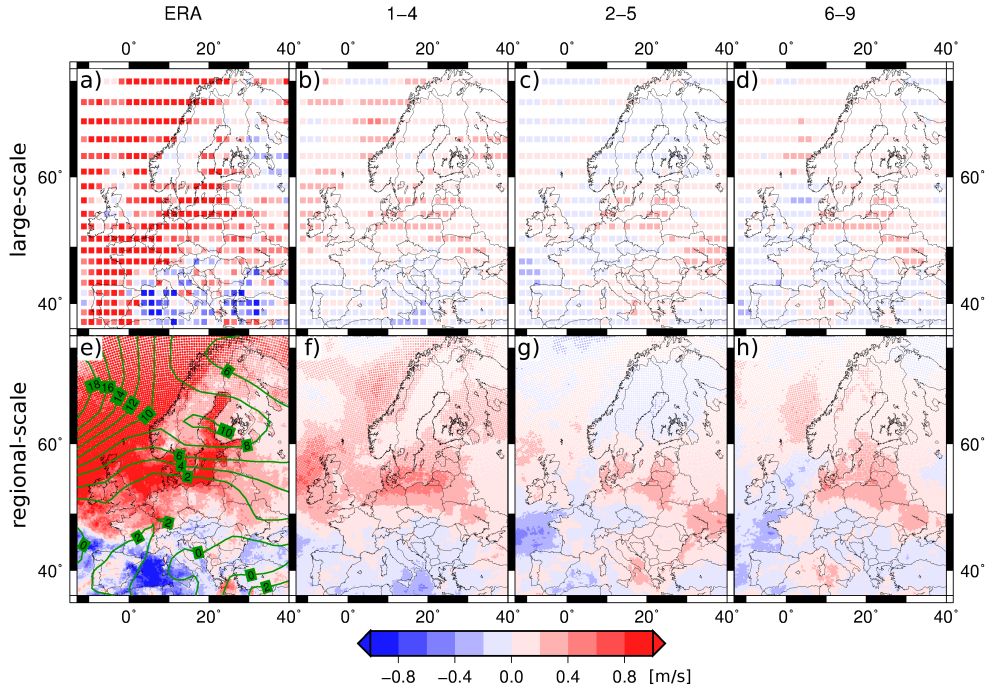
Figure 4: Deviations of the years 1990‑1993 from the climatology 1979‑2005. Top: 95 % quantiles of large-scale wind speed for (a) ERA-Interim data, (b) years 1‑4 from dec1989, (c) years 2‑5 from dec1988, and (d) years 6‑9 from dec1984. (b)‑(d) are deviations from uninitialized MPI-ESM-LR simulations of the years 1979‑2005. All MPI-ESM-LR simulations are ensemble means of ten realizations (initialized) or three realizations (uninitialized). Bottom: same as top row but for statistical-dynamically downscaled peak wind values. (e) Green: cyclone track density per year per $(deg.lat.)^2$ for the period 1990 to 1993 minus 1979 to 2005 (based on ERA-Interim).

The weaker predictive skill for later years after the initialization can be explained by an increasing ensemble spread with increasing forecast time, quantified by the standard deviation of the ten ensemble members. The corresponding standard deviations of the 10 realizations are shown in Figure 5 for the years 1‑4, 2‑5 and 6‑9. For all lead times, the standard deviation and thus the spread of the ensemble is highest over the sea, probably caused by higher offshore wind speeds. This is valid for both the large-scale MPI-ESM-LR wind speeds (Figure 5a-c) and SDD simulated peak wind speeds (Figure 5d-f). Over land, the standard deviation is similar for the years 1‑4 (Figure 5a,d) and the years 2‑5 (Figure 5b,e), and increases considerably for the years 6‑9 (Figure 5c,f). The higher the variation between the ensemble members, the wider the range of wind speeds, making the identification of outliers less probable. This leads to comparatively smaller deviations between this period and the climatology.
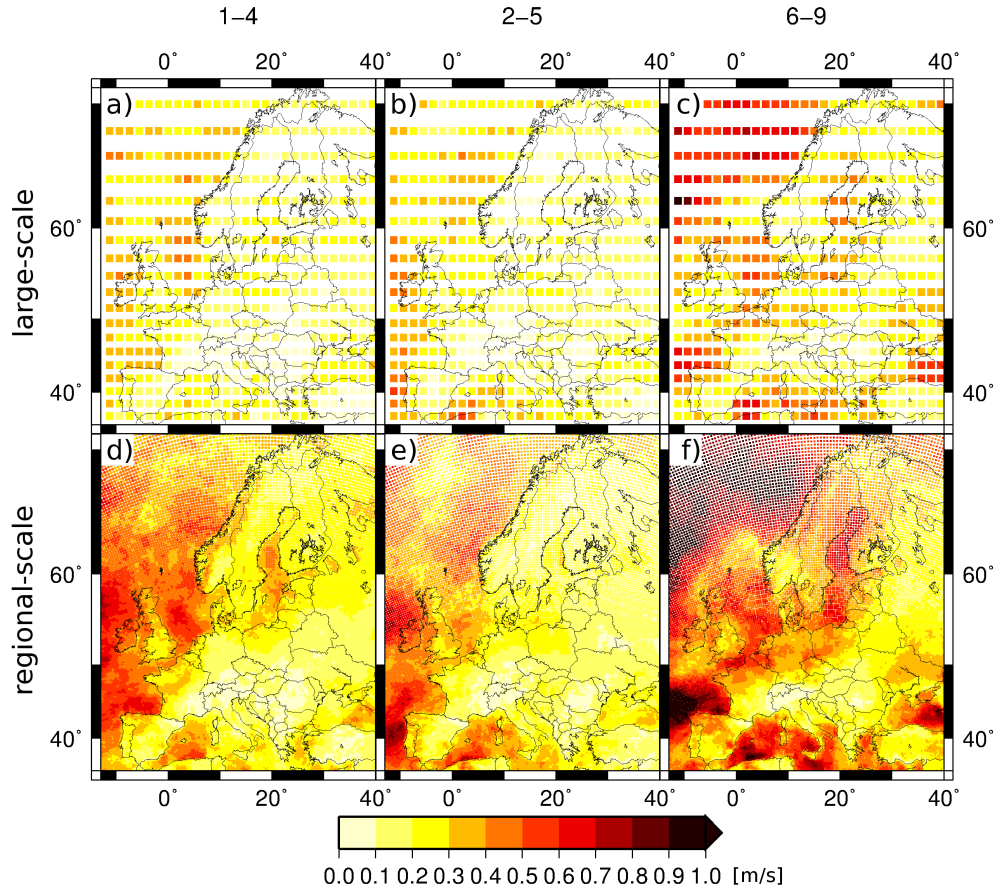
Figure 5: Ensemble spread of the 95 % wind speed quantiles of the ten initialized MPI-ESM-LR realizations quantified as its standard deviation. Top: (a) years 1 - 4 from decade starting in January 1990, (b) years 2 - 5 from decade starting in January 1989, and (c) years 6 - 9 from starting in January 1985 of large-scale wind speeds. Bottom: as (a) - (c), but for regional-scale SDD simulated peak winds.

To quantify the predictive skill of the MPI-ESM-LR before and after applying the downscaling technique, quantile verification skill scores are calculated (QVSS, see Section 3.2.). For this purpose, all the hindcasts initialized in the period 1979 - 2005 are taken into account to calculate ensemble mean quantiles for different lead times. In Figure 6, the QVSS of the 95 % quantiles is shown for both the large-scale MPI-ESM-LR wind speeds and the SDD regional-scale peak winds for four different lead times. The highest positive skill scores (averaged over all grid points) are found for year 1 after initialization, revealing that the initialization of the hindcasts enhances the predictability for short forecast periods (Figures 6a and 6e). Skill scores are highest over Central Europe. While the negative skill score in the south of the investigation area increase, the positive skill score over Central Europe

decreases with increasing time after the initialization and turns negative over parts of the North Sea. Over land, the QVSS decreases slightly with increasing forecast time, but the values are still positive except for parts of the Alpine region. Overall, these results indicate that the decadal hindcasts are closer to the reanalysis than the uninitialized historical runs and that the initialization with realistic boundary conditions improves the predictive skill over Central Europe, in particular for short lead times. This is valid for both MPI-ESM-LR wind speeds and SDD regional-scale peak winds speeds.
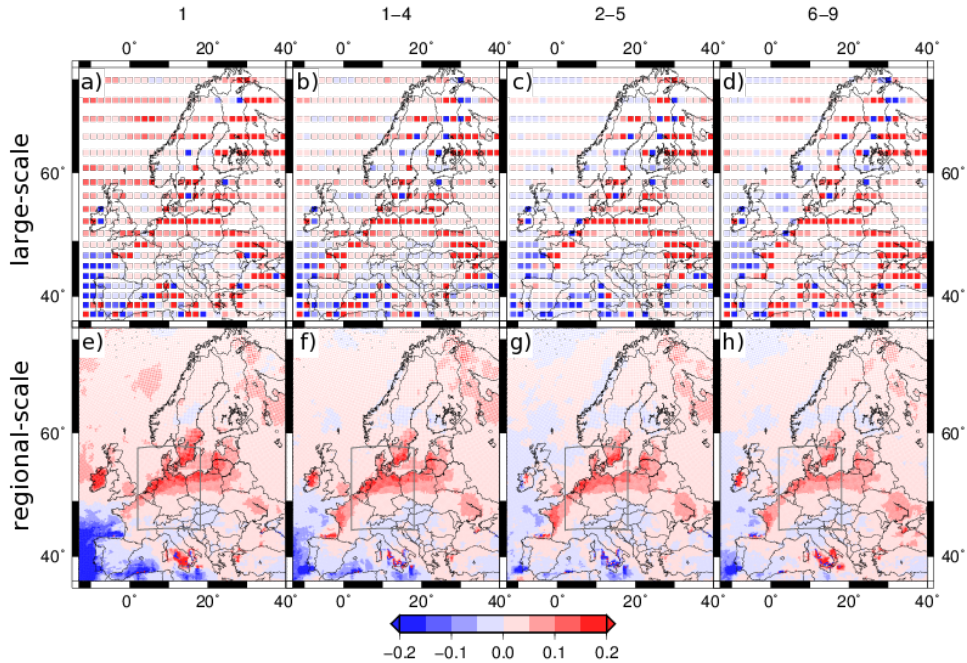
Figure 6: Quantile verification skill scores of the 95 % wind speed and peak wind speed quantiles for different lead times. Top: (a) year 1, (b) years 1 - 4, (c) years 2 - 5, and (d) years 6 - 9 for large-scale MPI-ESM-LR winds speeds. Bottom: same as top but SDD simulated regional-scale peak wind speeds. Grey rectangle: Smaller investigation area (cf. Tables 1 and 2).

The QVSS is subsequently determined for different quantiles of the SDD peak wind speeds. This is shown in Figure 7 for year 1 - 4 after the initialization for the quantiles 5 %, 50 %, 75 %, 90 %, 98 %, and 99 %. For all quantiles equal or above 75 %, the spatial QVSS patterns are quite similar, exhibiting the highest skills along a belt extending from the UK to the Baltic Sea (Figure 7c-f). Although a similar pattern is also observable for the 50 % quantile (Figure 7b), there are some negative values within the areas of positive QVSS. For quantiles below 50 %, the structure of positive and negative skill scores is quite diffuse. A very heterogeneous QVSS for example is found for the 5 %

quantile (Figure 7a), which indicates that it is generally difficult to predict weak wind periods. While this is probably associated with the large-scale weak pressure gradients during these periods, it is unclear why the distribution of the QVSS for this percentile is quite patchy, with high values over e. g. Central Europe and low values over Scandinavia.
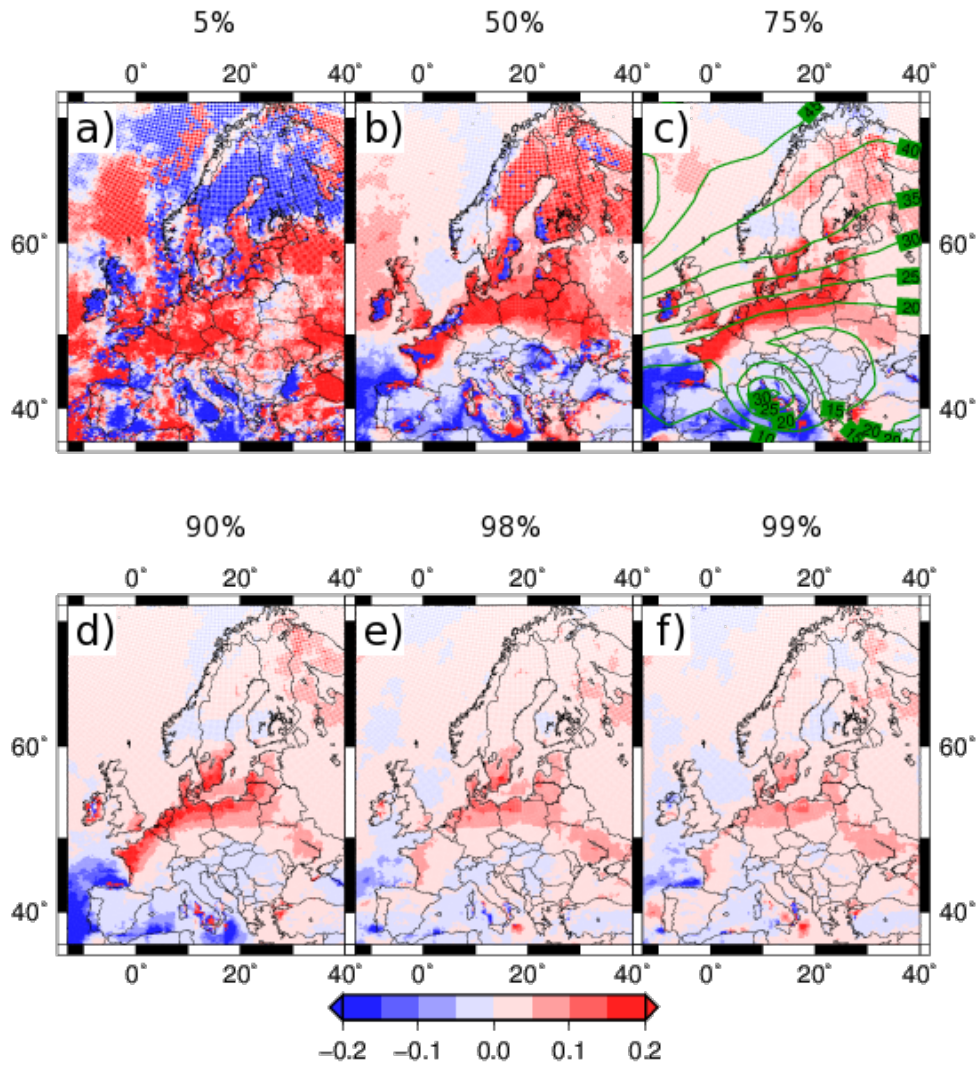
Figure 7: Quantile verification skill scores for SDD simulated regional-scale peak winds for years 1 - 4 after initialization and for different quantiles: (a) 5 %, (b) 50 %, (c) 75 %, (d) 90 %, (e) 98 %, and (f) 99 %. Green lines: cyclone track density per year per $(deg.lat.)^2$ for the period 1979 to 2005 (based on ERA-Interim).

The observed structure for the high quantiles over Northern and Central Europe corresponds well to the climatology of cyclones per year determined

from ERA-Interim, which shows a North-South gradient over this area (green lines in Figure 7c). This implies that the best performance can be found for strong wind speeds associated with extratropical cyclones. However, the agreement between cyclone activity and the QVSS is less tight for Southern Europe. With increasing quantiles, the magnitude of the skill score decreases. Nevertheless, for the highest quantile (99 %, Figure 7f) QVSS is predominantly positive over land, which means that the initialization provides an added value with respect to the decadal predictability.

Finally, the QVSS is determined for quantiles of spatially accumulated wind speeds. This is done for all grid points within the investigation area (Figure 1a) and within a smaller domain including Germany and parts of its neighboring countries (see grey rectangle in Figure 6). Table 1 summarizes the skill scores for large-scale wind speeds in the original MPI-ESM-LR resolution. If only quantiles greater than or equal 50 % are considered, the highest skill scores are obtained for the first year after initialization. For quantiles greater than or equal to 90 % the skill scores typically decrease with increasing lead time. While this finding is valid for both investigation areas, better values are found for the smaller area, which includes primarily onshore areas. The results for all lead times and both regions indicate that the enhancement of the decadal predictability by initialization of the hindcasts is highest for upper wind quantiles.

Table 1: QVSS for MPI-ESM-LR large-scale wind speeds. The QVSS values are spatially accumulated over all grid points within the investigation area (EU, Figure 1) and within a smaller domain including Germany (DE, Figure 6) for selected quantiles and different lead times (years).

Lead times	Area	Quantiles									
		1 %	5 %	10 %	25 %	50 %	75 %	90 %	95 %	98 %	99 %
1	EU	-0.060	-0.045	-0.044	-0.024	-0.007	0.009	0.029	0.038	0.045	0.053
	DE	-0.029	-0.027	-0.029	-0.032	0.011	0.060	0.060	0.060	0.060	0.061
1-4	EU	0.002	-0.008	0.004	0.019	0.029	0.027	0.024	0.027	0.027	0.028
	DE	-0.016	-0.018	-0.018	0.005	0.050	0.072	0.057	0.051	0.047	0.045
2-5	EU	0.003	0.007	0.022	0.030	0.040	0.030	0.020	0.020	0.019	0.021
	DE	-0.011	-0.007	0.015	0.029	0.071	0.077	0.051	0.043	0.039	0.035
6-9	EU	-0.003	-0.003	0.010	0.019	0.028	0.028	0.021	0.022	0.022	0.025
	DE	-0.025	-0.029	-0.030	-0.009	0.046	0.067	0.042	0.034	0.030	0.028

The results are less clear for the SDD simulated regional-scale peak wind speeds (Table 2). For high quantiles (90 % or higher) the skill scores are higher for the smaller domain than for the large European sector across all lead times except for year 1 after the initialization. The differences between the maxima of the QVSS of the MPI-ESM-LR wind speeds and of SDD simulated peak winds may be induced by a stronger influence of the SDD

underestimation of the high quantiles on either the hindcasts or the historical runs. Tables 1 and 2 cannot be directly compared as the first includes results of the large-scale wind speed quantiles, while the second summarizes the regional-scale peak wind speed results. The generally lower skill scores for the latter can be attributed to the higher variability of gust / peak wind speeds compared to wind speeds (e.g. BORN et al., 2012; HAAS et al., 2014). Therefore, it is not unexpected to find lower skill for regional scale peak winds than for global scale winds. Nevertheless, the results clearly indicate an improvement of the predictive skill for both the MPI-ESM-LR large-scale wind speeds and the SDD regional-scale peak wind speeds in the initialized hindcasts compared to the uninitialized historical runs. Additionally to the identified predictive skill of the MPI-ESM-LR wind speeds, the SDD allows for the estimation of peak wind speeds as a proxy for gusts.

Table 2: Same as Table 1 but for SDD simulated regional-scale peak wind speeds.

Lead times	Area	Quantiles									
		1 %	5 %	10 %	25 %	50 %	75 %	90 %	95 %	98 %	99 %
1	EU	-0.134	-0.234	-0.211	-0.067	-0.003	0.002	0.010	0.016	0.021	0.023
	DE	-0.209	-0.280	-0.253	-0.059	0.022	0.011	0.011	0.014	0.020	0.021
1-4	EU	0.027	0.034	0.019	0.001	0.023	0.014	0.011	0.012	0.013	0.012
	DE	0.154	0.085	0.040	-0.004	0.018	0.016	0.014	0.015	0.016	0.014
2-5	EU	-0.015	-0.008	-0.025	-0.032	0.038	0.020	0.010	0.010	0.010	0.009
	DE	-0.107	-0.038	-0.037	-0.071	0.037	0.024	0.014	0.014	0.013	0.012
6-9	EU	-0.083	-0.011	-0.007	-0.005	0.019	0.016	0.011	0.011	0.012	0.013
	DE	-0.153	-0.030	-0.007	-0.023	-0.005	0.015	0.015	0.015	0.016	0.015

6. Summary and Conclusion

In this study, the decadal predictability of large-scale wind speeds from MPI-ESM-LR hindcasts and of SDD simulated regional-scale peak wind speeds over Europe is evaluated. The SDD model uses a linear transfer function to derive the peak wind speeds from large-scale MPI-ESM-LR wind speeds. The transfer function is trained with the ERA-Interim reanalysis data and CCLM wind gust speeds. In HAAS and PINTO (2012), this approach has already been applied on a selection of severe windstorms. Here, we showed that the SDD approach is also able to provide a good estimate for the complete range of peak wind speeds. Still, the SDD shows an overestimation for the low quantiles and an underestimation for the high quantiles, which leads to a narrower PDF of the peak wind speeds.

The period 1990 - 1993 is characterized by a strong windstorm activity. In order to evaluate the skill of our methodology, we have compared the 95 % quantiles of this period to the value of the whole climatology (1979 -

2005). As already found for reanalysis data, the large-scale MPI-ESM-LR wind speeds as well as the downscaled regional-scale peak wind speeds show a positive anomaly of the 95 % quantile during this time period over the North Atlantic, the North Sea and Central Europe. The magnitudes of the anomalies in the hindcasts for the period 1990 - 1993 are generally smaller than for ERA-Interim and depend on the forecast time. In particular, the positive anomalies of the 95 % quantile are best captured by the MPI-ESM-LR hindcast simulations for short lead times (years 1 - 4). This may be due to the enhanced ensemble spread with increasing forecast times.

To analyze the performance of the decadal hindcasts both in its original MPI-ESM-LR resolution and in the high resolution after the application of the SDD, quantile verification skill scores are calculated. These skill scores are key for the quantification of the added value of the initialized simulations compared to uninitialized historical runs. Regarding different lead times, we achieved the best QVSS for the first years after the initialization. The skill score values typically decrease with increasing time after the initialization, sometimes becoming negative, especially over offshore regions. Nevertheless, the results suggest that the observations used for initialization still play an important role at forecast times up to year 6 - 9 after the initialization. If different quantiles are considered, the QVSS patterns are almost unchanged for quantiles equal to or above 75 %, but the magnitude slightly decreases for higher quantiles.

The accumulated QVSS has been considered over two investigation areas (Europe versus Germany) and confirms the above results, especially for the MPI-ESM-LR wind speeds. The skill scores of the downscaled regional-scale peak wind speeds are generally smaller compared to the MPI-ESM-LR wind speeds. These differences can be partially attributed to the fact that peak wind speeds estimated by the SDD approach are a proxy for gust speeds, which have a higher variability than wind speeds and are thus more difficult to predict (i.e. smaller QVSS). Nevertheless, the added value is given before and after the downscaling when considering the initialized hindcasts and predictions instead of the uninitialized historical runs. This is the case particularly for quantiles equal and above 75 %.

The predominantly positive skill scores over Europe and the Eastern North Atlantic are in line with the results of MÜLLER et al. (2012), who compared surface temperatures of MPI-ESM-LR decadal hindcasts (1st generation ensemble) with observed surface temperatures. MIERUCH et al. (2014) obtained good results using these hindcasts for the prediction of decadal anomalies of temperature over Central Europe, while the results for precipitation were less promising.

Our results indicate that the predictive skill for large-scale MPI-ESM-LR wind speeds and regional-scale SDD simulated peak winds over Europe in the

2nd generation MiKlip ensemble runs is particularly promising for the 1 - 4 years lead time. This result is in line with the findings of KRUSCHKE et al. (2014), who analyzed the predictive skill of cyclone tracks over the Northern Hemisphere in the same simulations, and with REYERS et al. (2015), who identified a positive skill for wind energy applications over Europe, particularly for Northern and Western Germany. Such results suggest further applications of the SDD method to additional parameters to evaluate the skill of decadal hindcasts for Europe.

While providing an adequate method to obtain regional-scale peak winds from large-scale wind speeds, the SDD method leads to overestimated low quantiles and underestimated high quantiles. For further applications, a bias correction should be applied to adjust the peak wind speed results towards realistic wind gust distributions. For this study, the over- and underestimations were neglected, as they are systematic and concern the downscaling of all datasets used for comparisons, i.e. the initialized and uninitialized simulations. Our analyses showed that the initialized runs are appropriate for decadal predictions of wind and peak wind speeds. For predictions on the regional scale, our methodology is beneficial as it allows for the estimation of peak wind speeds as a proxy for gusts. Furthermore, it enables to quantify whether the probability of occurrence of strong wind events is above or below average for specific periods (an example is shown for the period 1990 - 1993 in this study). The proposed cost-efficient downscaling technique is therefore adequate for an application to large ensemble datasets and thus also for an implementation to operational decadal prediction systems.

Acknowledgments

References

ALEXANDERSSON, H., H. TUOMENVIRTA, T. SCHMITH, K. IDEN, 2000: Trends of storms in NW Europe derived from an updated pressure data set. – Clim. Res. **14**, 71–73.

BALMASEDA, M. A., K. MOGENSEN, A. T. WEAVER, 2012: Evaluation of the ECMWF ocean reanalysis system ORAS4. – Q. J. R. Meteorol. Soc. **139**, 1132–1161. DOI: 10.1002/qj.2063.

BOER, G. J., S. J. LAMBERT, 2008: Multi-model decadal potential predictability of precipitation and temperature. – Geophys. Res. Lett. **35**, L05706. DOI: 10.1029/2008GL033234.

BORN, K., P. LUDWIG, J. G. PINTO, 2012: Wind gust estimation for Mid-European winter storms: towards a probabilistic view. – Tellus A **64**, 17471. DOI: 10.3402/tellusa.v64i0.17471.

DEE, D. P., S. M. UPPALA, A. J. SIMMONS, P. BERRISFORD, P. POLI, S. KOBAYASHI, U. ANDRAE, M. A. BALMASEDA, G. BALSAMO, P. BAUER, P. BECHTOLD, A. C. M. BELJAARS, L. VAN DE BERG, J. BIDLOT, N. BORMANN, C. DELSOL, R. DRAGANI, M. FUENTES, A.J. GEER, L. HAIMBERGER, S. B. HEALY, H. HERSBACH, E.V. HÓLM, L. ISAKSEN, P. KÅLLBERG, M. KÖHLER, M. MATRICARDI, A.P. MC-NALLY, B. M. MONGE-SANZ, J.-J. MORCRETTE, B.-K. PARK, C. PEUBEY, P. DE ROSNAY, C. TAVOLATO, J.-N. THÉPAUT, F. VITART, 2011: The ERA-Interim reanalysis: Configuration and performance of the data assimilation system. – Q. J. R. Meteorol. Soc. **137**, 553–597. DOI: 10.1002/qj.828.

FESER, F., M. BARCIKOWSKA, O. KRUEGER, F. SCHENK, R. WEISSE, L. XIA, 2014: Storminess over the North Atlantic and northwestern Europe - A review. – Q.J.R. Meteorol. Soc. DOI: 10.1002/qj.2364.

FUENTES, U., and D. HEIMANN, 2000: An Improved Statistical-Dynamical Downscaling Scheme and its Application to the Alpine Precipitation Climatology. – Theor. Appl. Climatol. **65**, 119–135. DOI: 10.1007/s007040070038.

FRIEDERICHS, P., A. HENSE, 2007: A Probabilistic Forecast for Daily Precipitation Totals. – Weather and Forecasting, 23, 659–673. DOI: 10.1175/2007WAF2007051.1.

HAAS, R., J. G. PINTO, 2012: A combined statistical and dynamical approach for downscaling large-scale footprints of European windstorms. – Geophys. Res. Lett. **39**, L23804. DOI: 10.1029/2012GL054014.

HAAS, R., J. G. PINTO, K. BORN, 2014: Can dynamically downscaled windstorm footprints be improved by observations through a probabilistic approach? – J. Geophys. Res. - Atmospheres. DOI:10.1002/2013JD020882.

IFS DOKUMENTATION Cy40r1, 2013: Part IV physical processes. Chapter 3.10.4. Edited by Peter W. White. http://old.ecmwf.int/research/ifsdocs/CY40r1/IFSPart4.pdf

IPCC, 2012: Managing the Risks of Extreme Events and Disasters to Advance Climate Change Adaptation. A Special Report of Working Groups I and II of the Intergovernmental Panel on Climate Change [FIELD, C.B., V. BARROS, T.F. STOCKER, D. QIN, D.J. DOKKEN, K.L. EBI, M.D. MAS-TRANDREA, K.J. MACH, G.-K. PLATTNER, S.K. ALLEN, M. TIGNOR, AND P.M. MIDGLEY (eds.)] – Cambridge University Press, Cambridge, UK, and New York, NY, USA, 582 pp.

IPCC, 2013: Summary for Policymakers. In: Climate Change 2013: The Physical Science Basis. Contribution of Working Group I to the Fifth Assessment Report of the Intergovernmental Panel on Climate Change [STOCKER, T.F., D. QIN, G.-K. PLATTNER, M. TIGNOR, S. K. ALLEN, J. BOSCHUNG, A. NAUELS, Y. XIA, V. BEX AND P.M. MIDGLEY (eds.)]. – Cambridge University Press, Cambridge, UK, and New York, NY, USA.

JUNGCLAUS, J. H., N. FISCHER, H. HAAK, K. LOHMANN, J. MA-ROTZKE, D. MATEI, U. MIKOLAJEWICZ, D. NOTZ, J.-S. VON STORCH, 2013: Characteristics of the ocean simulations in MPIOM, the ocean component of the MPI Earth System Model. – Journal of Advances in Modeling Earth Systems, 5, 422–446. doi:10.1002/jame.20023.

KRUSCHKE, T., H. W. RUST, C. KADOW, G. C. LECKEBUSCH, U. ULBRICH, 2014: Evaluating decadal predictions of northern hemispheric cyclone frequencies. – Tellus A 66, 22830. DOI: 10.3402/tellusa.v66.22830.

MIERUCH, S., H. FELDMANN, G. SCHÄDLER, C.-J. LENZ, S. KOTHE, C. KOTTMEIER, 2014: The regional MiKlip decadal forecast ensemble for Europe. – Geosci. Model Dev. Discuss. **6**, 5711–5745. DOI: 10.5194/gmdd-6-5711-2013.

MSADEK, R., K. W. DIXON, T. L. DELWORTH, W. HURLIN, 2010: Assessing the predictability of the Atlantic meridional overturning circulation and associated fingerprints. – Geophys. Res. Lett. **37**, L19608. DOI: 10.1029/2010GL044517.

MÜLLER, W. A., J. BAEHR, H. HAAK, J. H. JUNGCLAUS, J. KRÖGER, D. MATEI, D. NOTZ, H. POHLMANN, J. S. VON STORCH, J. MAROTZKE, 2012: Forecast skill of multi-year seasonal means in the decadal prediction system of the Max Planck Institute for Meteorology. – Geophys. Res. Lett.

39, L22707. DOI: 10.1029/2012GL053326.

MURRAY, R. J., I. SIMMONDS, 1991: A numerical scheme for tracking cyclone centres from digital data. Part I: Development and operation of the scheme. – Aust. Meteor. Mag. **39**, 155–166.

OLDENBORGH, G. J. VAN, F. J. DOBLAS-REYES, B. WOUTERS, W. HAZELEGER, 2012: Skill in the trend and internal variability in a multi-model decadal prediction ensemble. – Clim. Dyn. **38**, 1263–1280. DOI: 10.1007/s00382-012-1313-4.

PFAHL S., 2014: Characterising the relationship between weather extremes in Europe and synoptic circulation features. – Nat. Hazards Earth Syst. Sci. 14, 1461–1475. DOI:10.5194/nhess-14-1461-2014.

PINTO, J. G., T. SPANGEHL, U. ULBRICH, P. SPETH, 2005: Sensitivities of a cyclone detection and tracking algorithm: Individual tracks and climatology. – Meteor. Z. **14**, 823–838. DOI: 10.1127/0941-2948/2005/0068.

PINTO, J. G., C. P. NEUHAUS, G. C. LECKEBUSCH, M. REYERS, M. KERSCHGENS, 2010: Estimation of wind storm impacts over West Germany under future climate conditions using a statistical-dynamical downscaling approach. – Tellus A **62**, 188–201. DOI: 10.1111/j.1600-0870.2009.00424.x.

PINTO, J. G., M. K. KARREMANN, K. BORN, P. M. DELLA-MARTA, AND M. KLAWA, 2012: Loss potentials associated with European windstorms under future climate conditions. – Clim. Res., 54, 1–20. DOI: 10.3354/cr01111.

PINTO, J. G., I. GÎMARA, G. MASATO, H. F. DACRE, T. WOOLLINGS, AND R. CABALLERO, 2014: Large-scale dynamics associated with clustering of extratropical cyclones affecting Western Europe, – J. Geophys. Res. - Atmospheres, 119, 13704–13719. DOI: 10.1002/2014JD022305.

POHLMANN, H., W. A. MÜLLER, K. KULKARNI, M. KAMESWAR-RAO, D. MATEI, F. S. E. VAMBORG, C. KADOW, S. ILLING, J. MAROTZKE, 2013: Improved forecast skill in the tropics in the new MiKlip decadal climate predictions. – Geophys. Res. Lett. **40**, 5798–5802. DOI: 10.1002/2013GL058051.

REYERS, M., J. G. PINTO, J. MÖMKEN, 2015: PINTO, J. G., I. GÎMARA, G. MASATO, H. F. DACRE, T. WOOLLINGS, AND R. CABALLERO, 2014: Large-scale dynamics associated with clustering of extratropical cyclones affecting Western Europe, – J. Geophys. Res. - Atmospheres, 119, 13704–13719. DOI: 10.1002/2014JD022305.

ROCKEL, B., A. WILL, A. HENSE, 2008: The regional climate model

COSMO-CLM (CCLM). – Meteorol. Z. **17**, 347–348.

ROCKEL, B., K. WOTH, 2007: Extremes of near surface wind speed over Europe and their future changes as estimated from an ensemble of RCM simulations. – Clim. Change 81, 267Ð280. DOI: 10.1007/s10584-006-9227-y.

SCHULZ, J. P., 2008: Revision of the turbulent gust diagnostics in the COSMO model. – COSMO Newsl. **8**, 17–22.

SMITH, D., S. CUSACK, A. COLMAN, C. FOLLAND, G. HARRIS, J. MURPHY, 2007: Improved surface temperature prediction for the coming decade from a global circulation model. – Science **317**, 796–799. DOI: 10.1126/science.1139540.

SMITH, D. M., A.A. SCAIFE, G. J. BOER, M. CAIAN, F. J. DOBLAS-REYES, V. GUEMAS, E. HAWKINS, W. HAZELEGER, L. HERMANSON, C. K. HO, M. ISHII, V. KHARIN, M. KIMOTO, B. KIRTMAN, J. LEAN, D. MATEI, W. J. MERRYFIELD, W. A. MÜLLER, H. POHLMANN, A. ROSATI, B. WOUTERS, K. WYSER, 2013: Real-time multi-model decadal climate predictions. – Clim. Dyn. **41**, 2875–2888. DOI: 10.1007/s00382-012-1600-0.

SOLOMON, A., L. GODDARD, A. KUMAR, J. CARTON, C. DESER, I. FUKUMORI, A.M. GREENE, G. HEGERL, B. KIRTMAN, Y. KUSHNIR, M. NEWMAN, D. SMITH, D. VIMONT, T. DELWORTH, G.A. MEEHL, AND T. STOCKDALE, 2011: Distinguishing the roles of natural and anthropogenically forced decadal climate variability implications for prediction. – Bull. Amer. Meteor. Soc. 92, 141–156. doi: 10.1175/2010BAMS2962.1.

STEVENS, B., M. A. GIORGETTA, M. ESCH, T. MAURITSEN, T. CRUEGER, S. RAST, M. SALZMANN, H. SCHMIDT, J. BADER, K. BLOCK, R. BROKOPF, I. FAST, S. KINNE, L. KORNBLUEH, U. LOHMANN, R. PINCUS, T. REICHLER, E. ROECKNER, 2013: Atmospheric component of the MPI-M Earth System Model: ECHAM6. – Journal of Advances in Modeling Earth Systems, 5, 146–172. doi:10.1002/jame.20015.

TAYLOR, K. E., R. J. STOUFFER, G. A. MEEHL, 2012: An Overview of CMIP5 and the Experiment Design. – Bull. Amer. Meteor. Soc. **93**, 485–498. DOI: 10.1175/BAMS-D-11-00094.1.

TENG, H., G. BRANSTATOR, G. A. MEEHL, 2011: Predictability of the Atlantic overturning circulation and associated surface patterns in two CCSM3 climate change ensemble experiments. – J. Clim. **24**, 6054–6076. DOI: 10.1175/2011JCLI4207.1.

Abbreviations

BMBF .... Federal Ministry of Education and Research (**B**undes**M**inisterium für **B**ildung und **F**orschung)

CCLM .... RCM of the **CO**nsortium for **S**mall-scale **MO**delling in **CL**imate **M**ode (COSMO-CLM)

CDF .... **C**umulative **D**ensity **F**unction

CMIP5 .... **C**oupled **M**odel **I**ntercomparison **P**roject Phase 5

DD .... **D**ynamical **D**ownscaling

ECHAM .... **EC**MWF **HAM**burg

ECMWF .... **E**uropean **C**entre for **M**edium-Range **W**eather **F**orecasts

MiKlip .... Decadal predictions (**Mi**ttelfristige **Kli**ma**p**rognosen)

MPI-ESM-LR .... **M**ax-**P**lanck-**I**nstitute **E**arth **S**ystem **M**odel in its **L**ower **R**esolution

MPIOM .... **M**ax-**P**lanck-**I**nstitute **O**cean **M**odel

ORAs4 .... **O**cean **R**e-**A**nalysis System of the ECMWF

PDF .... **P**robabilistic **D**ensity **F**unction

PRODEF .... **PRO**babilistic **DE**cadal **F**orecast for Central and Western Europe

QVSS .... **Q**uantile **V**erification **S**kill **S**core

RCM .... **R**egional **C**limate **M**odel

RMSE .... **R**oot **M**ean **S**quared **E**rror

SDD .... **S**tatistical-**D**ynamical **D**ownscaling

SS_{RMSE} .... RMSE **S**kill **S**core

6 Summary and discussion

The aim of this work is to optimize the prediction of gust speeds by combining wind and/or gust speeds of different data sets with different temporal and spatial resolutions. This is important for the analysis of windstorms and their impacts under current and future climate conditions. For this purpose, appropriate techniques have been developed and validated. These techniques imply mainly a statistical-dynamical downscaling tool, which allows to downscale and investigate large ensembles of large-scale wind data, and a MOS approach, which aims at adjusting simulated gust speeds closer to observations. Concerning future climate conditions, the prediction on a time horizon of about ten years is particularly interesting for adaption strategies. Therefore, the applicability of the developed downscaling methodology for decadal predictions is shown.

The first part of this work (Haas and Pinto, 2012, Chapter 2) deals with the development of a statistical-dynamical downscaling approach. For this purpose, 100 events between 1989 and 2010 are selected. Three days around each of these top-ranked windstorm events are considered to train MLR models. These models relate RCM data and large-scale data. In this study, transfer functions between CCLM simulations of gust speed and ERA-Interim wind speeds are estimated, i.e. each CCLM grid point is related to the surrounding 16 ERA-Interim grid points. The approach is tested by leave-one-out validation, that is for each windstorm the transfer function is determined with the information of the 99 other events. The CCLM footprints are then reproduced by applying the transfer functions on ERA-Interim reanalysis data. RMSEs between the original CCLM footprints and the reproduced footprints show relative errors of 10 - 20 % per event. Best results are achieved for strong events with a broad footprint, while the method produces larger errors for windstorms associated to uncommon cyclone tracks or multiple cyclones. Further factors that could lead to larger deviations between dynamically and statistical-dynamically downscaled footprints are explosive cyclogenesis or high altitudes. In order to make the results independent from altitude, an implementation of an exposure correction based on topographic data or other local-scale characteristics like roughness length would be advisable for further developments.

A comparison to observations at 39 test sites of the DWD shows similar results for CCLM footprints and for the footprints reproduced by the statistical-dynamical downscaling. Thus, this kind of statistical-dynamical downscaling delivers a cost-efficient alternative to pure dynamical downscaling with an RCM. Due to the straightforward nature of the methodology, it can be easily adjusted to other data sets or parameters. Thus, the methodology was also employed for a cooperation project with Aon Benfield Impact Forecasting in London. The insurances broker requested a windstorm catalogue including 10000 events as input for a windstorm model. For this purpose, the statistical-dynamical model was trained with gust speeds of 250 events simulated with the CCLM and according wind speeds from the reanalysis of the National Centers for Environmental Prediction (NCEP) and the National Center for Atmospheric Research (NCAR). The MLR coefficients were afterwards applied to wind speeds of 10000 events simulated with the ECHAM5 GCM. These downscaled gust footprints are now part of the windstorm catalogue and the windstorm model launched in March 2014. For further other applications, it would e.g. be reasonable to enhance the temporal resolution of the downscaled parameters from daily to e.g. hourly values by replacing the training data and / or the input data for the transfer function. However, the results are always dependent on the RCM and reanalysis data sets used to train the transfer functions, so that the downscaled gust speeds can be only as good as the input data.

The similar findings of the dynamical and the statistical-dynamical downscaling in comparison to observations shown in Haas and Pinto (2012) lead to the assumption that the RCM output as training data should be adjusted to observations first to improve the skill of the combined approach. For this purpose, a MOS technique is applied in the second part of this work (Haas et al., 2014a, Chapter 3). This methodology is performed with the same selection of events and the same CCLM simulations as presented in Haas and Pinto (2012). The special feature of the introduced methodology compared to former studies using MOS approaches is the adjustment to observations not only for specific locations but for a regular grid corresponding to the RCM resolution. For a selection of test sites (173 for wind and 111 for gust) and each grid point, the wind and gust speeds are fitted by the Weibull distribution. In order to compare observations and CCLM simulations, the distribution parameters of the observations are interpolated to the RCM grid. A probability mapping combines the two pairs of distribution parameters (interpolated and simulated) for wind and gust separately at each grid point so that the CCLM simulations can be corrected.

Both uncorrected and corrected CCLM simulations are validated against observations using RMSEs. Regarding the spatial average of errors, 99 of 100 events are improved for wind and 88 of 100 events are improved in terms of gusts. Similar results are obtained when investigating the percentage of

improved test sites per event. For a detailed analysis, Circulation Weather Types (CWTs) are ascertained for each event. These CWTs show that the best results are achieved for events with a westerly or an anticyclonic-westerly flow. The RMSEs as averages over all events demonstrates that 145 of the 173 test sites selected for wind are in a better congruence to the observations after the correction. Concerning gust speeds, the RMSE is after the correction lower at 71 of the 111 selected test sites. For both meteorological parameters, the improved sites are randomly distributed over Germany.

In summary, improvements by the MOS approach are better with respect to wind speeds than for gusts. The application on gust data is more challenging due to the higher spatial and temporal variability of gust data in comparison to wind data. Additionally, the available time series for gust speeds are considerably shorter than for wind speeds. These shortcomings are reflected in the weaker results. Thus, the methodology should be further adjusted for the application on gust speeds. One possibility to enlarge the amount of gust data is a wind-gust model as introduced in Seregina et al. (2014). This methodology is based on the anticorrelation of both distribution parameters, which is noticeable for both wind and gust measurements. However, for daily values as taken into consideration in Haas et al. (2014a), such a wind-gust model is less suitable (c. f. Chapter 4). On the other hand, the hourly gust measurements used in Seregina et al. (2014) have the weakness of a threshold of 12.5 m/s before 2001. This means that 12 years of the investigation period (1989 - 2010) would not be covert or, if the threshold would be included, at least not the full range of gust speeds would be covered. One possibility would be to shorten the training period for the downscaling transfer function and for the Weibull fitting to the years 2001 - 2010; the other possibility would be to test the methodology with other gust observations, e. g. from other European countries, where no thresholds are applied. An expansion to other European countries is also desirable for wind observations, in order to combine the MOS approach with the statistical-dynamical downscaling presented in the first part of this work. The methodology introduced by Seregina et al. (2014) also enables to estimate return periods of intense windstorms for Germany. By an extended wind and gust data set, this methodology would have the potential for an implementation to the techniques of this work.

In the third part of this work (Haas et al., 2014b, Chapter 5), the statistical-dynamical downscaling approach introduced in Haas and Pinto (2012) is applied on decadal hindcasts and predictions. The decadal predictability of the MPI-ESM-LR (baseline1) is analyzed using simulations in its original lower resolution and in the higher resolution after downscaling. For each decade 10 yearly initialized realizations and 3 additional realizations of uninitialized runs as reference (historical) simulations are available. Considering the investigation period 1979 - 2010, this adds up to 96 historical runs and 320

hindcasts in the original resolution. Thus, the application of an RCM is hard to realize for the entire investigation period. Therefore, the statistical-dynamical downscaling is a cost-efficient option for downscaling the full ensemble. The downscaling approach is for this third study slightly adapted: a) the ERA-Interim data as large-scale training data is interpolated to the MPI-ESM-LR grid for consistency reasons; b) the regional simulations are realized with the CCLM on a 25 km x 25 km grid within a slightly enlarged investigation area; and c) all days between 1979 and 2010 are considered and not only a selection of intense windstorms. As output, selected quantiles are stored for each grid point and each decade considering both resolutions and the different data sets (ERA-Interim, hindcasts and historical simulations).

The reproduction of the CCLM simulations delivers good results with an overall RMSE of 2.98 m/s. Comparing different quantiles shows that especially the medians of the RCM and the statistical-dynamical downscaling are almost equal, while the low quantiles are overestimated and the high quantiles are underestimated by the combined approach. The analysis of an example period known for several windstorms (1990 - 1993), shows that the hindcasts are able to represent the above-average wind speeds caused by an unusual number of intense cyclones in the original resolution and after downscaling. The performance is best shortly after the initialization, when the ensemble spread is smallest. In order to quantify the predictive skill of the initialized hindcasts vs. the uninitialized simulations, they are each compared to ERA-Interim quantiles by means of RMSEs. The skill scores of the 95 % quantile are best for small lead times (1 - 4 years) in both resolutions, which evidences that the initialization of the GCM with observed sea surface temperatures and salinity as starting conditions has a strong influence beside model physics. For longer lead times, they are still positive over land but negative over sea. The pattern of the skill scores over Europe are similar for the high quantiles greater or equal 75 %. These pattern are in congruence with the number of cyclones per year. As midlatitude cyclones cause rather high wind speeds equal to high quantiles, the lower quantiles do not have such distinct pattern. Averages over the entire investigation area also show that the best skill scores are achieved for the higher quantiles in both resolutions, although they are somewhat smaller for the higher resolution. However, a direct comparison of the skill scores of both resolutions is not meaningful, because the downscaling to the high resolution also implies the estimation of peak wind speeds as a proxy for gusts. Due to the higher variability of gusts, an estimation is more challenging than for wind speeds. The RMSE-based skill score as average over the entire investigation area and over a reduced area are despite this enhanced variability positive. This means, an added value of initialization is still given after the downscaling. The above mentioned overestimation (underestimation) of low (high) quantiles is not relevant here, as it affects both the downscaling of the initialized and of the uninitialized simulations and is compensated. Nonetheless, a bias

correction would be meaningful for further studies analyzing the direct results of downscaled decadal predictions and not the ration between initialized and uninitialized simulations.

In order to allow for a comparison between the skill scores of the high and the low resolution and thus analyze the added value of downscaling, the statistical-dynamical downscaling approach could be trained with CCLM (or other RCM) wind speeds to predict high resolution wind speeds instead of peak winds. For a direct comparison, the hindcasts should be interpolated to the CCLM grid. However, compared to observations it is likely that errors and biases of the hindcasts and predictions are still present after the downscaling. Thus, a distinct improvement of high-resolution wind speeds or peak wind speeds is dependent on the further development of decadal prediction systems. Within the MiKlip project some improvements could already be found for the baseline1 system compared to baseline0 (e.g. Pohlmann et al., 2013). The methodology will also be applied to the MiKlip prototype system, which is currently in progress. Compared to the baseline1 hindcasts and predictions, for this new system, the initialization is enhanced using additional data sets for ocean and atmosphere.

An important point when using statistical approaches like those presented here, is the temporal stationarity of the estimated transfer functions. This means it has to be assumed that the relation between regional-scale and large-scale data (parts 1 and 3) or between observations and simulations (part 2) does not change under future climate conditions. For Haas and Pinto (2012), the 100 events are split into a training period and a validation period, each consisting of 50 events. For validation, the transfer function is determined from the first 50 events and afterwards applied on the large-scale data of the later 50 events, and the other way round. The resulting RMSE of the first period averaged over the entire investigation area is comparable to the RMSE obtained from leave-one-out validation. The RMSE of the gusts of the later period, estimated with the transfer function of the earlier events, is slightly enhanced (about 17 % compared to 16 %, c.f. Table 1 in Chapter 2). This may be induced by more uncommon cyclones during the later events. Nevertheless, the similar results even for the quite small samples support the assumption of stationarity for the statistical-dynamical downscaling technique. Thus, the technique can be recommended for investigations with respect to near future climate conditions. For Haas et al. (2014a), the same splitting of events can be carried out, i.e. the Weibull parameters are calculed for each period separately. These build four new transfer functions: one for wind speeds of the first 50 events ($T_{1,50,wind}$), one for wind speeds of the events 51 to 100 ($T_{51,100,wind}$), one for gust speeds of the first 50 events ($T_{1,50,gust}$), and one for gust speeds of the events 51 to 100 ($T_{51,100,gust}$). For wind speed, exemplary values between 1 m/s and 20 m/s in $T_{1,50,wind}$ and $T_{51,100,wind}$ are inserted. The same is done for gust speed with values between 1 m/s and

40 m/s. The resulting corrected wind / gust speeds of both periods can be plotted against each other and a regression line can be fitted for each grid point (Figure S5 in Chapter 3). These regression lines differ only marginally from the identity line over most parts of northern Germany, i. e. stationarity can be assumed for these areas for wind and gusts (Figure S6 in Chapter 3). Larger deviations can be found over Southern Germany, where single test sites have large influence on the overall pattern. Therefore, the assumption of stationarity is not unfounded but should be proofed again with a larger data set for future investigations with the MOS approach. For the study of Haas et al. (2014b), stationarity is not tested again. Since it has been proven for the selected 100 windstorms, it can be assumed to be valid also for a larger data set consisting of all days between 1979 and 2010. Furthermore, for the calculation of skill scores, an unchanging transfer function is less important, because it effects both the downscaled hindcasts or predictions and the downscaled uninitialized simulations.

Summarizing the results of the three publications shows that it is possible to effectively combine different wind and gust speed data sets. These are important to analyze windstorms, as they have a large impact on Europe. The individual advantages of the different data sets are still existent, while the shortcomings are minimized:

- The coarse resolution of ERA-Interim reanalysis data and of MPI-ESM-LR decadal hindcasts is increased by the statistical-dynamical downscaling from 0.75° x 0.75° (T255) to 0.0625° x 0.0625° (7 km x 7 km) and from 1.875° x 1.875° (T63) to 0.22° x 0.22° (25 km x 25 km), respectively.

- Due to the statistical transfer function between local-scale and large-scale wind / gust footprints, the approach is cost-efficient compared to pure dynamical downscaling, and thus applicable for large data sets.

- Unlike pure statistical downscaling the combined approach includes small-scale features parameterized by the CCLM.

- The MOS approach based on Weibull distribution parameters is able to adjust CCLM simulations to observations, provided that the amount of measurements is large enough. So far, this is only given for wind speeds.

- The downscaling approach is applicable for decadal hindcasts and has the advantage to make conclusions on peak winds as a proxy for gusts in addition to large-scale wind speeds in the lower resolution.

- The techniques build a complete model chain, which enables to bridge the gap between the different scales.

Following studies should focus on the spatial and temporal enlargement of the data sets. Gusts are regionally very heterogeneous, induced by specific local conditions like land use or the arrangement of buildings. Therefore, the estimation of gusts on a grid below the investigated 7 km-resolution could be appropriate for detailed studies. As peak gusts most times only last for several seconds and are thus also very variable in time, it could be meaningful to increase the temporal resolution from daily maxima to at least hourly maximum gusts. However, data amount and related computation time should be always balanced with the resulting benefit. Additionally, the implementation of further parameters at different stages of the methods could help to capture small-scale features even better. For example, roughness length is a factor with a large impact on near-surface winds and gusts. There is also potential to apply the combination of all techniques or only single parts to other meteorological parameters like temperature or precipitation. Only the choice of the Weibull distribution has to be revised for these purposes. Such a change would be easy to implement because the different techniques can be seen as parts of a modular construction system.

So far, the methodologies are tested with historical data, but the approach is also applicable for future climate investigations, if stationarity is assumed. A possible field of application with respect to renewable energy is the examination of wind energy potential like done in Reyers et al. (2014) or Hueging et al. (2013). Their findings could e. g. be compared to results of the statistical-dynamical downscaling. Climate change impacts are not only important for energy supply, but also for economy like reinsurance companies, which are dependent on reliable risk assessments to calculate their required capital and to adjust the contracts with their customers. This shows, that statements for the near future and especially for the coming decade are important for politics and economy in order to react on climate change and resulting changes in meteorological parameters like wind and gust, and to develop adaption strategies. Although information on wind and gust speeds are in particular demanded, studies on these parameters were so far rather underrepresented in comparison to temperature and precipitation. Thus, the findings of this work deliver a valuable contribution to the existing research on downscaling in particular for gusts and wind.

7   References

Adamson, D. S., Belcher, S. E., Hoskins, B. J., and Plant, R. S. (2006). Boundary-layer friction in midlatitude cyclones. *Q. J. R. Meteorol. Soc*, 132:101–124. `http://dx.doi.org/10.1256/qj.04.145`.

Bjerknes, J. and Solberg, H. (1922). Life cycle of cyclones and the polar front theory of atmospheric circulation. *Grondahl*.

Boé, J., Terray, L., Habets, F., and Martin, E. (2006). A simple statistical-dynamical downscaling scheme based on weather types and conditional resampling. *J. Geophys. Res.*, 111:D23106. `http://dx.doi.org/10.1029/2005JD006889`.

Charney, J. G. (1947). The dynamics of long waves in a baroclinic westerly current. *J. Meteor.*, 4:136–162. `http://dx.doi.org/10.1175/1520-0469(1947)004<0136:TDOLWI>2.0.CO;2`.

Davis, W. M. (1899). The circulation of the atmosphere. *Q. J. R. Meteorol. Soc*, 25:160–172. `http://dx.doi.org/10.1002/qj.49702511003`.

Dee, D. P., Uppala, S. M., Simmons, A. J., Berrisford, P., Poli, P., Kobayashi, S., Andrae, U., Balmaseda, M. A., Balsamo, G., Bauer, P., Bechtold, P., Beljaars, A. C. M., van de Berg, L., Bidlot, J., Bormann, N., Delsol, C., Dragani, R., Fuentes, M., Geer, A. J., Haimberger, L., Healy, S. B., Hersbach, H., Hólm, E. V., Isaksen, L., Kållberg, P., Köhler, M., Matricardi, M., McNally, A. P., Monge-Sanz, B. M., Morcrette, J.-J., Park, B.-K., Peubey, C., de Rosnay, P., Tavolato, C., Thépaut, J.-N., and Vitart, F. (2011). The ERA-Interim reanalysis: Configuration and performance of the data assimilation system. *Q. J. R. Meteorol. Soc.*, 137:553–597. `http://dx.doi.org/10.1002/qj.828`.

Della-Marta, P. M., Mathis, H., Frei, C., Liniger, M. A., Kleinn, J., and Appenzeller, C. (2009). The return period of wind storms over Europe. *Int. J. Climatol.*, 29:437–459. `http://dx.doi.org/10.1002/joc.1794`.

Fuentes, U. and Heimann, D. (2000). An improved statistical-dynamical downscaling scheme and its application to the alpine precipitation climatol-

ogy. *Theor. Appl. Climatol.*, 65:119–135. `http://dx.doi.org/10.1007/s007040070038`.

Goyette, S., Brasseur, O., and Beniston, M. (2003). Application of a new wind gust parameterization: Multiscale case studies performed with the canadian regional climate model. *J. Geophys. Res.*, 108:4374. `http://dx.doi.org/10.1029/2002JD002646`.

Haas, R. and Pinto, J. G. (2012). A combined statistical and dynamical approach for downscaling large-scale footprints of european windstorms. *Geophys. Res. Lett.*, 39:L23804. `http://dx.doi.org/10.1029/2012GL054014`.

Haas, R., Pinto, J. G., and Born, K. (2014a). Can dynamically downscaled wind- storm footprints be improved by observations through a probabilistic approach? *J. Geophys. Res. Atmos*, 119:713–725. `http://dx.doi.org/10.1002/2013JD020882`.

Haas, R., Reyers, M., and Pinto, J. G. (2014b). Decadal predictability of regional-scale peak winds over europe based on MPI-ESM-LR. *Meteorol. Z.*, submitted.

Hack, J. J. (1994). Parameterization of moist convection in the national center for atmospheric research community climate model (CCM2). *J. Geophys. Res.*, 99:5551–5568. `http://dx.doi.org/10.1029/93JD03478`.

Hadley, G. (1735). Concerning the cause of the general trade-winds: By geo. hadley, esq; frs. *Philosophical Transactions*, 39:58–62.

Hueging, H., Haas, R., Born, K., Jacob, D., and Pinto, J. G. (2013). Regional changes in wind energy potential over europe using regional climate model ensemble projections. *J. Appl. Meteorol. Climatol.*, 52:903–917. `http://dx.doi.org/10.1175/JAMC-D-12-086.1`.

Klawa, M. and Ulbrich, U. (2003). A model for the estimation of storm losses and the identification of severe winter storms in germany. *Nat. Hazards Earth Syst. Sci.*, 3:725–732.

Klein, W. H. and Glahn, H. R. (1974). Forecasting local weather by means of model output statistics. *Bull. Amer. Meteor. Soc.*, 55:1217–1227.

Maraun, D., Wetterhall, F., Ireson, A. M., Chandler, R. E., Kendon, E. J., Widmann, M., Brienen, S., Rust, H. W., Sauter, T., Themeßl, M., Venema, V. K. C., Chun, K. P., Goodess, C. M., Jones, R. G., Onof, C., Vrac, M., and Thiele-Eich, I. (2010). Precipitation downscaling under climate change: Recent developments to bridge the gap between dynamical models and the end user. *Rev. Geophys.*, 48:RG3003. `http://dx.doi.org/10.1029/2009RG000314`.

Mieruch, S., Feldmann, H., Schädler, G., Lenz, C.-J., Kothe, S., and Kottmeier, C. (2013). The regional MiKlip decadal forecast ensemble for europe. *Geosci. Model Dev. Discuss.*, 6:5711–5745. `http://dx.doi.org/10.5194/gmdd-6-5711-2013`.

Noilhan, J. and Planton, S. (1989). A simple parameterization of land surface processes for meteorological models. *Mon. Wea. Rev.*, 117:536–549. `http://dx.doi.org/10.1175/1520-0493(1989)117<0536:ASPOLS>2.0.CO;2`.

Pohlmann, H., Müller, W. A., Kulkarni, K., Kameswarrao, M., Matei, D., Vamborg, F. S. E., Kadow, C., Illing, S., and Marotzke, J. (2013). Improved forecast skill in the tropics in the new miklip decadal climate predictions. *Geophys. Res. Lett*, 40:5798–5802. `http://dx.doi.org/10.1002/2013GL058051`.

Reyers, M., Pinto, J. G., and Moemken, J. (2014). Statistical-dynamical downscaling for wind energy potentials: Evaluation and applications to decadal hindcasts and climate change projections. *Int. J. Climatol.*, page accepted.

Rockel, B., Will, A., and Hense, A. (2008). The regional climate model cosmo-clm (cclm). *Meteorol. Z.*, 17:347–348.

Schönwiese, C.-D. (1994). *Klimatologie*, chapter 5.2 Planetarische (globale) Zirkulation, pages 163–169. Verlag Eugen Ulmer GmbH & Co, Stuttgart (Hohenheim).

Seregina, L. S. (2012). Untersuchungen zur räumlichen variabilität von verteilungsparametern der windgeschwindigkeit zur entwicklung einer wind-böe-beziehung. Master's thesis, Institute for Geophysics and Meteorology, University of Cologne, Germany.

Seregina, L. S., Haas, R., Born, K., and Pinto, J. G. (2014). Development of a wind gust model to estimate gust speeds and their return periods. *Tellus A*, accepted.

Stevens, B., Giorgetta, M., Esch, M., Mauritsen, T., Crueger, T., Rast, S., Salzmann, M., Schmidt, H., Bader, J., Block, K., Brokopf, R., Fast, I., Kinne, S., Kornblueh, L., Lohmann, U., Pincus, R., Reichler, T., and Roeckner, E. (2013). Atmospheric component of the mpi-m earth system model: Echam6. *J. Adv. Model. Earth Syst.*, 5:146–172. `http://dx.doi.org/10.1002/jame.20015`.

Taylor, K. E., Stouffer, R. J., and Meehl, G. A. (2012). An overview of CMIP5 and the experiment design. *Bull. Amer. Meteor. Soc.*, 93:485–498. `http://dx.doi.org/10.1175/BAMS-D-11-00094.1`.

Wilby, R., Charles, S., Zorita, E., Timbal, B., Whetton, P., and Mearns, L. (2004). Guidlines for Use of Climate Scenarios Developed from Statistical Downscaling Methods. Technical report, IPCC Task Group on Data and Scenario Support for Impacts and Climate Analysis (TGCIA). `http://www.narccap.ucar.edu/doc/tgica-guidance-2004.pdf`.

8 List of Abbreviations

CCLM .... RCM of the **CO**nsortium for **S**mall-scale **MO**delling in **CL**imate **M**ode (COSMO-CLM)

CDF .... **C**umulative **D**ensity **F**unction

CMIP5 .... **C**oupled **M**odel **I**ntercomparison **P**roject Phase 5

CWT .... **C**irculation **W**eather **T**ype

DWD .... German Weather Service (**D**eutscher **W**etterdienst)

ECHAM .... **EC**MWF **HAM**burg

ECMWF .... **E**uropean **C**entre for **M**edium-Range **W**eather **F**orecasts

GCM .... **G**eneral **C**irculation **M**odel

MiKlip .... Decadal predictions (**Mi**ttelfristige **Kli**ma**p**rognosen)

MLR .... **M**ultiple **L**inear **R**egression

MOS .... **M**odel **O**utput **S**tatistics

MPI-ESM-LR .... **M**ax-Planck-**I**nstitute **E**arth **S**ystem **M**odel in its **L**ower **R**esolution

MPIOM .... **M**ax-Planck-**I**nstitute **O**cean **M**odel

NCAR .... **N**ational **C**enter for **A**tmospheric **R**esearch

NCEP .... **N**ational **C**enters for **E**nvironmental **P**rediction

NH . . . . **N**orthern **H**emisphere

PRODEF . . . . **PRO**babilistic **DE**cadal **F**orecast for Central and Western Europe

RCM . . . . **R**egional **C**limate **M**odel

RMSE . . . . **R**oot **M**ean **S**quared **E**rror

SH . . . . **S**outhern **H**emisphere

Danksagung

An dieser Stelle möchte ich mich bei allen Personen bedanken, die mich in den letzten Jahren unterstützt haben.

Als erstes danke ich Prof. Dr. Michael Kerschgens dafür, dass er die Rolle des Doktorvaters übernommen hat. Außerdem danke ich Prof. Dr. Andreas Fink für die Begutachtung dieser Arbeit.

Insbesondere möchte ich mich bei Dr. Joaquim G. Pinto für die Betreuung, die Zusammenarbeit und die wertvollen Diskussionen bedanken. Ebenso danke ich ihm für das Korrekturlesen und die hilfreichen Rückmeldungen.

Mein Dank gilt außerdem allen Kollegen am Institut für Geophysik und Meteorologie für die tolle Arbeitsatmosphäre und vor allem den Mitarbeitern der AG RegClim, die mir mit Rat und Tat geholfen haben. Insbesondere danke ich Kai Born, der mich während der ersten Phase der Promotion unterstützt hat. Danke an Melanie Karremann für die vielen Stunden im gemeinsamen Büro. Ich danke Mark Reyers und Sabine Lennartz-Sassinek für das Korrekturlesen und die hilfreichen Kommentare.

Abschließend möchte ich mich bei meiner Familie und meinen Freunden für jegliche Unterstützung bedanken.

Beiträge zu den Publikationen

Publikation 1 (Chapter 2)

Das Konzept für diese Veröffentlichung wurde in Zusammenarbeit mit Dr. Joaquim Pinto erstellt. Für diese Arbeit wurden mir Simulationen des Regionalmodels COSMO-CLM zur Verfügung gestellt. Des Weiteren habe ich zur Ereignisauswahl Ergebnisse einer bereits bestehenden Methode genutzt. Alle Arbeiten zur Entwicklung und Validierung der präsentierten Methode, sowie der erste Textentwurf stammen von mir. Die Ausarbeitung des Textes fand in enger Zusammenarbeit mit meinem Koautor Dr. Joaquim Pinto statt.

Publikation 2 (Chapter 3)

Das Konzept für diesen Artikel wurde in Zusammenarbeit mit Dr. Joaquim Pinto und Dr. Kai Born entwickelt. Auch für diese Arbeit wurden die oben genannten COSMO-CLM Simulationen genutzt. Die Umsetzung in Form von entsprechenden Programmen und Analysen wurde von mir persönlich realisiert. Der ursprüngliche Textentwurf stammt ebenfalls von mir. Die Ausarbeitung des Textes fand zusammen mit meinen Koautoren Dr. Joaquim Pinto und Dr. Kai Born statt.

Publikation 3 (Chapter 5)

Das Konzept für dieses Manuskript ist zusammen mit Dr. Joaquim Pinto und Dr. Mark Reyers erstellt worden. Für diese Arbeit wurden dekadische Ensemble-Simulation des MiKlip Projekts als großskalige Antriebsdaten genutzt. Die Vorbereitung dieser Daten und die Berechnung der dynamischen Regionalmodel Simulationen wurden von Dr. Mark Reyers übernommen. Die Anwendung des in Publikation 1 entwickelten Verfahrens, die statistischen Auswertungen und der erste Textentwurf sind mein maßgeblicher Anteil zu dieser Arbeit. Der finale Inhalt und Text wurde mit den Koautoren Dr. Mark Reyers und Dr. Joaquim Pinto abgestimmt.

Erklärung

Ich versichere, dass ich die von mir vorgelegte Dissertation selbständig angefertigt, die benutzten Quellen und Hilfsmittel vollständig angegeben und die Stellen der Arbeit - einschließlich Tabellen, Karten und Abbildungen -, die anderen Werken im Wortlaut oder dem Sinn nach entnommen sind, in jedem Einzelfall als Entlehnung kenntlich gemacht habe; dass diese Dissertation noch keiner anderen Fakultät oder Universität zur Prüfung vorgelegen hat; dass sie - abgesehen von unten angegebenen Teilpublikationen - noch nicht veröffentlicht worden ist sowie, dass ich eine solche Veröffentlichung vor Abschluss des Promotionsverfahrens nicht vornehmen werde. Die Bestimmungen der Promotionsordnung sind mir bekannt. Die von mir vorgelegte Dissertation ist von Prof. Dr. Michael Kerschgens betreut worden.

Köln, den 28.03.2014

Folgende Teilpublikationen liegen vor:

Haas, R., and J. G. Pinto (2012), A combined statistical and dynamical approach for downscaling large-scale footprints of European windstorms, *Geophysical Research Letters*, **39**, L23804, doi:10.1029/ 2012GL054014.

Haas, R, J. G. Pinto, and K. Born (2014), Can dynamically downscaled windstorm footprints be improved by observations through a probabilistic approach? *Journal of Geophysical Research*, **119**, 713–725, doi: 10.1002/ 2013JD020882.

Haas, R., M. Reyers, and J. G. Pinto, Decadal predictability of regional-scale peak winds over Europe based on MPI-ESM-LR, *Meteorologische Zeitschrift*, in review.